



Geophysical Investigation of Asteroids by Spacecraft

UCLA seminar
1 March 2018

A. I. Ermakov¹ (eai@caltech.edu), R. S. Park¹, C. A. Raymond¹, M. T. Bland², M. T. Zuber³,
C. T. Russell⁴, R. R. Fu⁵

¹Jet Propulsion Laboratory, California Institute of Technology

²US Geological Survey, Astrogeology Science Center

³Department of the Earth, Atmospheric and Planetary Sciences, Massachusetts Institute of Technology

⁴University of California Los Angeles

⁵Department of Earth and Planetary Sciences, Harvard University.



Outline

- **Why do we need to study remnant planetesimals (a.k.a planetary embryos a.k.a protoplanets)?**
- **How do we study them?**
- **Dawn at Vesta**
- **Dawn at Ceres**
- **Future studies**

A decorative header featuring various celestial bodies and a satellite against a black background. From left to right, there is a large grey cratered sphere, a satellite with two long thin antennae, a large cratered sphere, the word 'Outline' in white, a green and white cratered sphere, a small grey sphere, and a small orange sphere.

Outline

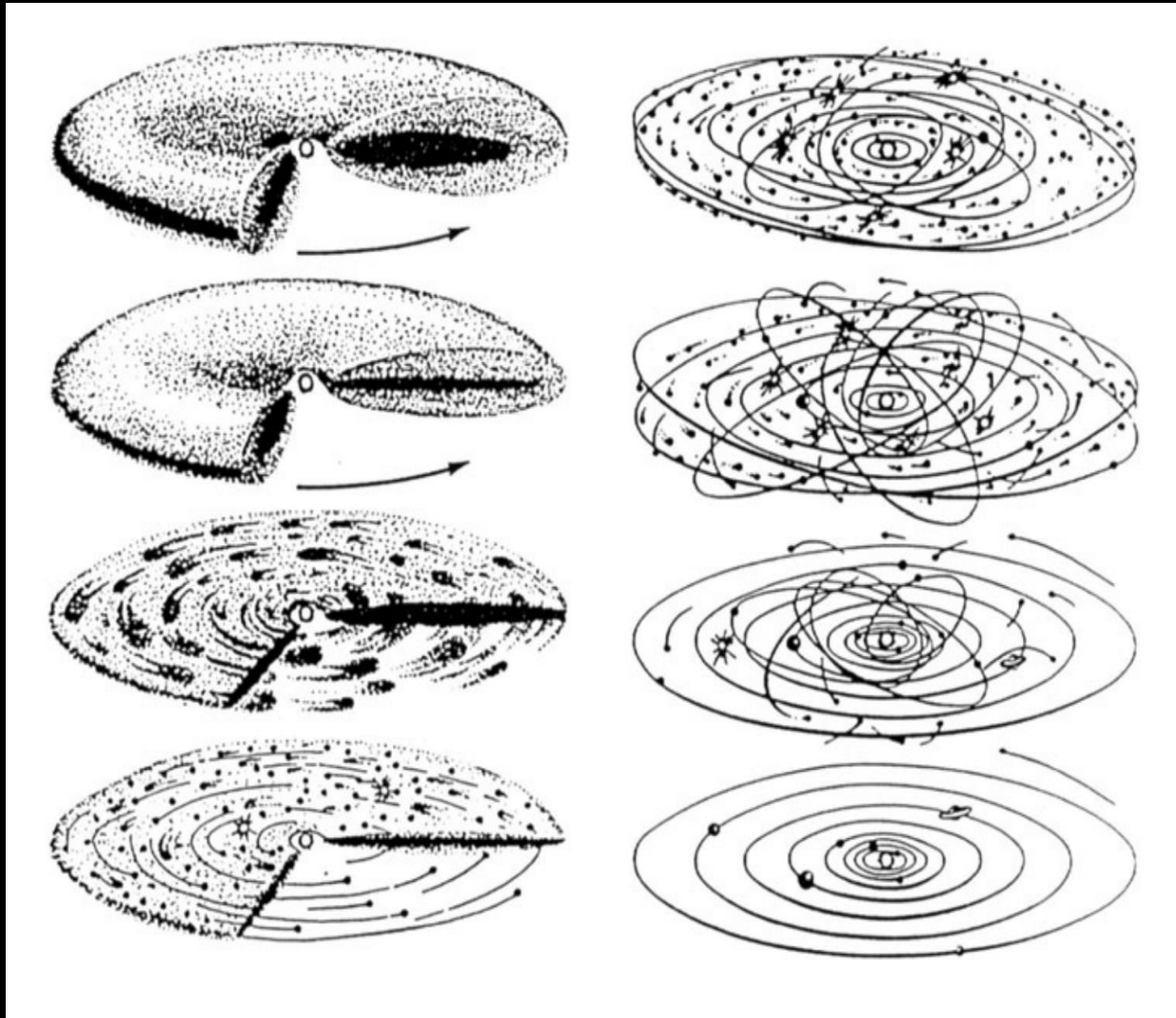
- **Why do we need to study remnant planetesimals (a.k.a planetary embryos a.k.a protoplanets)?**
- **How do we study them?**
- **Dawn at Vesta**
- **Dawn at Ceres**
- **Future studies**



Outline

- **Why do we need to study remnant planetesimals (a.k.a planetary embryos a.k.a protoplanets)?**
- **How do we study them?**
- **Dawn at Vesta**
- **Dawn at Ceres**
- **Future studies**

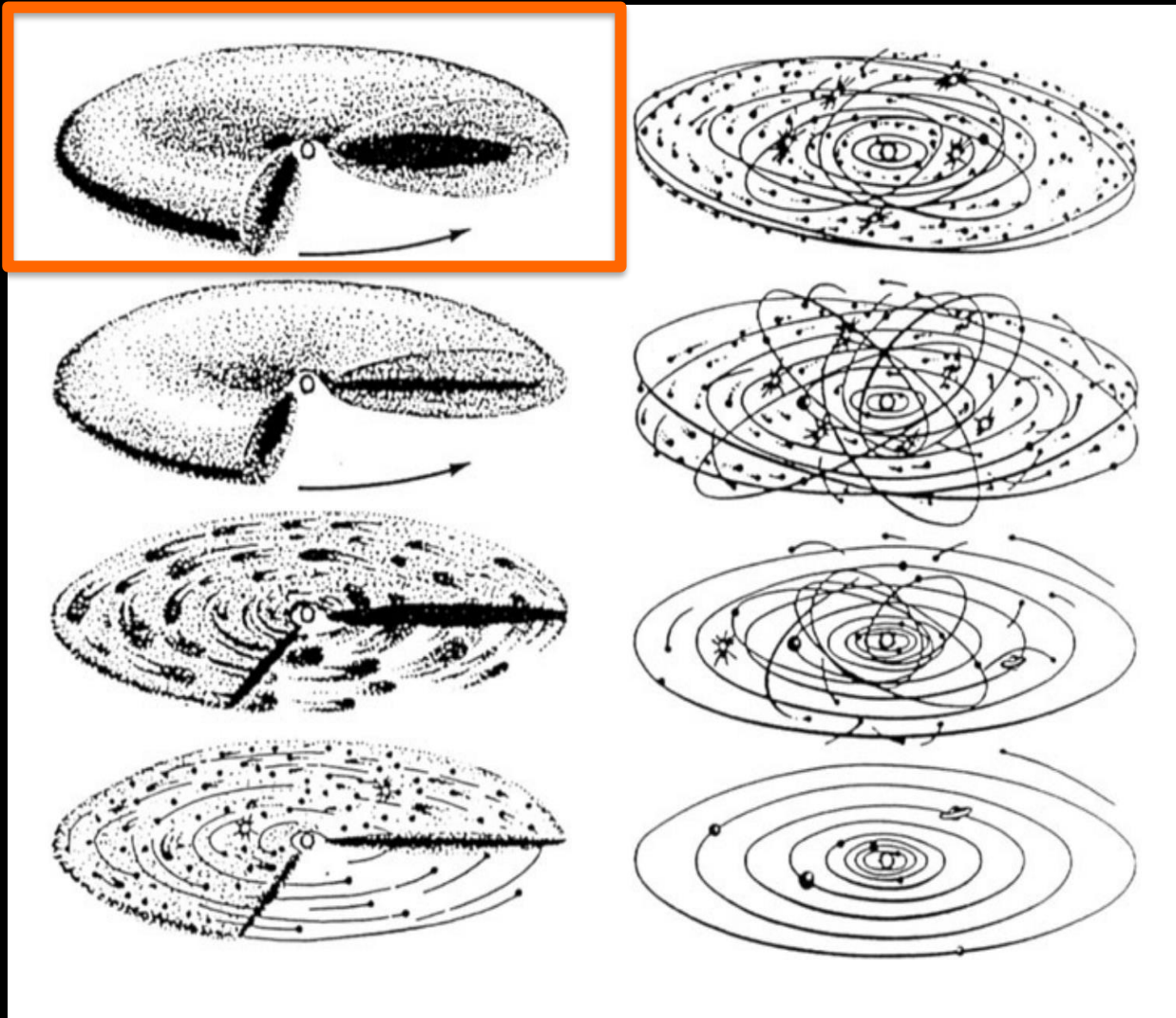
Brief reminder on planet formation



Safronov & Ruskol 1994

UCLA planetary seminar

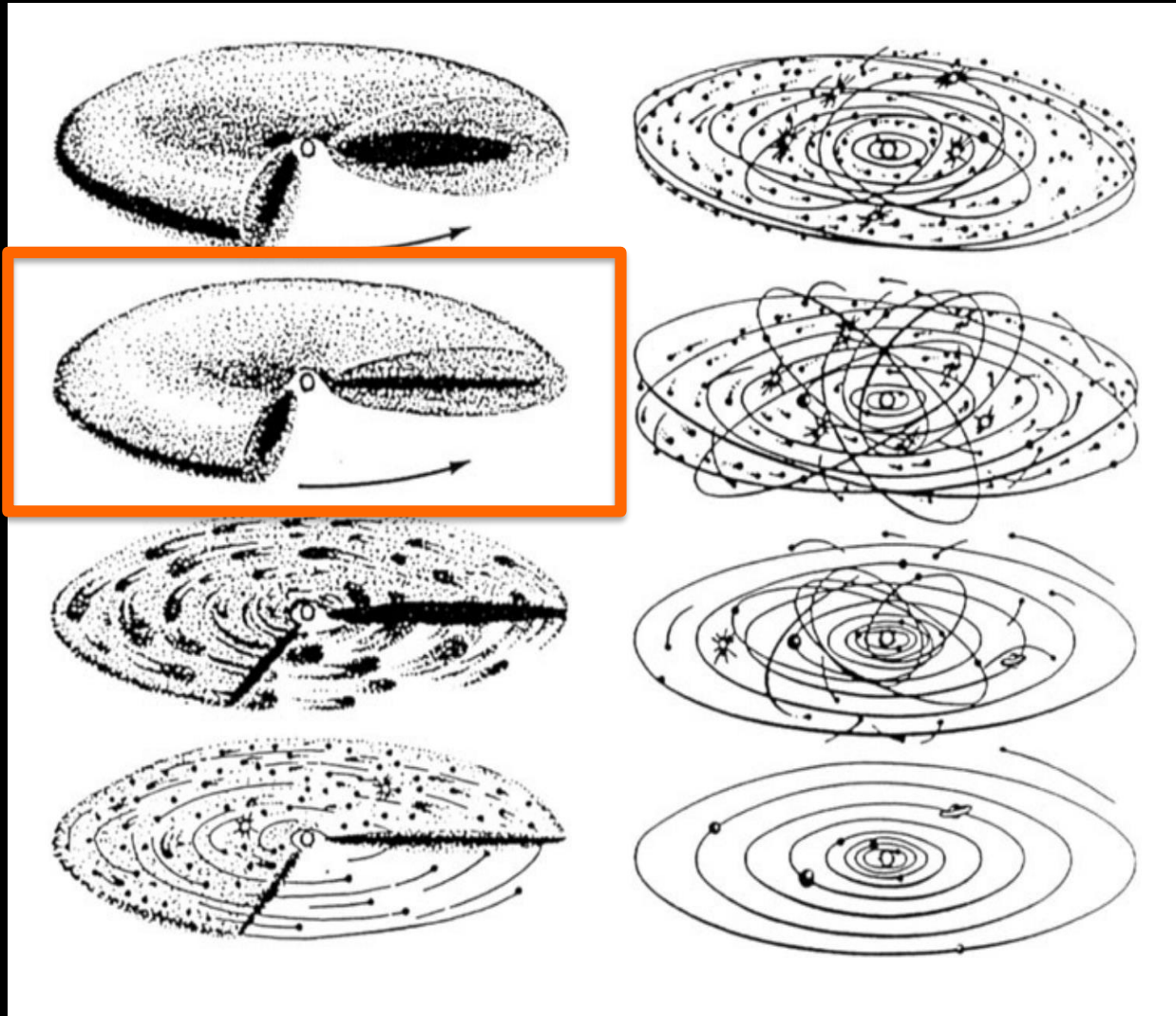
Disk formation



Safronov & Ruskol 1994

UCLA planetary seminar

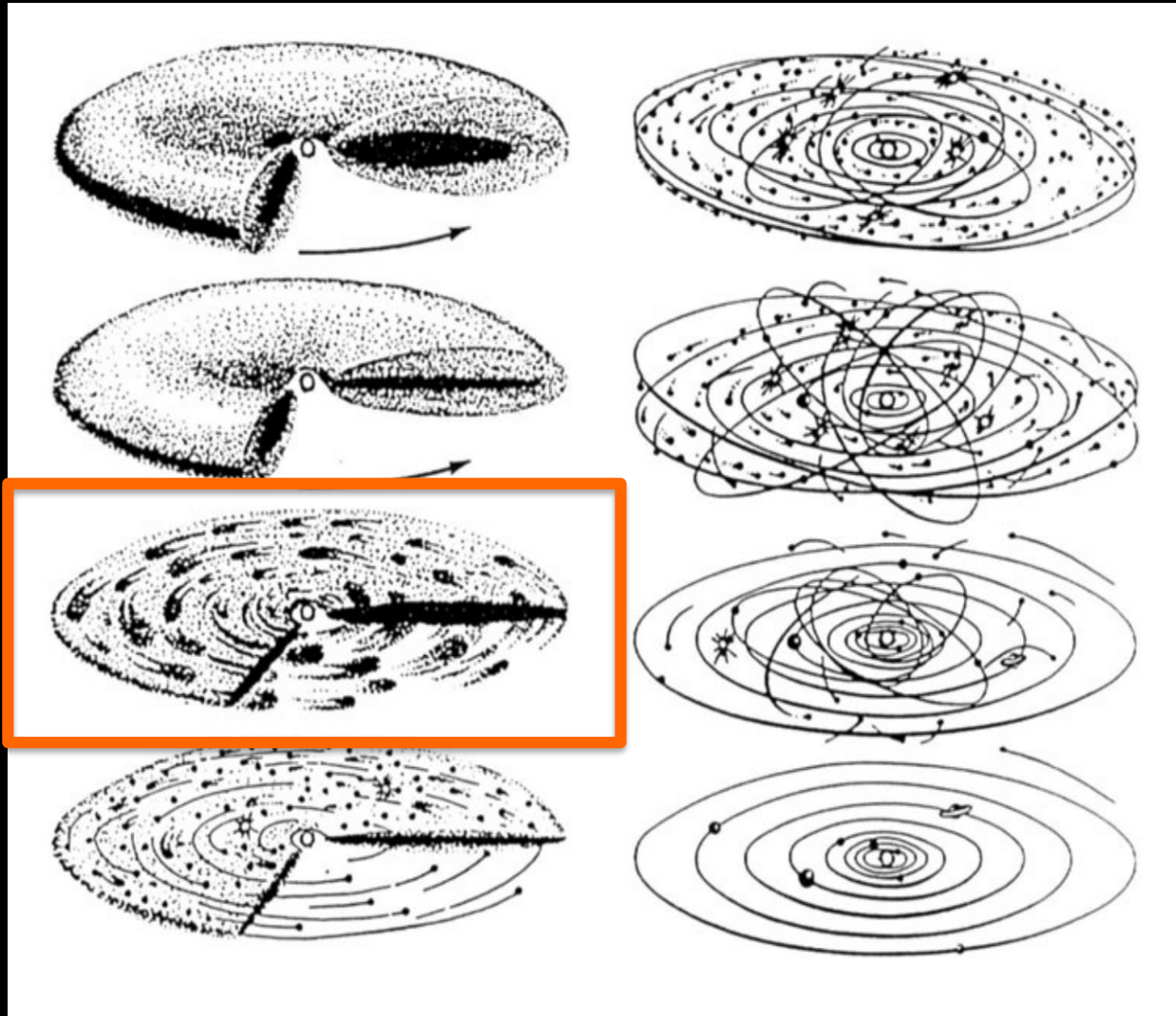
Settling to mid-plane



Safronov & Ruskol 1994

UCLA planetary seminar

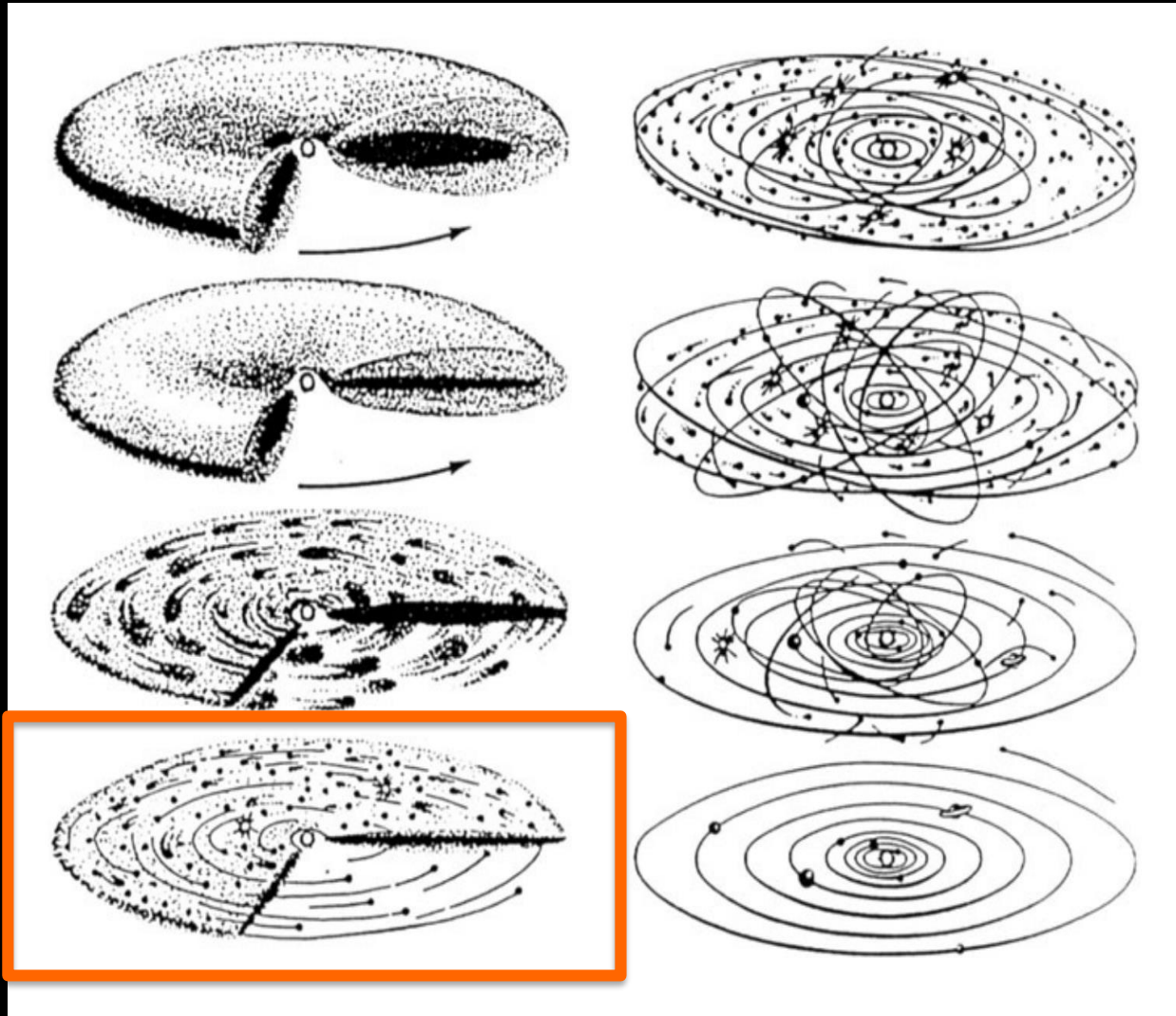
Dust coagulation



Safronov & Ruskol 1994

UCLA planetary seminar

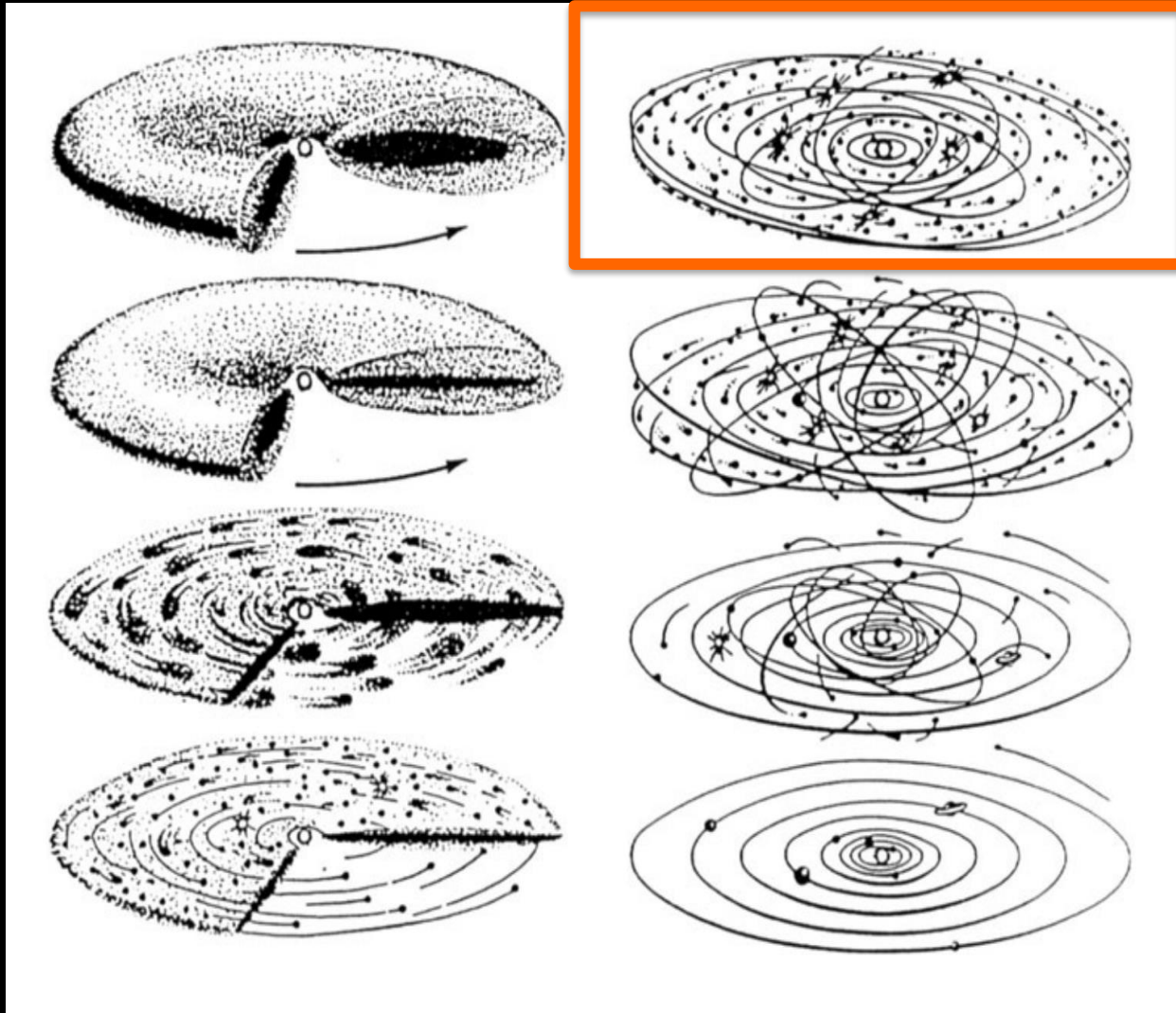
Ordinary growth



Safronov & Ruskol 1994

UCLA planetary seminar

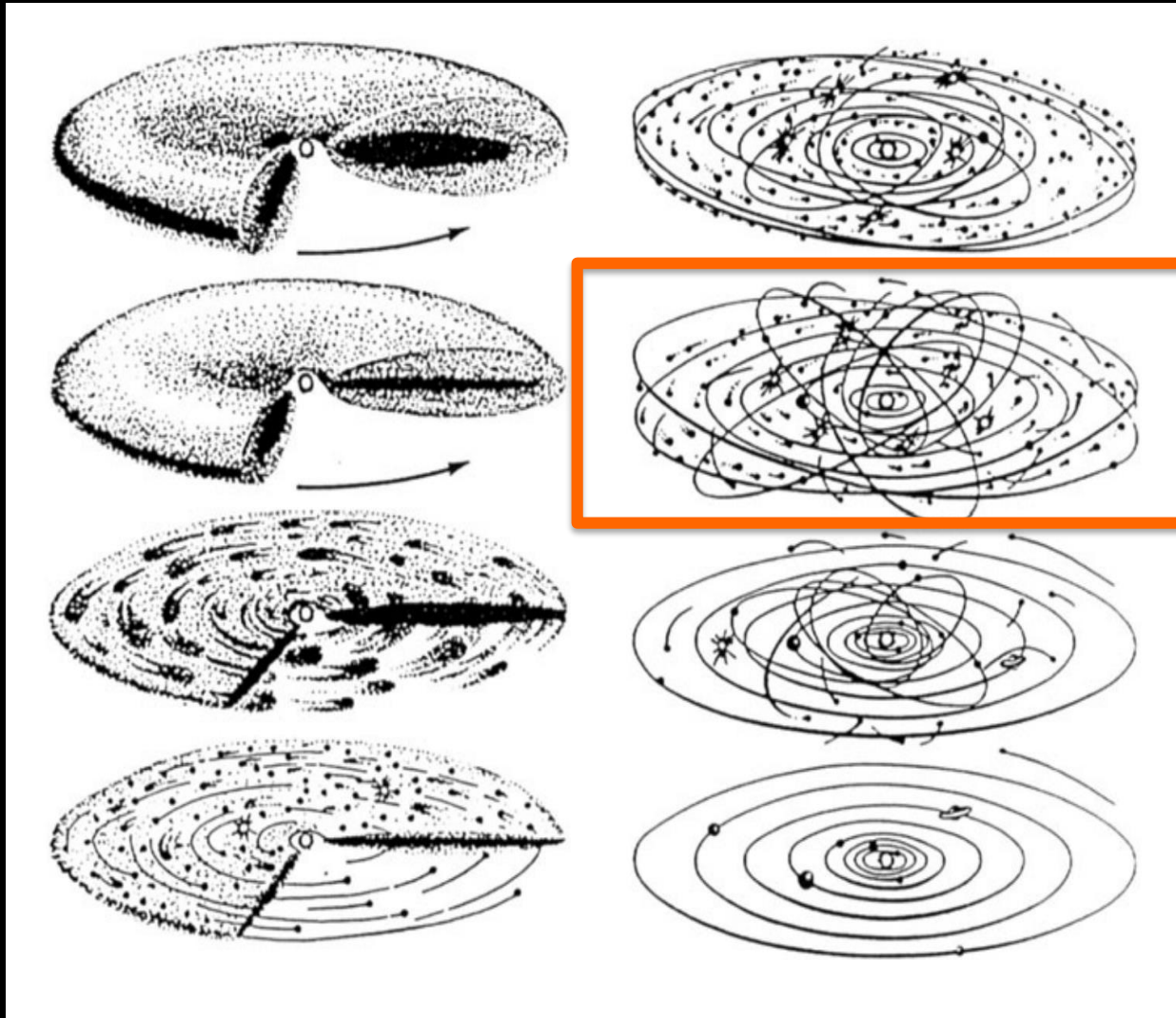
Run-away growth



Safronov & Ruskol 1994

UCLA planetary seminar

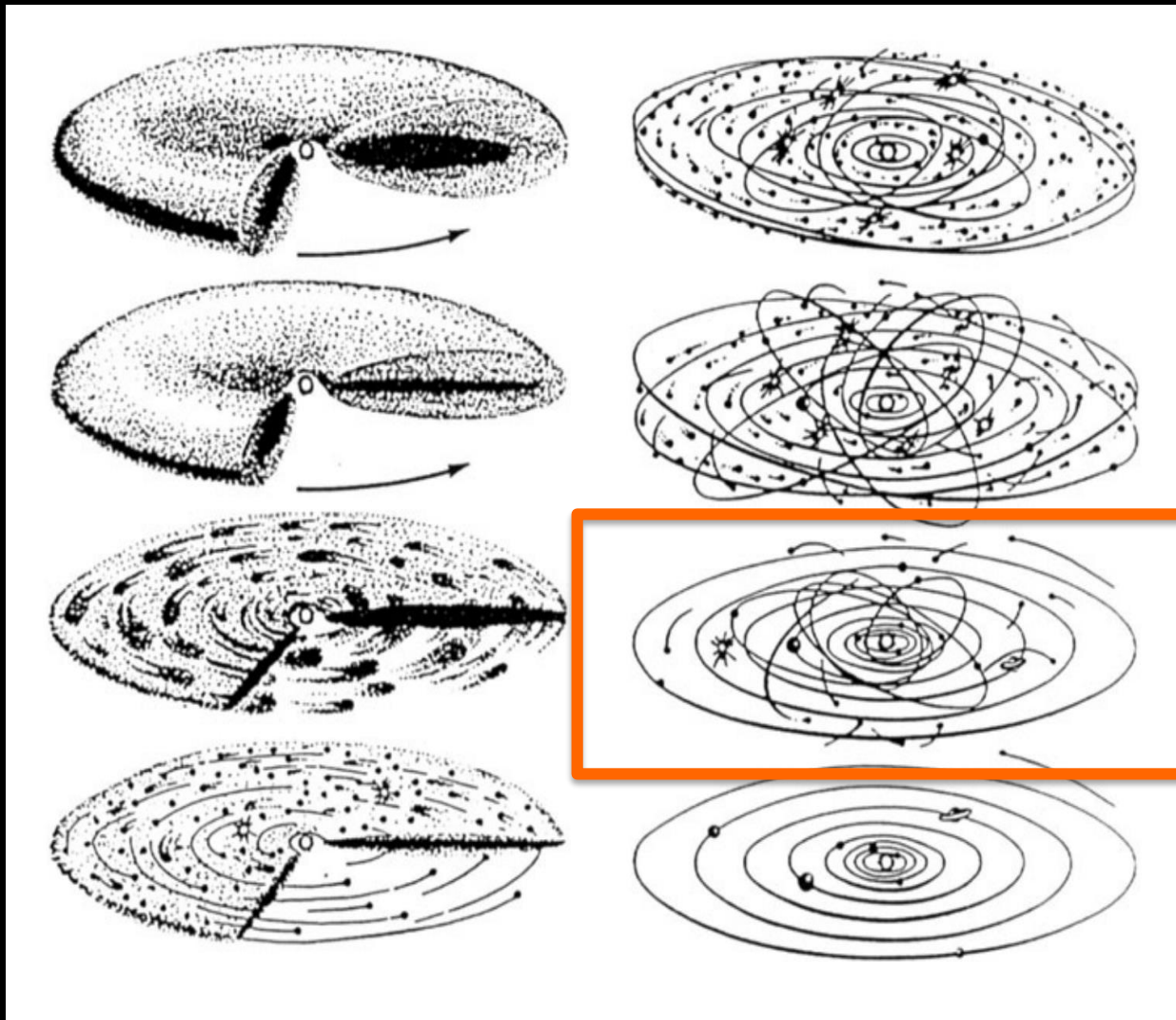
Gas dispersal



Safronov & Ruskol 1994

UCLA planetary seminar

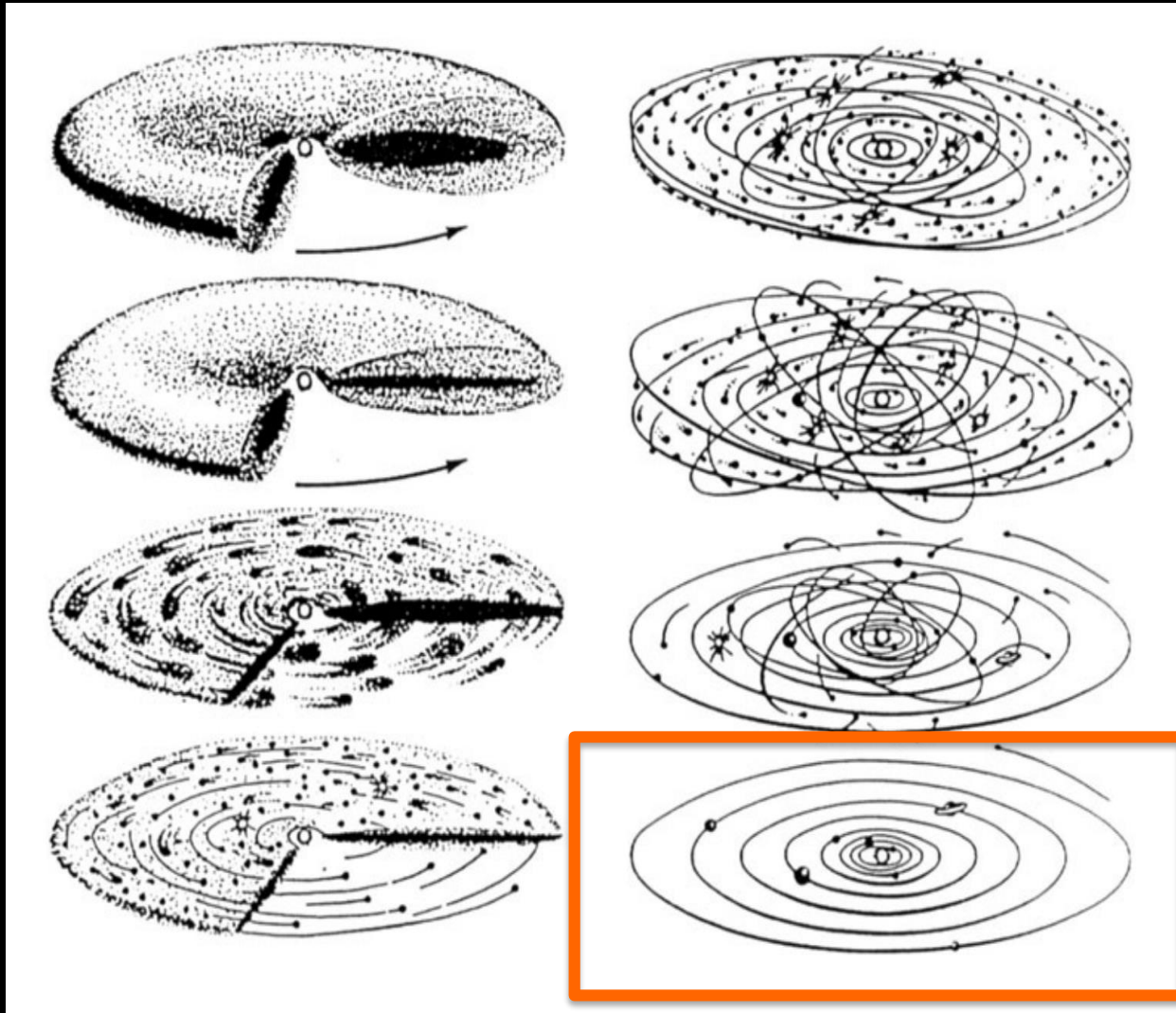
Giant mergers



Safronov & Ruskol 1994

UCLA planetary seminar

Present state

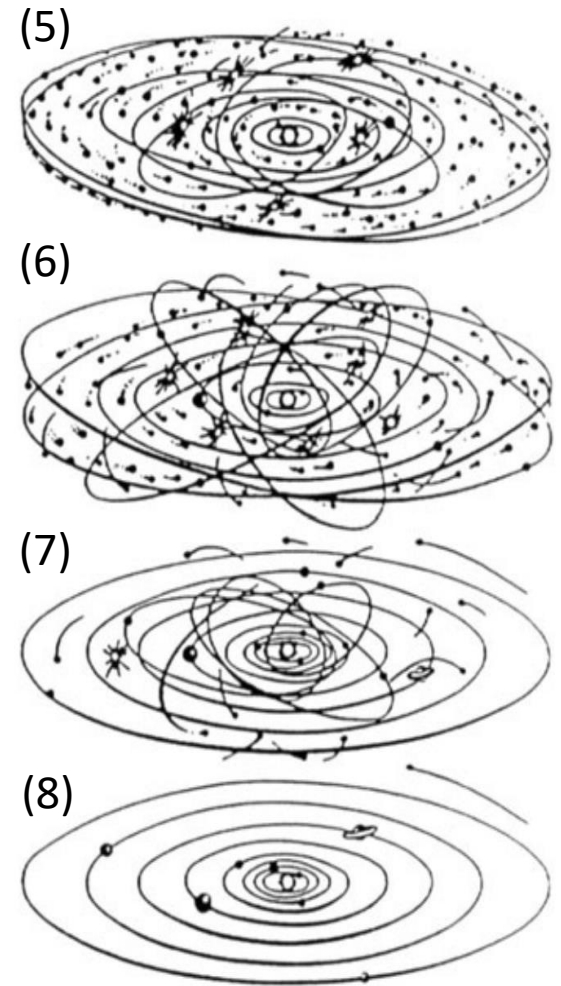
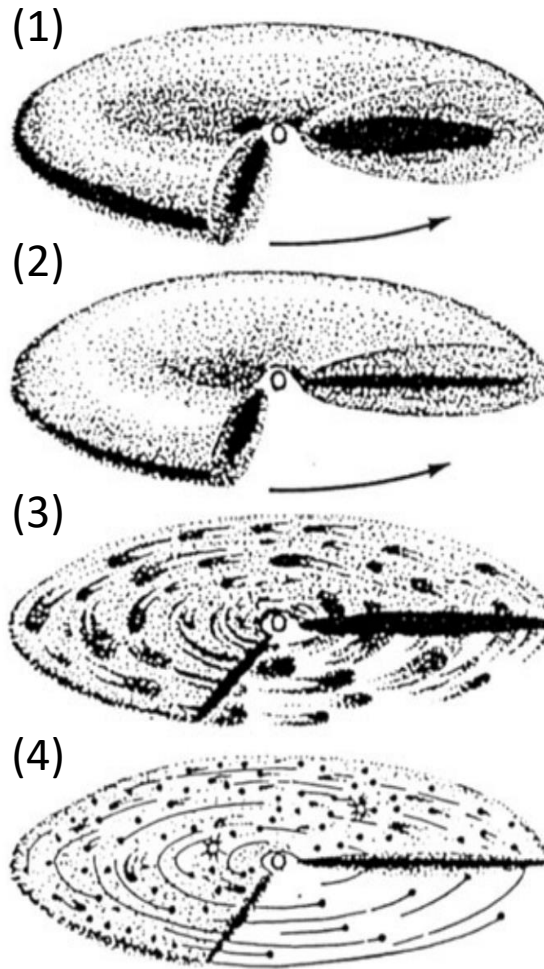


Safronov & Ruskol 1994

UCLA planetary seminar

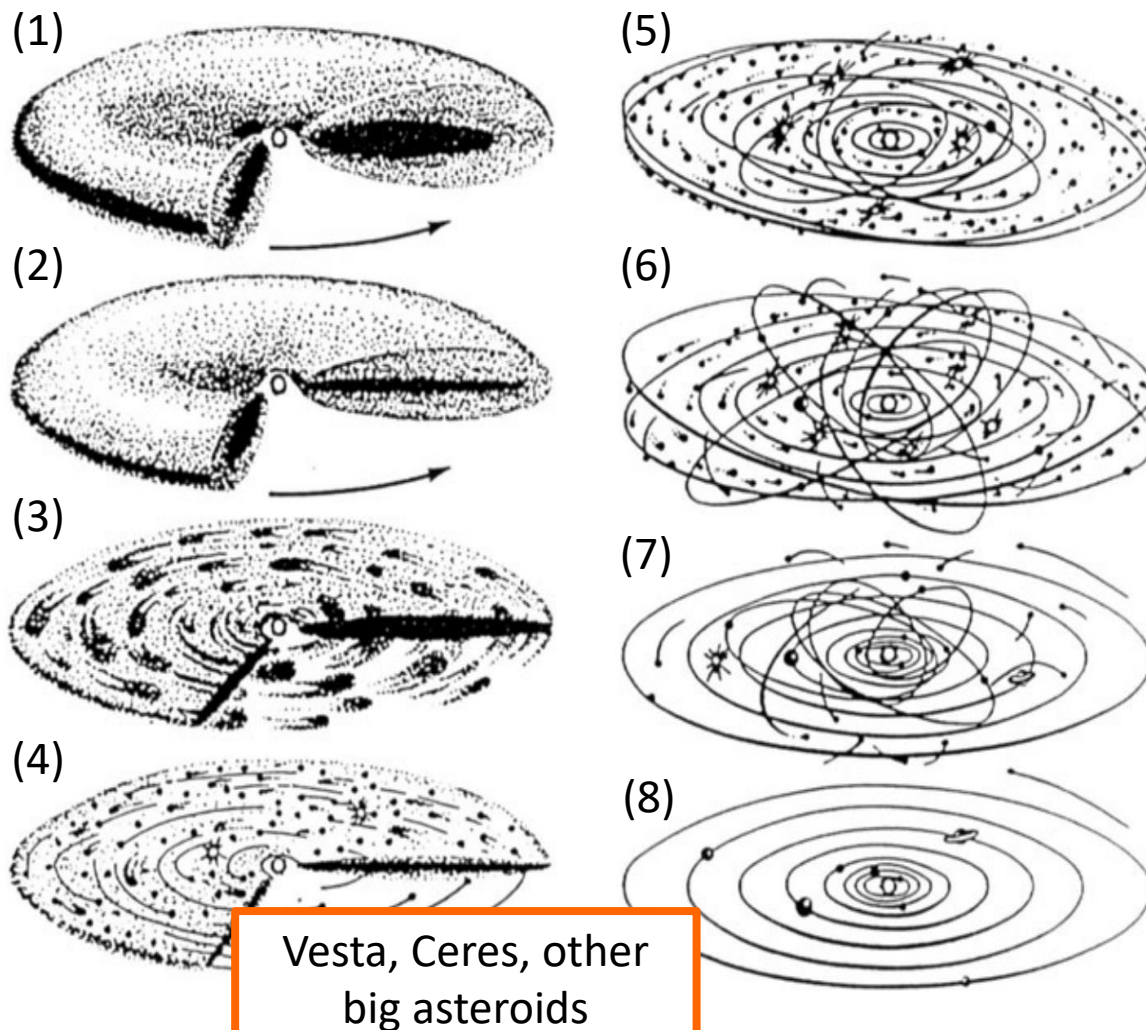
Planet formation

- ① Formation of a nebula disk
- ② Settling to mid-plane
- ③ Dust coagulation
- ④ Orderly growth
- ⑤ Run-away growth
- ⑥ Gas dispersal
- ⑦ Late-state mergers
- ⑧ Present state

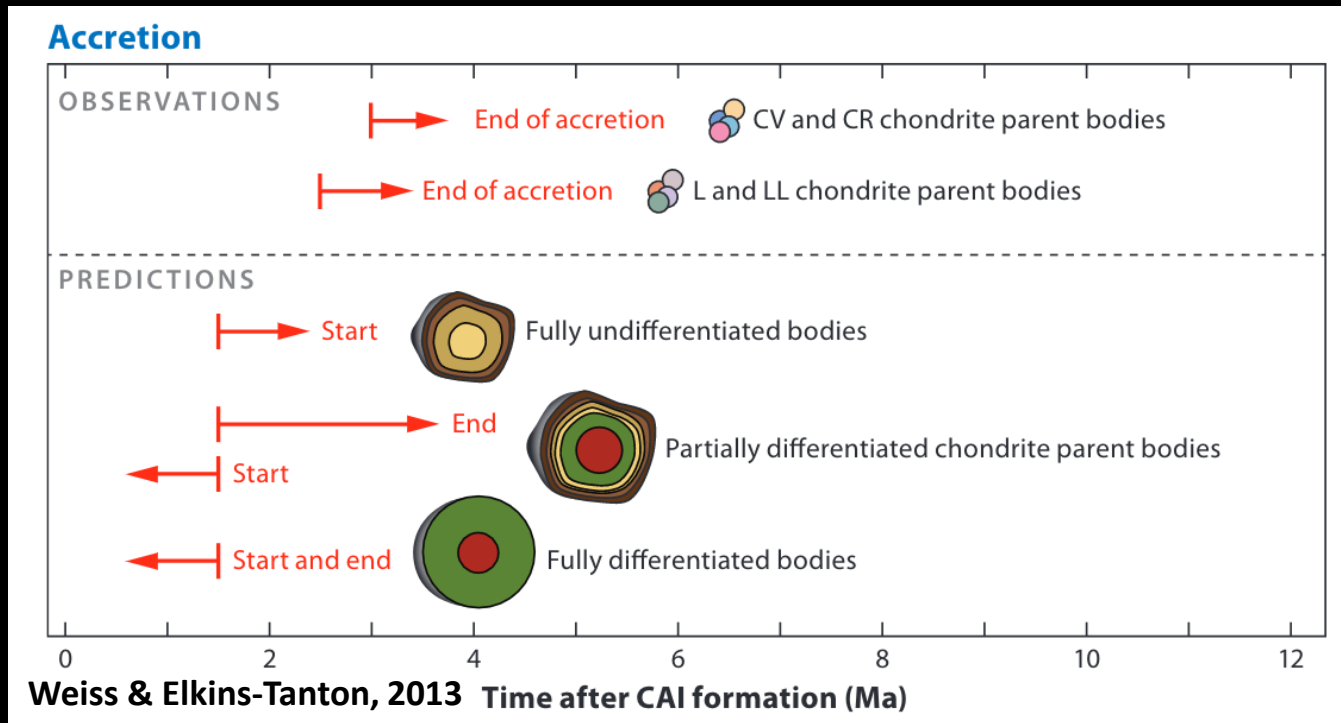


Planet formation

- ① Formation of a nebula disk
- ② Settling to mid-plane
- ③ Dust coagulation
- ④ Orderly growth
- ⑤ Run-away growth
- ⑥ Gas dispersal
- ⑦ Late-state mergers
- ⑧ Present state



A spectrum of protoplanet internal structure



- What was the differentiation state of planetesimals?
 - Differentiated or undifferentiated?
 - How much water?
- What can interior structure tell us about the accretion process?
 - Fast or slow
 - Early or late

A decorative header featuring several celestial bodies against a black background. From left to right, there is a large grey cratered sphere, a medium grey cratered sphere, a small green and white sphere with a dark ring, a small grey sphere, and a small orange sphere.

How do we study a planetary interior with gravity and topography?

- **We study the interior but looking at its response to various forcings such as:**
 - **Rotation**
 - **Surface loads**
 - **Subsurface loads**

A series of five celestial bodies are arranged horizontally across the top of the slide. From left to right: a dark, cratered sphere; a larger, grey, cratered sphere; a green and white planet with a prominent dark spot; a small, dark, cratered sphere; and a small, reddish-brown sphere.

Hydrostatic equilibrium

➤ In hydrostatic equilibrium

- Surfaces of constant density, pressure and potential coincide
- No shear stresses



Hydrostatic equilibrium

➤ **In** hydrostatic equilibrium



Hydrostatic equilibrium

➤ In hydrostatic equilibrium

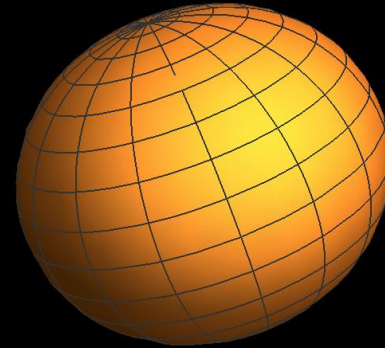
$$\rho = \rho(r), \omega$$

Hydrostatic equilibrium

➤ In hydrostatic equilibrium

$$\rho = \rho(r), \omega$$

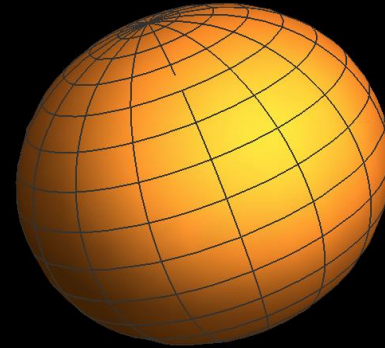
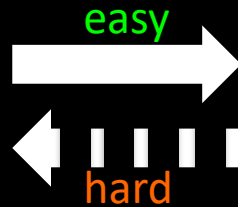
easy



Hydrostatic equilibrium

➤ In hydrostatic equilibrium

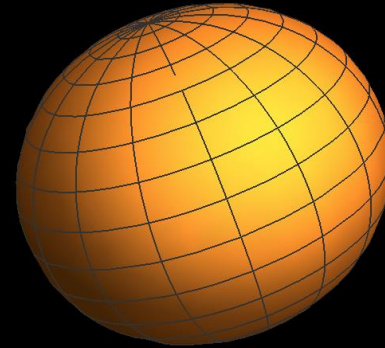
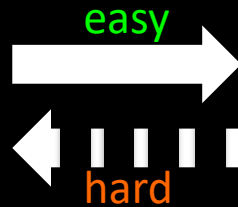
$$\rho = \rho(r), \omega$$



Hydrostatic equilibrium

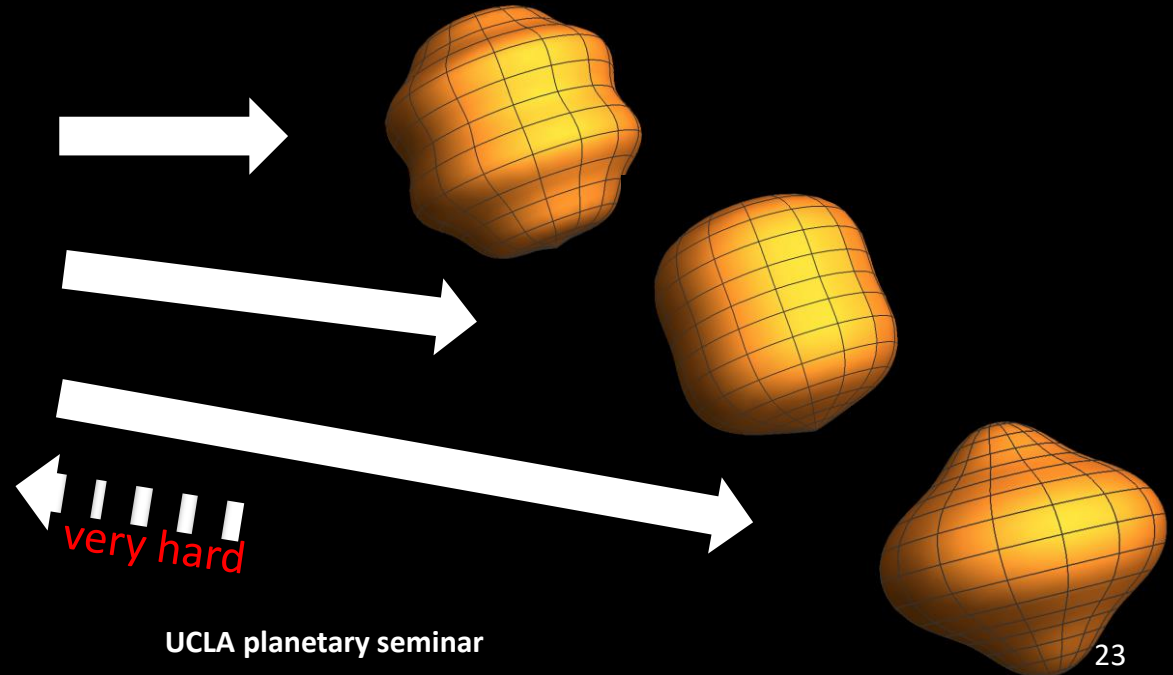
➤ **In** hydrostatic equilibrium

$$\rho = \rho(r), \omega$$



➤ **Not in** hydrostatic equilibrium

$$\rho = \rho(r), \omega$$



Spherical Harmonics

➤ Shape

$$r(f, l) = R_0 \sum_{n=1}^{\infty} \sum_{m=0}^n \left(A_{nm} \cos(m l) + B_{nm} \sin(m l) \right) P_{nm}(\sin f)$$

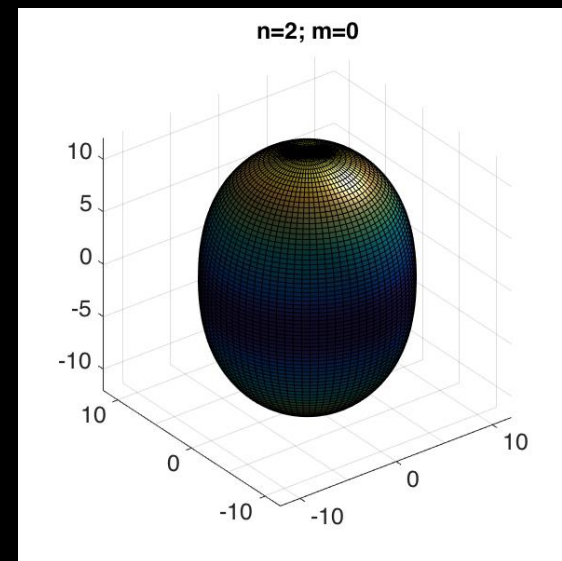
➤ Gravitational potential

$$U(r, \phi, \lambda) = \frac{GM}{R} \left[1 + \sum_{n=2}^{\infty} \sum_{m=0}^n \left(\frac{R_0}{r} \right)^n \left(C_{nm} \cos(m\lambda) + S_{nm} \sin(m\lambda) \right) P_{nm}(\sin \phi) \right]$$

➤ Power Spectral Density

$$s_n^{gg} = \sum_{m=0}^n \frac{C_{nm}^2 + S_{nm}^2}{2n+1} \quad \text{gravity}$$

$$s_n^{tt} = \sum_{m=0}^n \frac{A_{nm}^2 + B_{nm}^2}{2n+1} \quad \text{topography}$$



Spherical Harmonics

➤ Shape

$$r(\phi, \lambda) = R_0 \sum_{n=1}^{\infty} \sum_{m=0}^n \left(A_{nm} \cos(m\lambda) + B_{nm} \sin(m\lambda) \right) P_{nm}(\sin \phi)$$

➤ Gravitational potential

$$U(r, \phi, \lambda) = \frac{GM}{R} \left[1 + \sum_{n=2}^{\infty} \sum_{m=0}^n \left(\frac{R_0}{r} \right)^n \left(C_{nm} \cos(m\lambda) + S_{nm} \sin(m\lambda) \right) P_{nm}(\sin \phi) \right]$$

U – gravitational potential

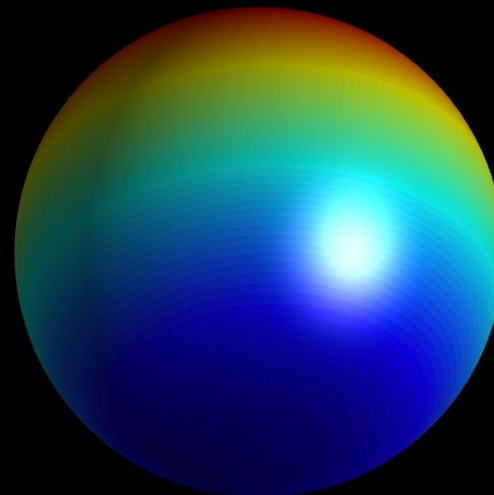
ϕ – latitude

λ – longitude

r – radial distance

n – degree

m – order



Spherical Harmonics

➤ Shape

$$r(\phi, \lambda) = R_0 \sum_{n=1}^{\infty} \sum_{m=0}^n (A_{nm} \cos(m\lambda) + B_{nm} \sin(m\lambda)) P_{nm}(\sin \phi)$$

➤ Gravitational potential

$$U(r, \phi, \lambda) = \frac{GM}{R} \left[1 + \sum_{n=2}^{\infty} \sum_{m=0}^n \left(\frac{R_0}{r} \right)^n (C_{nm} \cos(m\lambda) + S_{nm} \sin(m\lambda)) P_{nm}(\sin \phi) \right]$$

U – gravitational potential

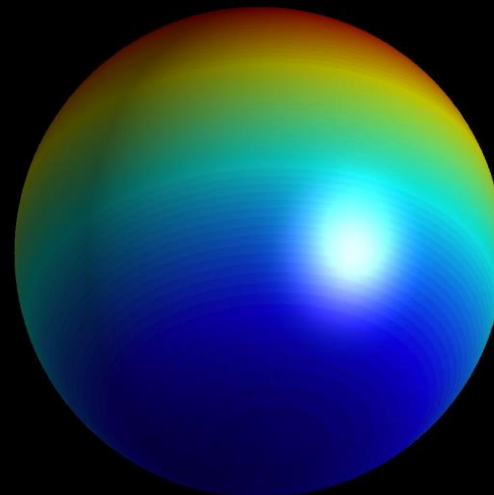
ϕ – latitude

λ – longitude

r – radial distance

n – degree

m – order





Admittance

Z_n - gravity-topography admittance

$$Z_n = \frac{\text{gravity}}{\text{topography}} \quad \text{for a given wavelength}$$



Admittance

Z_n - gravity-topography admittance

$$Z_n = \frac{\text{gravity}}{\text{topography}} \quad \text{for a given wavelength}$$

➤ Linear two-layer hydrostatic model

$$Z_n = \frac{GM}{R^3} \frac{3(n+1)}{2n+1} \frac{r_{crust}}{r_{mean}}$$



Admittance

Z_n - gravity-topography admittance

$$Z_n = \frac{\text{gravity}}{\text{topography}} \quad \text{for a given wavelength}$$

➤ Linear two-layer hydrostatic model

$$Z_n = \frac{GM}{R^3} \frac{3(n+1)}{2n+1} \frac{r_{crust}}{r_{mean}}$$

➤ Linear two-layer isostatic model

$$Z_n = \frac{GM}{R^3} \frac{3(n+1)}{2n+1} \frac{r_{crust}}{r_{mean}} \left(1 - \frac{\rho_c}{\rho_m} \right) - \frac{D_{comp}}{R} \frac{\ddot{u}_n}{u_n}$$

A decorative header featuring several celestial bodies: a dark, cratered sphere on the far left; a large, cratered sphere in the top center; a green and white planet with a prominent dark spot on the top right; a small dark sphere next to it; and a reddish-brown sphere on the far right.

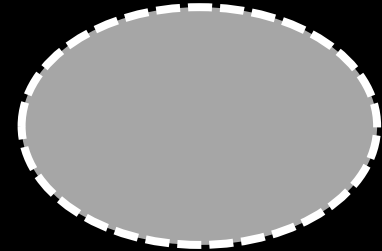
Gravity anomalies

- Free-air anomaly

$$\sigma_{\text{FA}} = \sigma_{\text{obs}} - \sigma_{\text{model}}$$

$$\sigma_{\text{model}} =$$

gravity of
hydrostatic figure





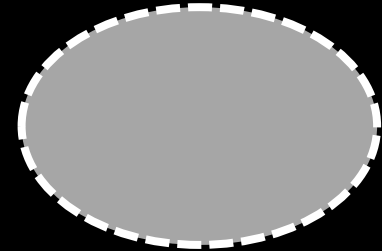
Gravity anomalies

- Free-air anomaly

$$\sigma_{\text{FA}} = \sigma_{\text{obs}} - \sigma_{\text{model}}$$

$$\sigma_{\text{model}} =$$

gravity of
hydrostatic figure

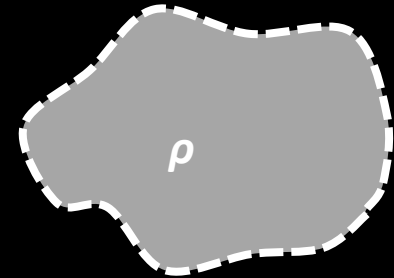


- Bouguer anomaly

$$\sigma_{\text{BA}} = \sigma_{\text{obs}} - \sigma_{\text{model}}$$

$$\sigma_{\text{model}} =$$

gravity of shape
assuming ρ



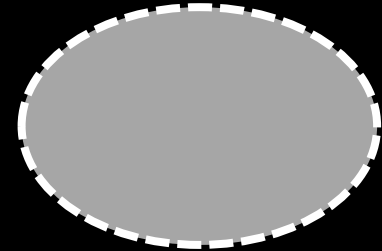


Gravity anomalies

- Free-air anomaly

$$\sigma_{\text{FA}} = \sigma_{\text{obs}} - \sigma_{\text{model}}$$

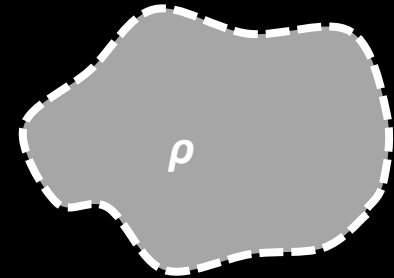
$\sigma_{\text{model}} =$ gravity of
hydrostatic figure



- Bouguer anomaly

$$\sigma_{\text{BA}} = \sigma_{\text{obs}} - \sigma_{\text{model}}$$

$\sigma_{\text{model}} =$ gravity of shape
assuming ρ

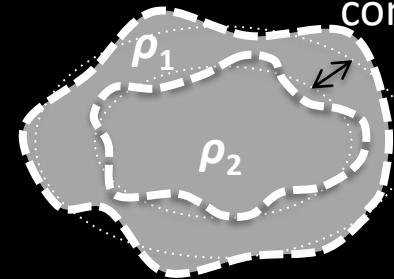


- Isostatic anomaly

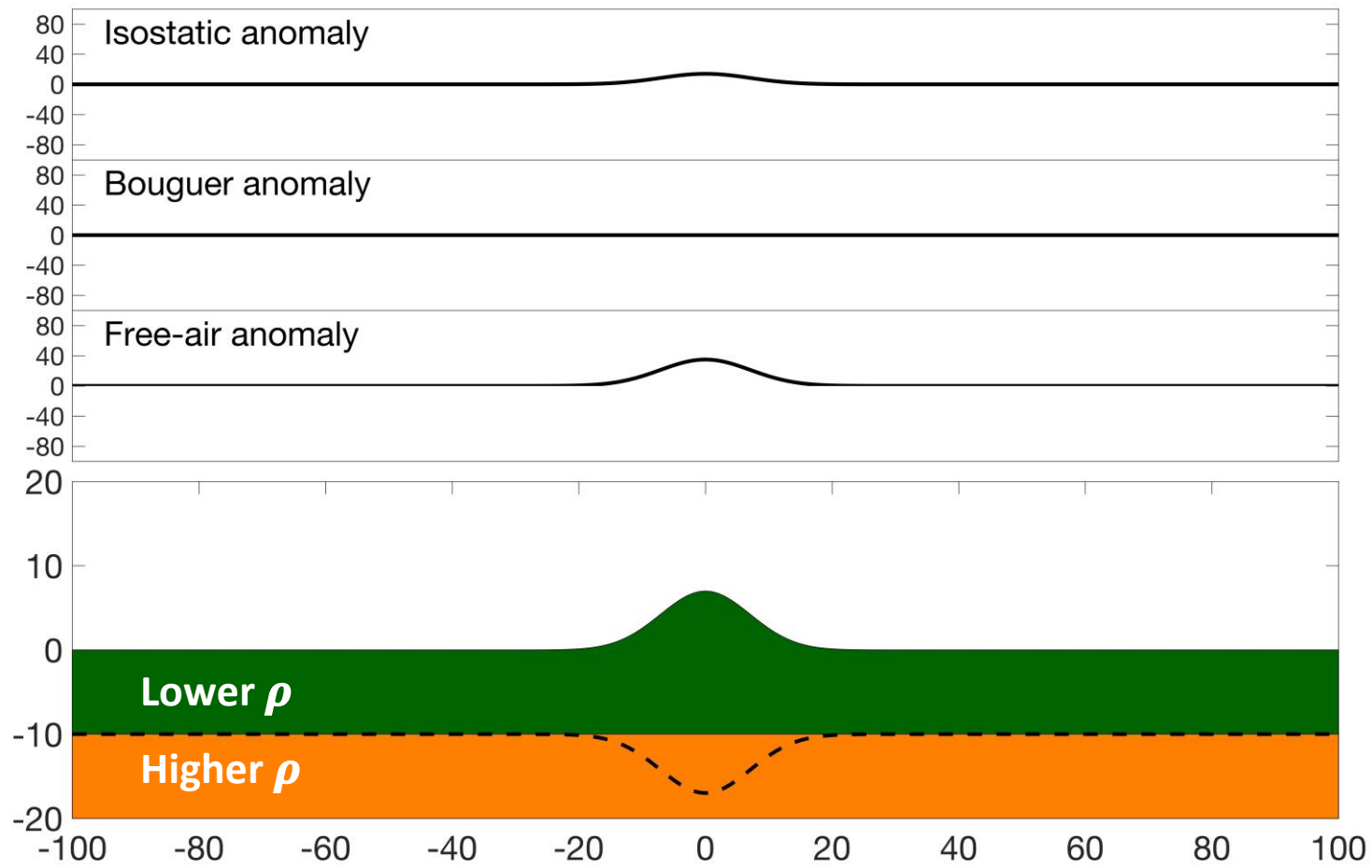
$$\sigma_{\text{IA}} = \sigma_{\text{obs}} - \sigma_{\text{model}}$$

h – depth of
compensation

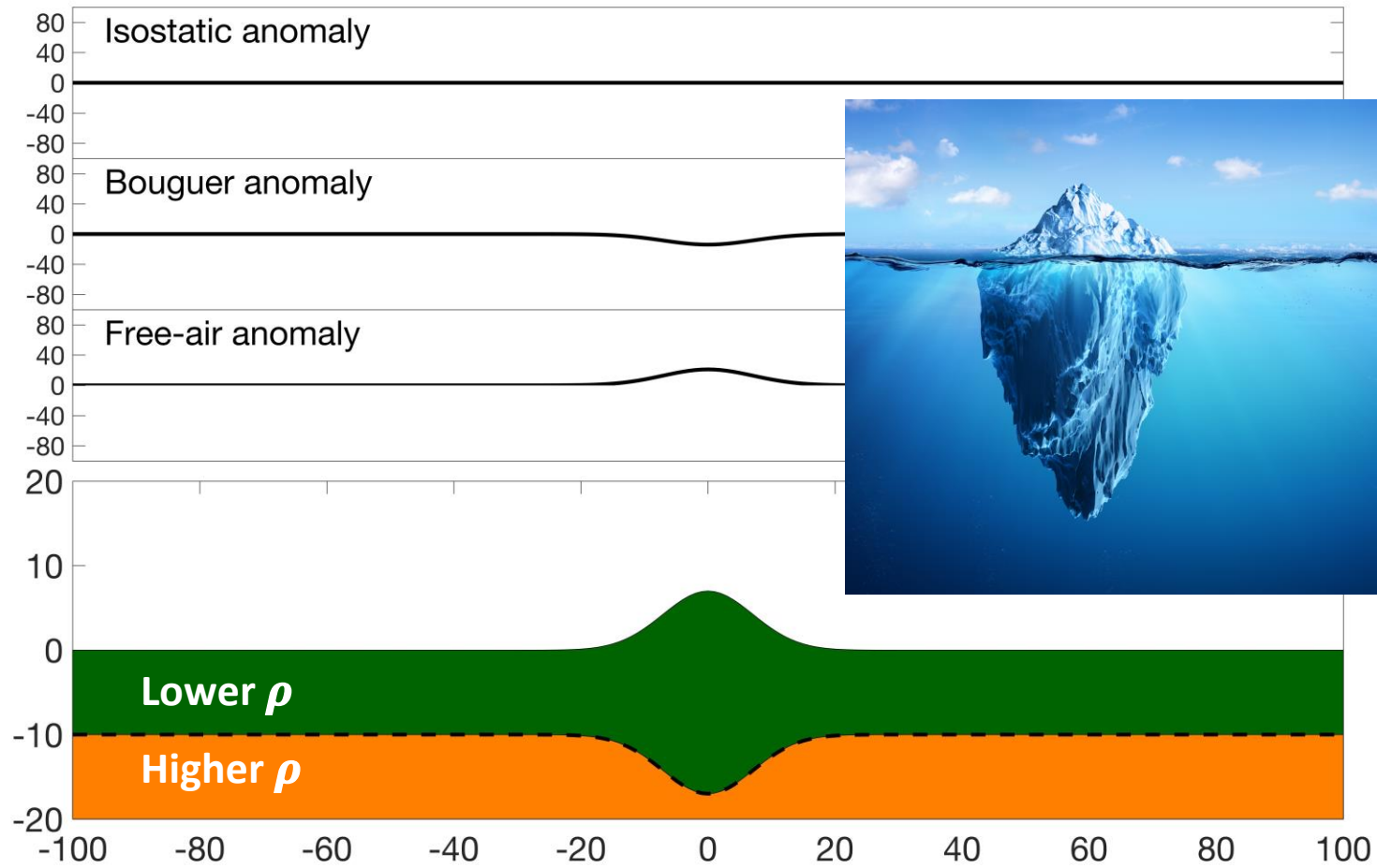
$\sigma_{\text{model}} =$ gravity assuming
isostasy for ρ_1, ρ_2, h



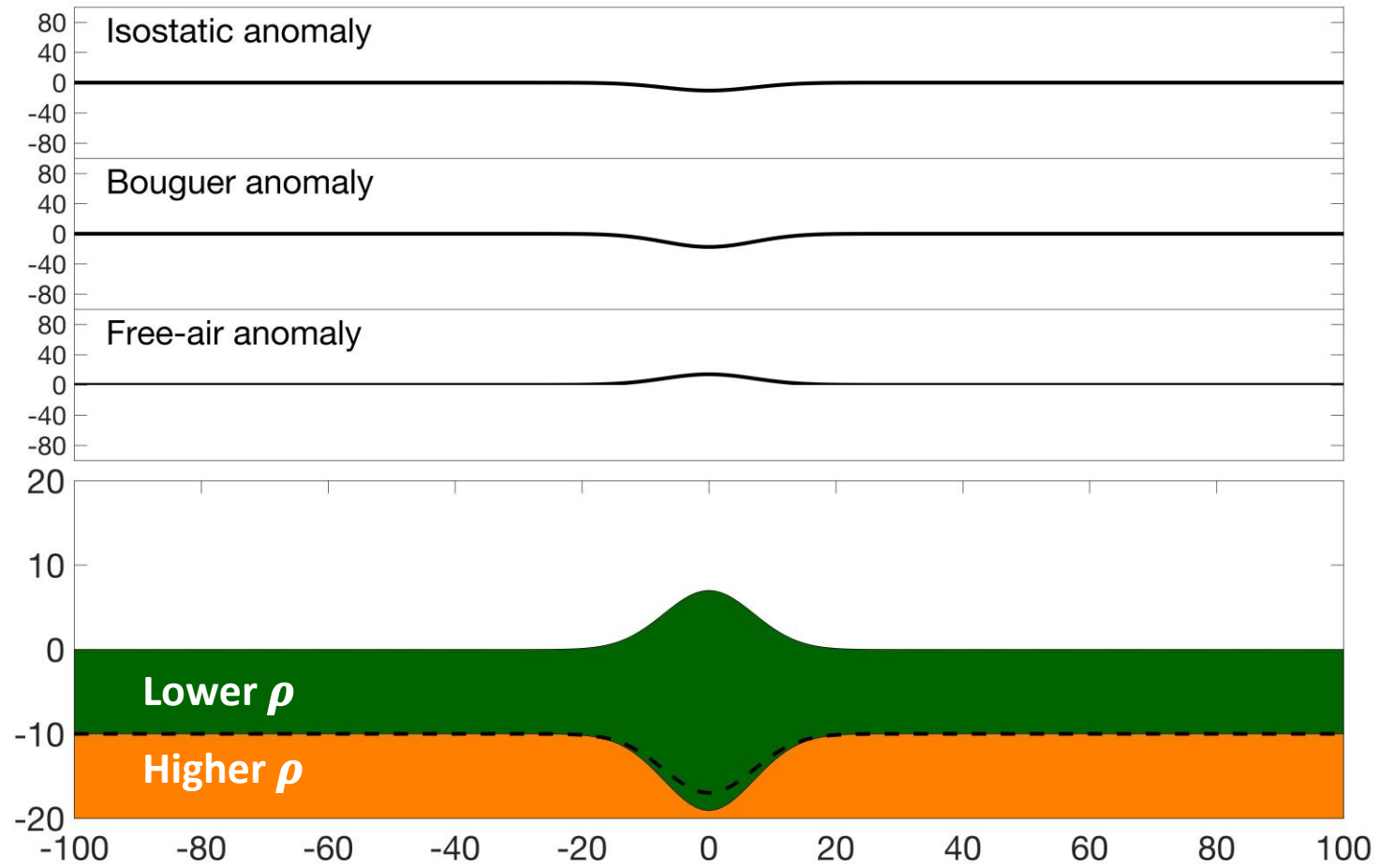
Example: uncompensated topography



Example: compensated topography



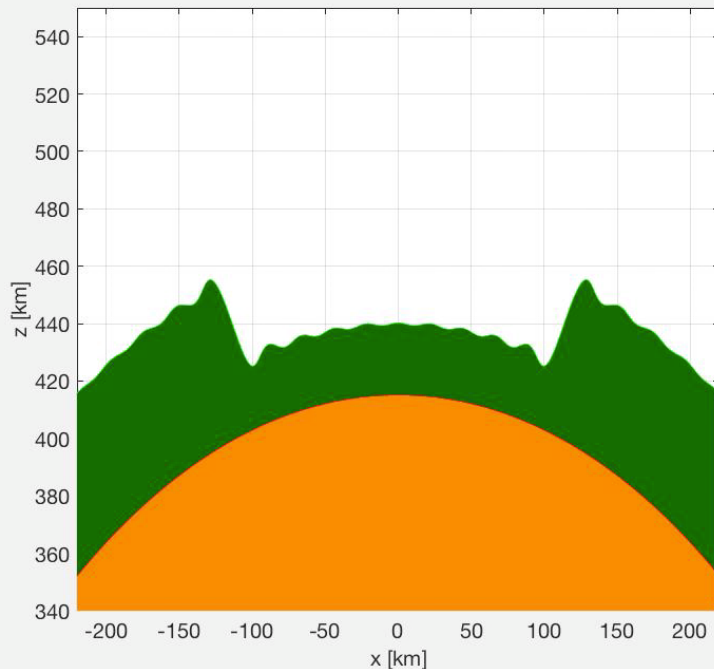
Example: supercompensated topography



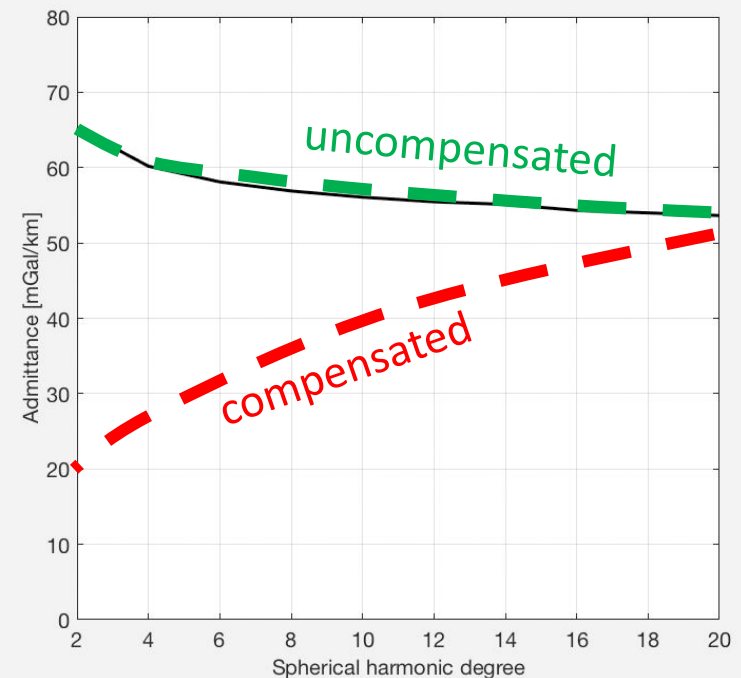
Isostatic compensation

➤ Example of a spherical cap (depression) relaxation

Interface evolution

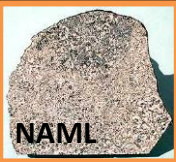


Admittance evolution



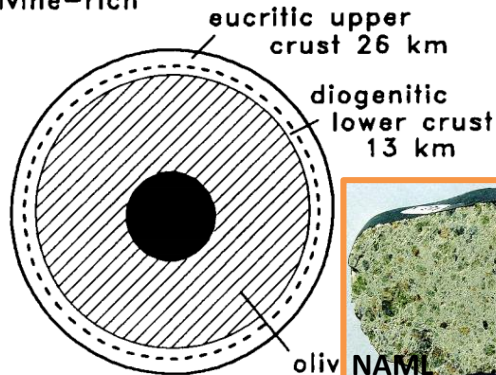
What did we know before Dawn?

Vesta



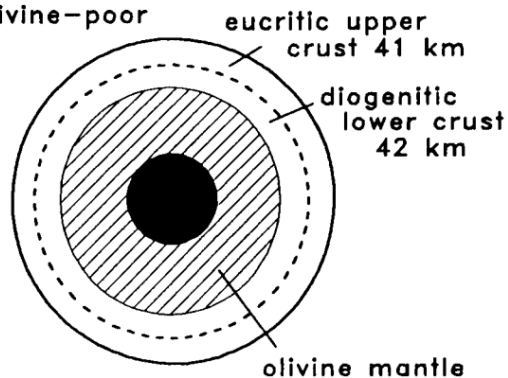
Vesta

olivine-rich



Vesta

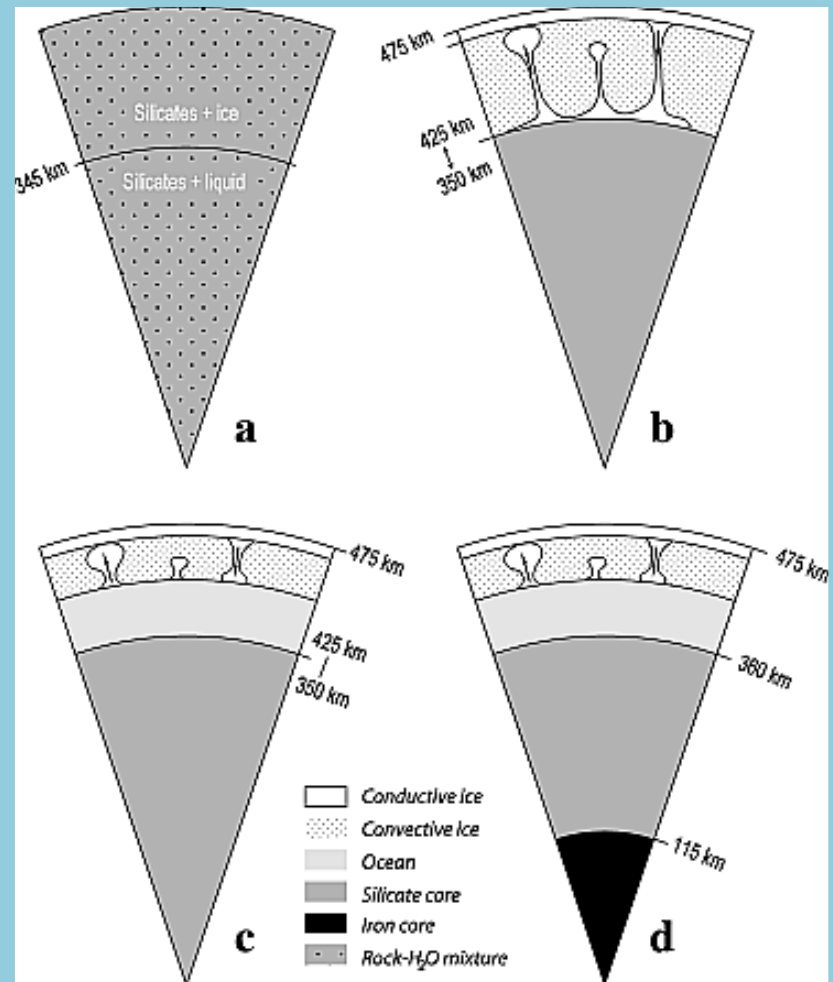
olivine-poor



core mass = 5%
core radius = 75 km
asteroid radius = 265 km

Ruzicka et al., 1997

Ceres



McCord and Sotin, 2005

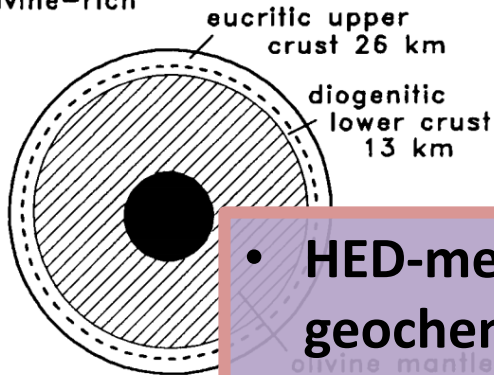
What did we know before Dawn?

Vesta

Ceres

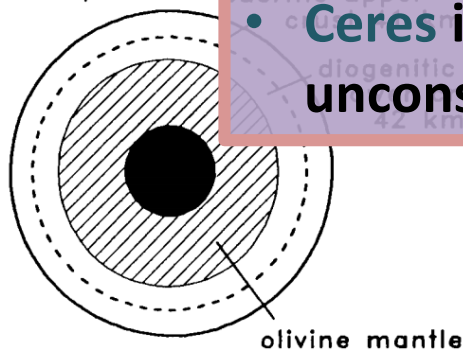
Vesta

olivine-rich



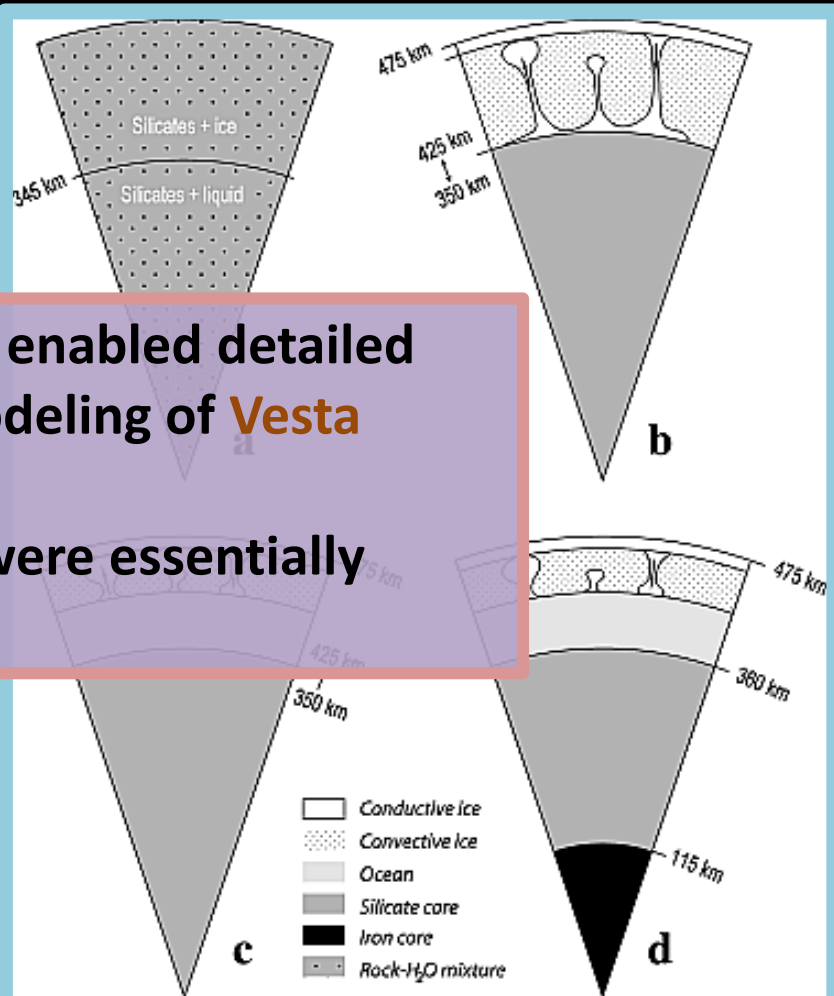
Vesta

olivine-poor



core mass = 5%
core radius = 75 km
asteroid radius = 265 km

- HED-meteorites enabled detailed geochemical modeling of **Vesta**
- **Ceres** interiors were essentially unconstrained



Ruzicka et al., 1997

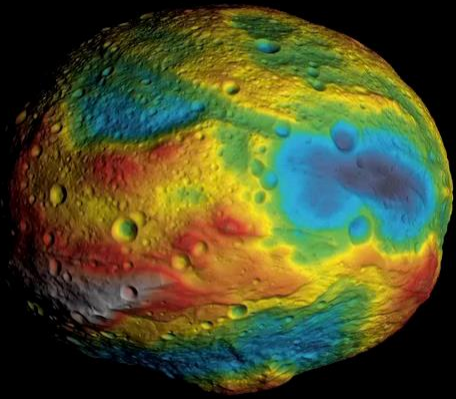
McCord and Sotin, 2005



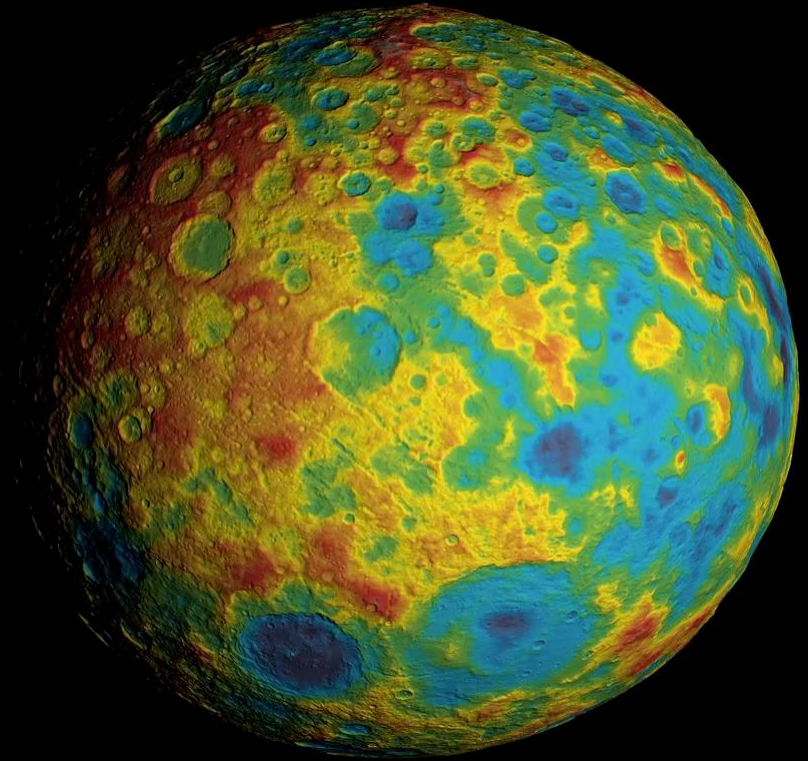
Dawn geophysical data

- Shape model
 - Stereophotogrammetry (SPG) from DLR
 - Stereophotoclinometry (SPC) from JPL
 - Mutually consistent with the accuracy much better than the spatial resolution of gravity field
- Gravity field
 - Accurate up to $n = 18$ ($\lambda=93$ km) for **Vesta** (Konopliv et al., 2014)
 - Accurate up to $n = 17$ ($\lambda=174$ km) for **Ceres** (Konopliv et al., 2017)
- Assumptions we have to make:
 - Multilayer model with uniform density layers
 - Range of core densities for **Vesta**
 - Range of crustal densities from HEDs for **Vesta**
 - Can't really assume anything for **Ceres**

Vesta and Ceres



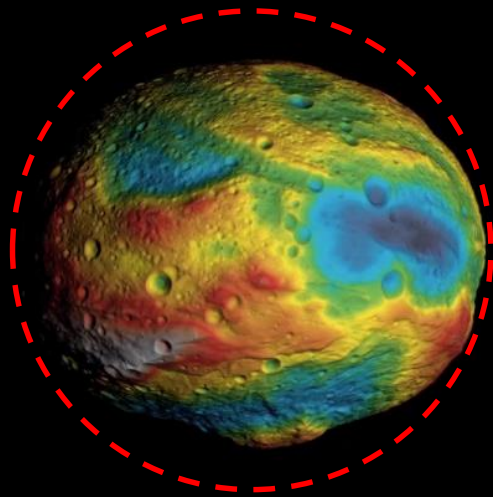
Gaskell, 2012



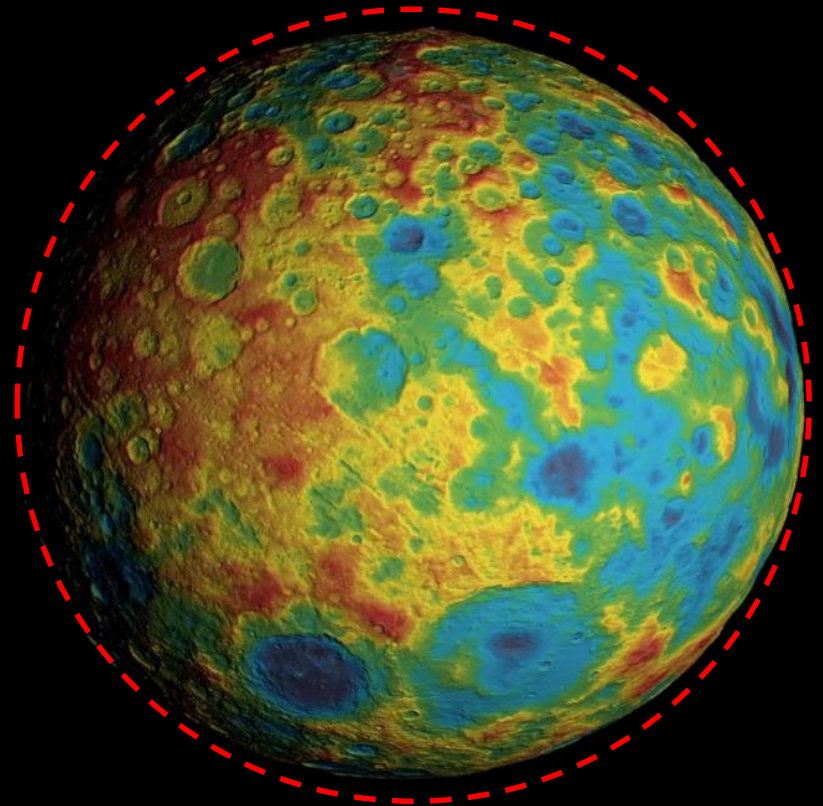
Park et al., 2016



Vesta and Ceres



Gaskell, 2012



Park et al., 2016

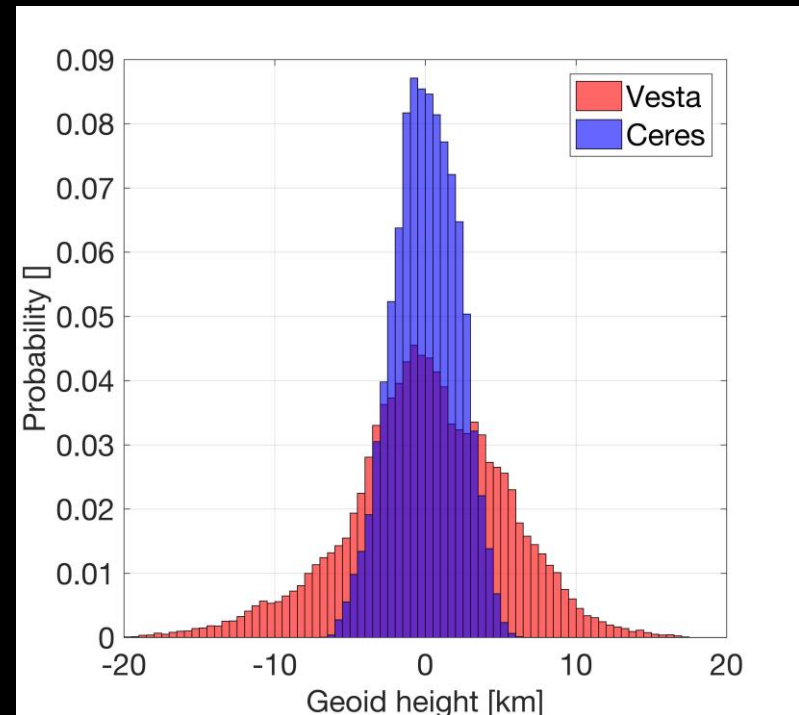
Vesta and Ceres topography

Shape statistics

Parameter	Vesta	Ceres
Equatorial flattening	0.0262	0.0043
Geoidal height range (km)	37.9	13.2
Geoidal height RMS (km)	5.2	2.1

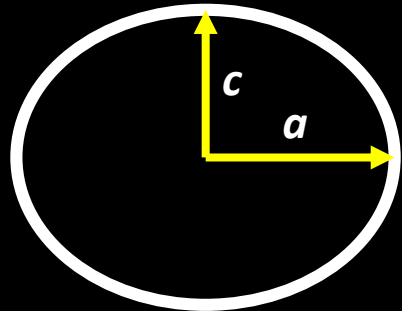
- Ceres is closer to hydrostatic equilibrium than Vesta
- Smoother topography at Ceres

Hypsograms of Vesta and Ceres

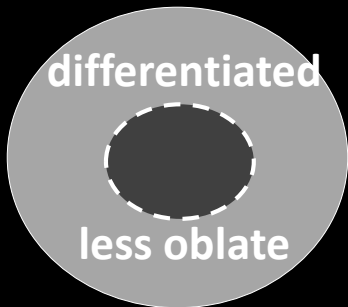


**Hypsogram is a fancy word for the “histogram of elevations”*

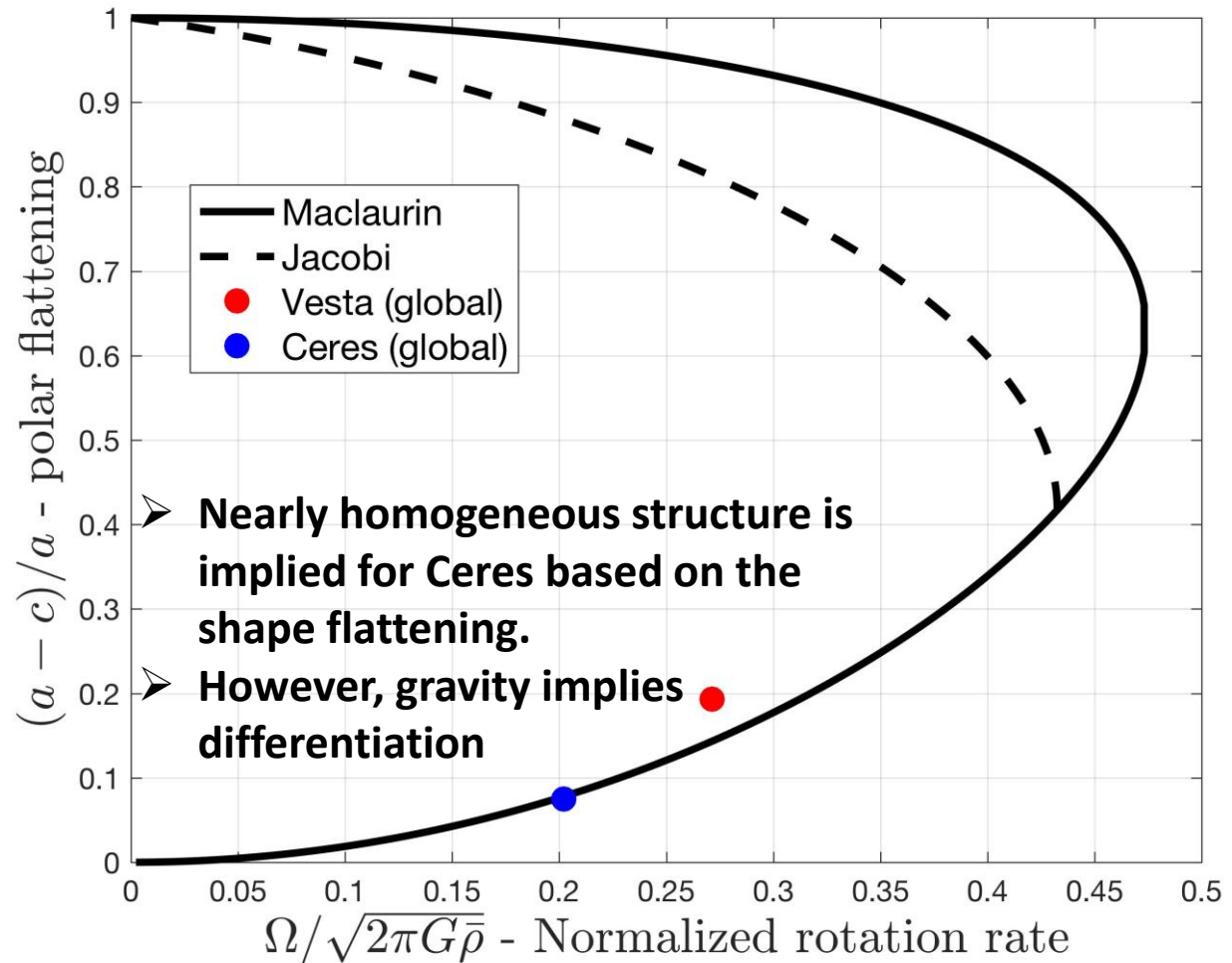
Flattening vs rotation rate



homogeneous
more oblate



differentiated
less oblate

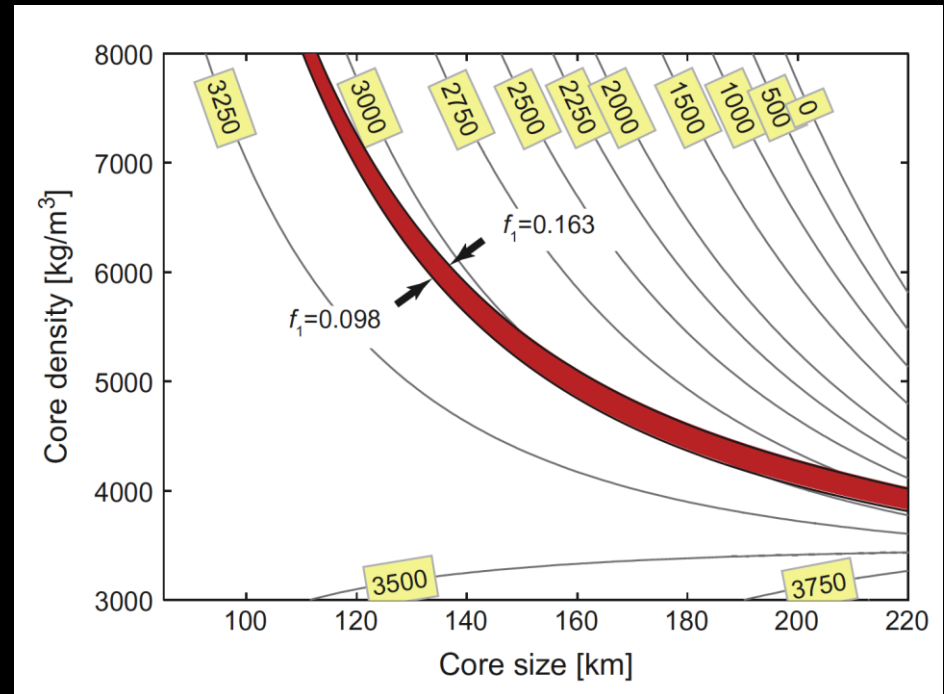




Vesta Internal Structure

- Vesta is not presently in hydrostatic equilibrium
- No unique solution only from gravity/topography, need an extra constraint
- Geochemically motivated 3-layer interior structure (Ruzicka et al., 1997)
- Densities constrained by the Howardite-Eucrite-Diogenite (HED) meteorites

Contours are mantle density [kg/m^3]



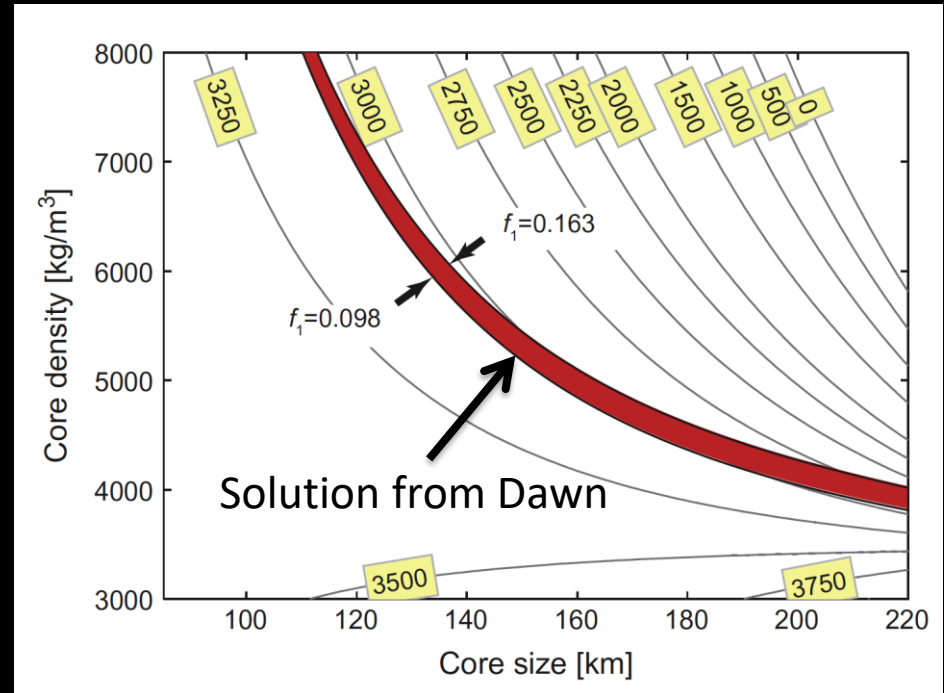
Ermakov et al., 2014



Vesta Internal Structure

- Vesta is not presently in hydrostatic equilibrium
- No unique solution **only** from gravity/topography, need an extra constraint
- Geochemically motivated 3-layer interior structure (Ruzicka et al., 1997)
- Densities constrained by the Howardite-Eucrite-Diogenite (HED) meteorites

Contours are mantle density [kg/m^3]



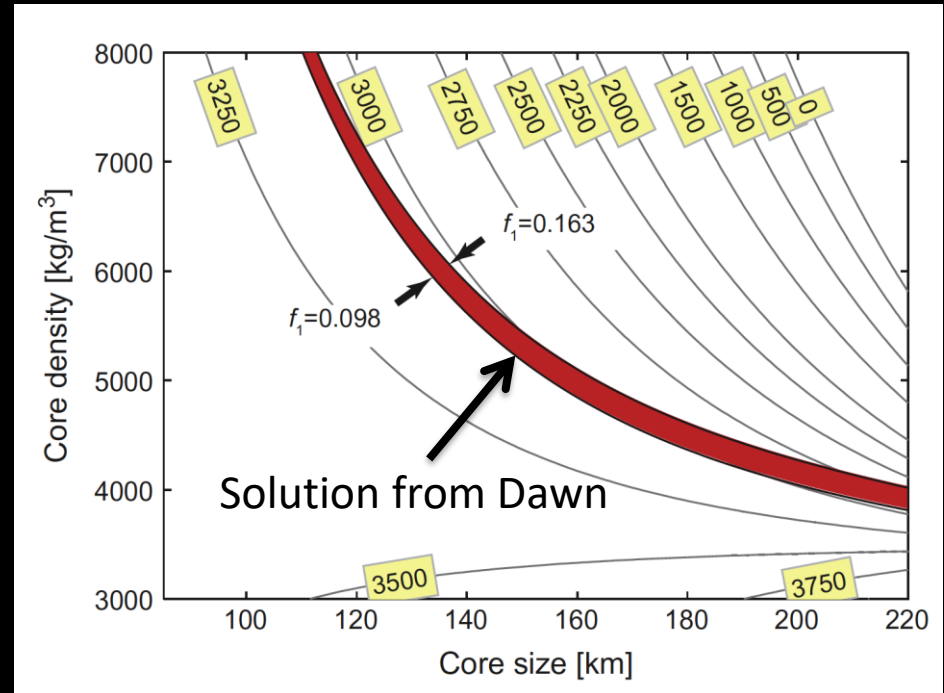
Ermakov et al., 2014



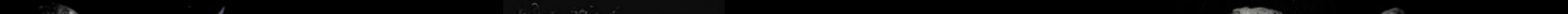
Vesta Internal Structure

- Vesta is not presently in hydrostatic equilibrium
- No unique solution **only** from gravity/topography, need an extra constraint
- Geochemically motivated 3-layer interior structure (Ruzicka et al., 1997)
- Densities constrained by the Howardite-Eucrite-Diogenite (HED) meteorites

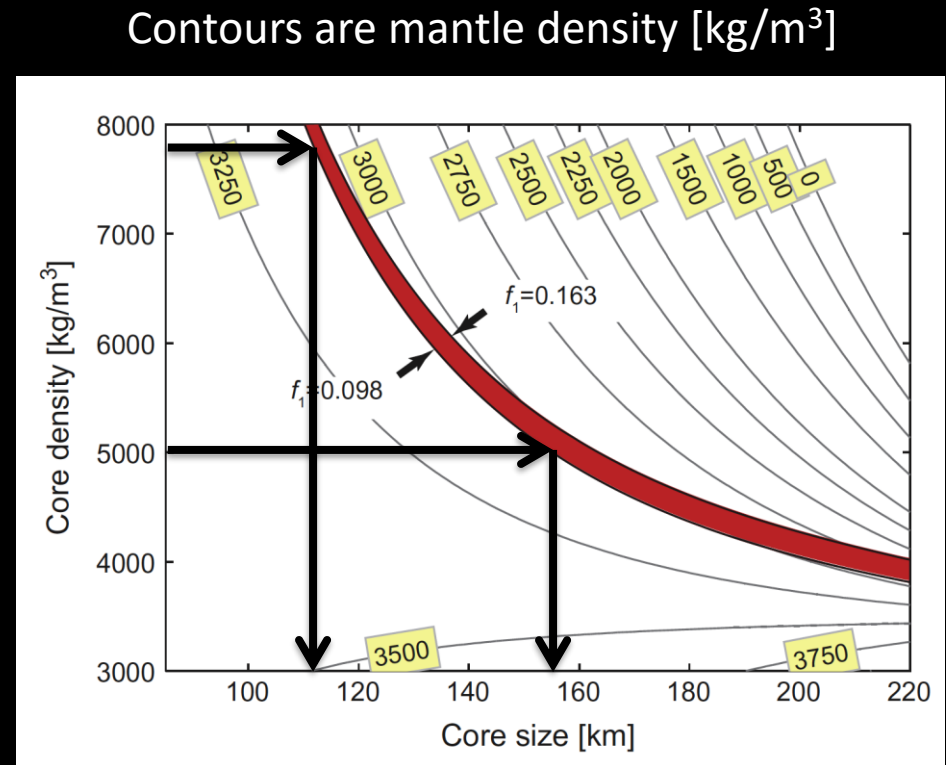
Contours are mantle density [kg/m^3]



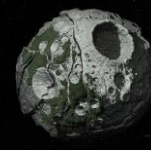
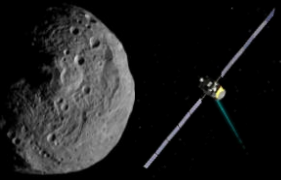
Ermakov et al., 2014



- Vesta is not presently in hydrostatic equilibrium
- No unique solution **only** from gravity/topography, need an extra constraint
- Geochemically motivated 3-layer interior structure (Ruzicka et al., 1997)
- Densities constrained by the Howardite-Eucrite-Diogenite (HED) meteorites



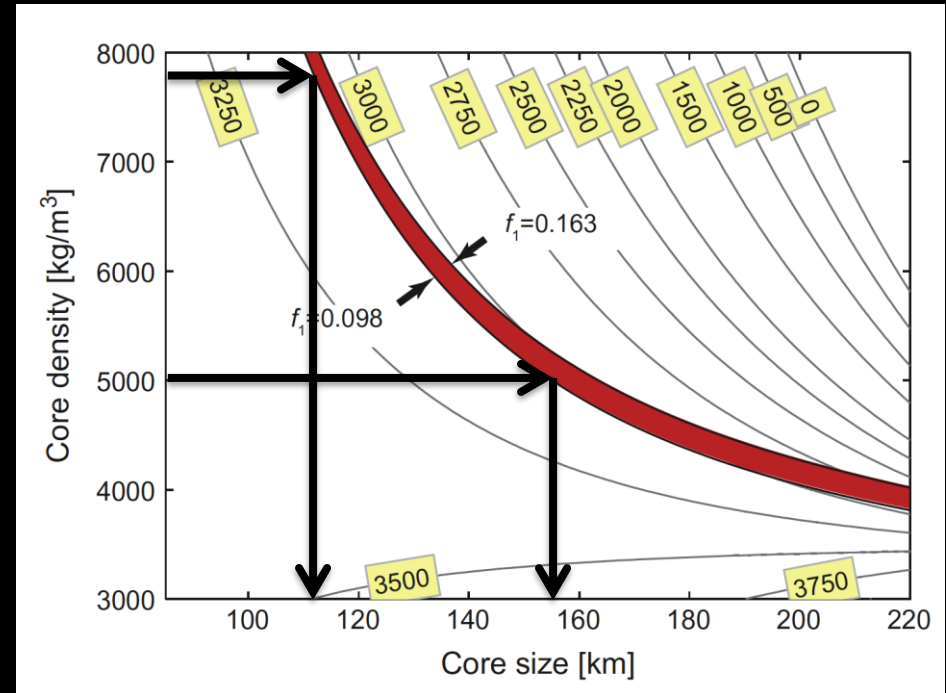
Ermakov et al., 2014



Vesta Internal Structure

- Vesta is not presently in hydrostatic equilibrium
- No unique solution **only** from gravity/topography, need an extra constraint
- Geochemically motivated 3-layer interior structure (Ruzicka et al., 1997)
- Densities constrained by the Howardite-Eucrite-Diogenite (HED) meteorites

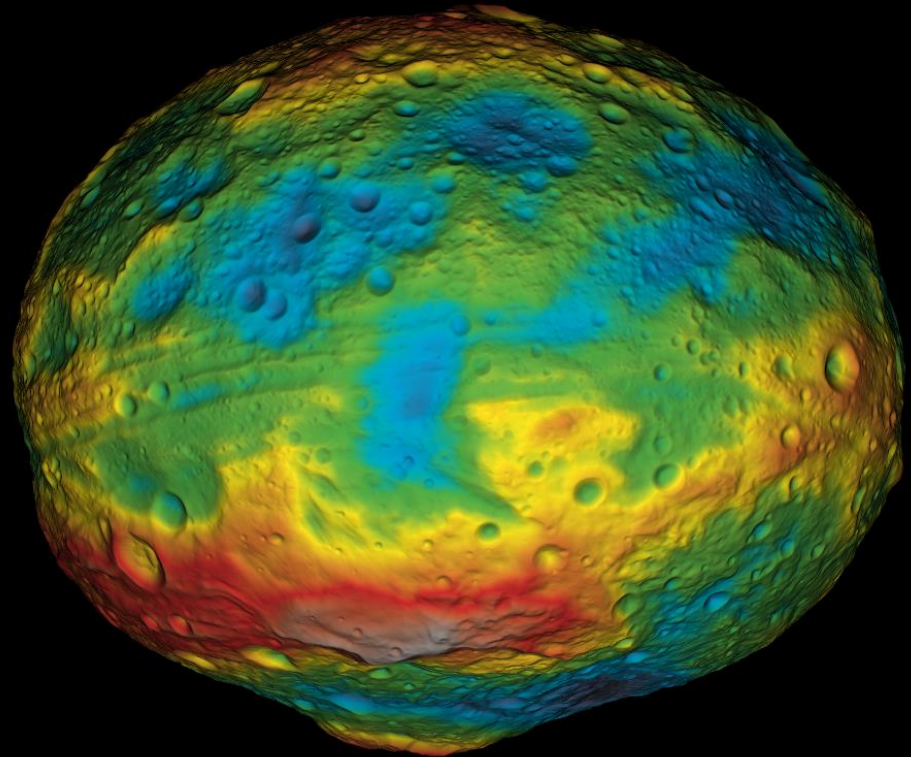
Contours are mantle density [kg/m^3]



Core radius of 110 to 155 km
Ermakov et al., 2014

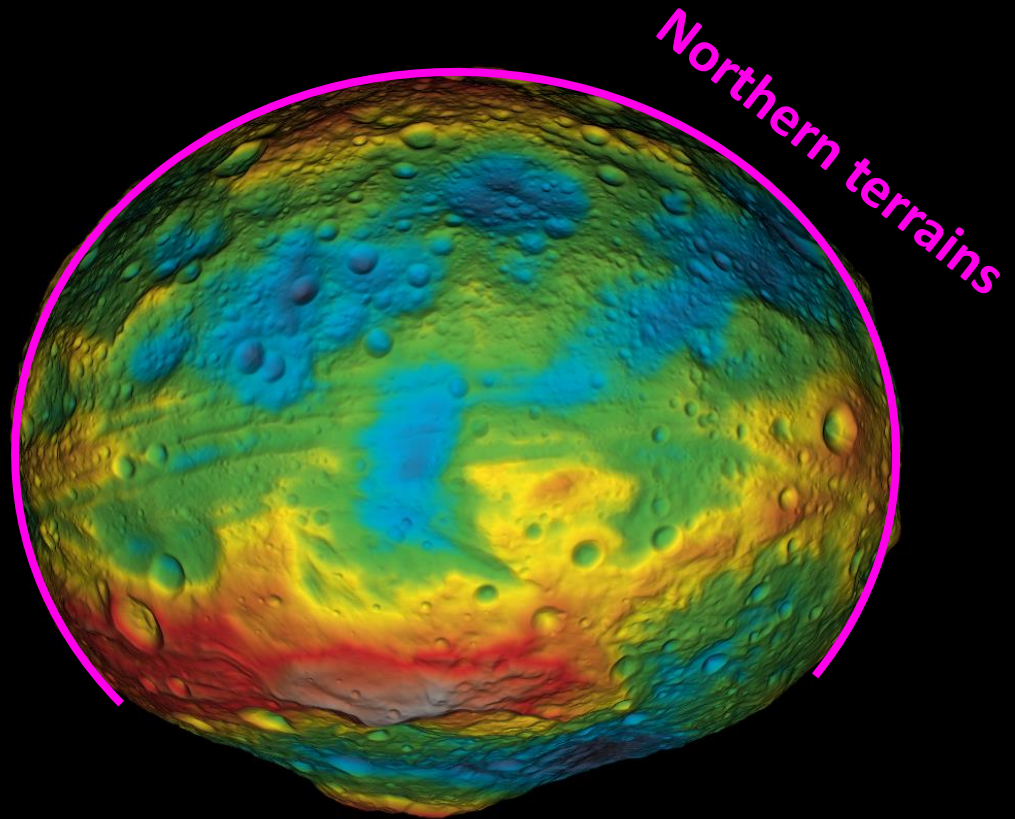
Early efficient viscous relaxation of Vesta

- Vesta was likely close to hydrostatic equilibrium in its early history (Fu et al., 2014).
- Vesta's northern terrains likely reflect its pre-impact equilibrium shape.
- Major impact occurred when Vesta was effectively non-relaxing leading to uncompensated Rheasilvia and Veneneia basins.



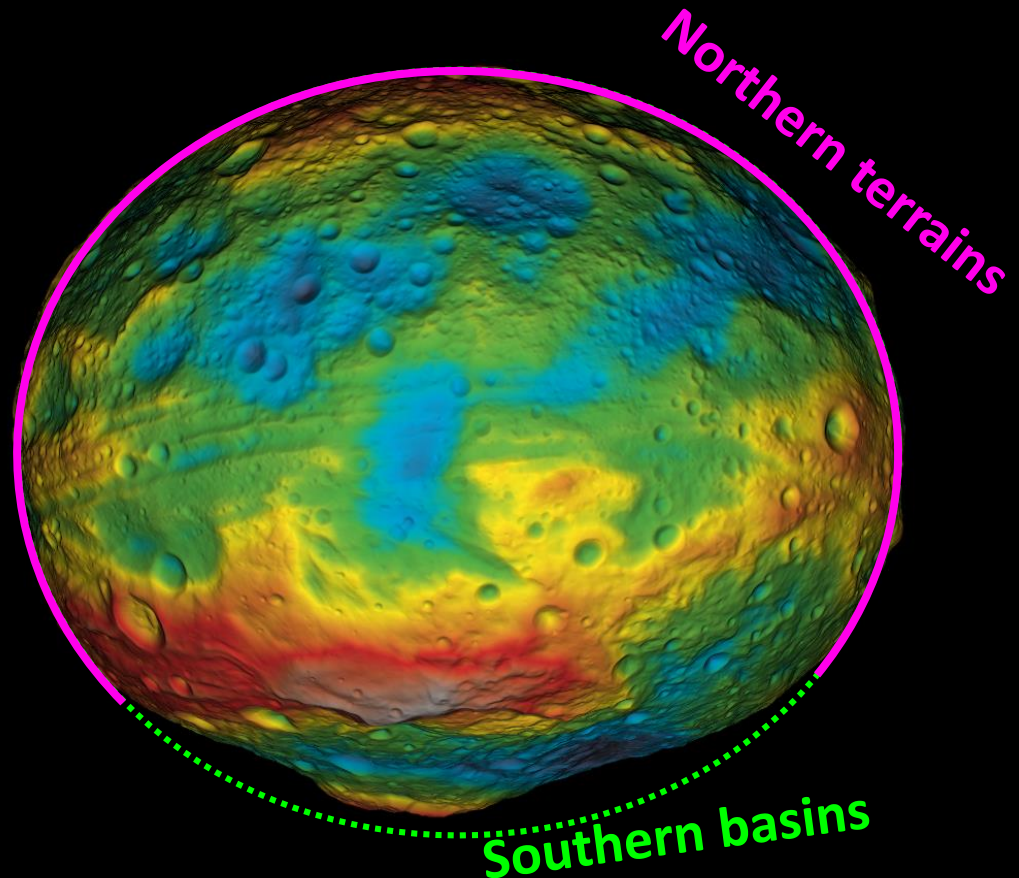
Early efficient viscous relaxation of Vesta

- Vesta was likely close to hydrostatic equilibrium in its early history (Fu et al., 2014).
- Vesta's northern terrains likely reflect its pre-impact equilibrium shape.
- Major impact occurred when Vesta was effectively non-relaxing leading to uncompensated Rheasilvia and Veneneia basins.

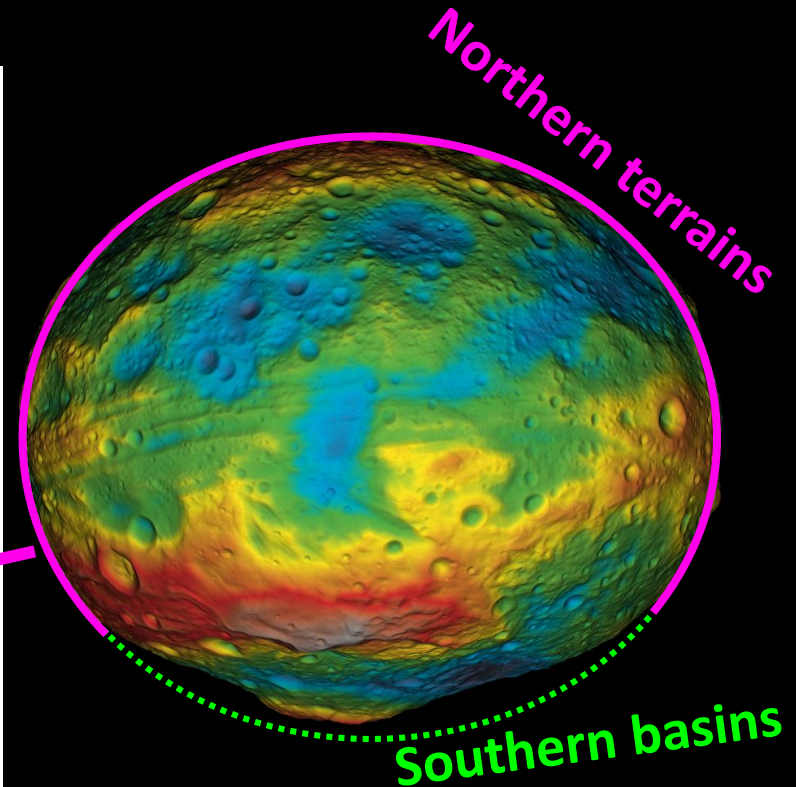
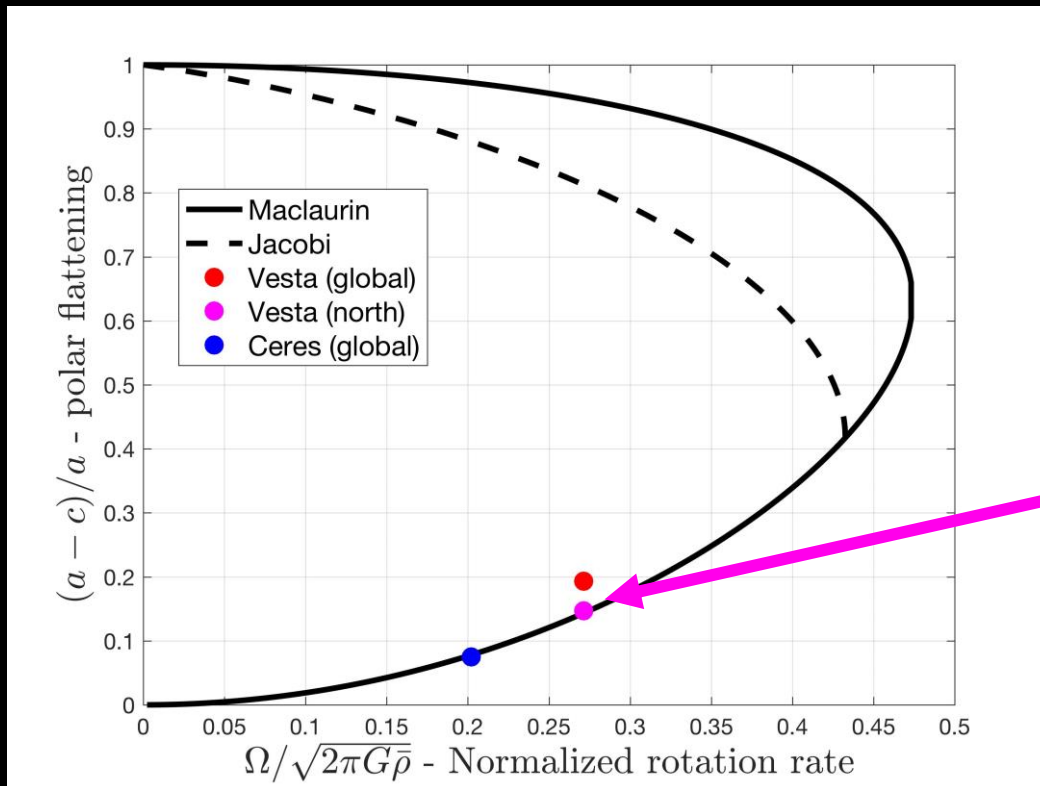


Early efficient viscous relaxation of Vesta

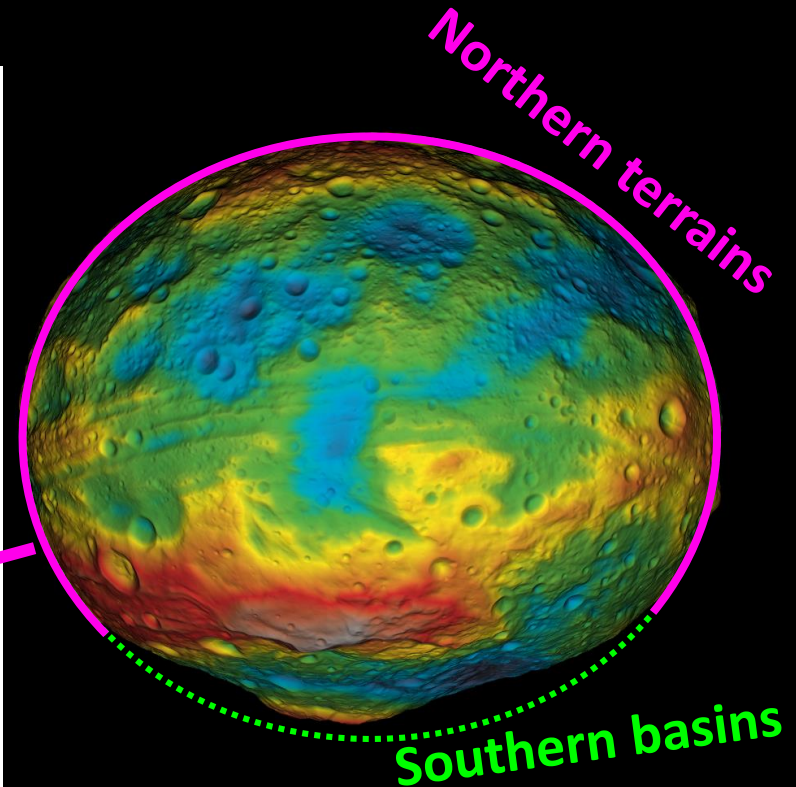
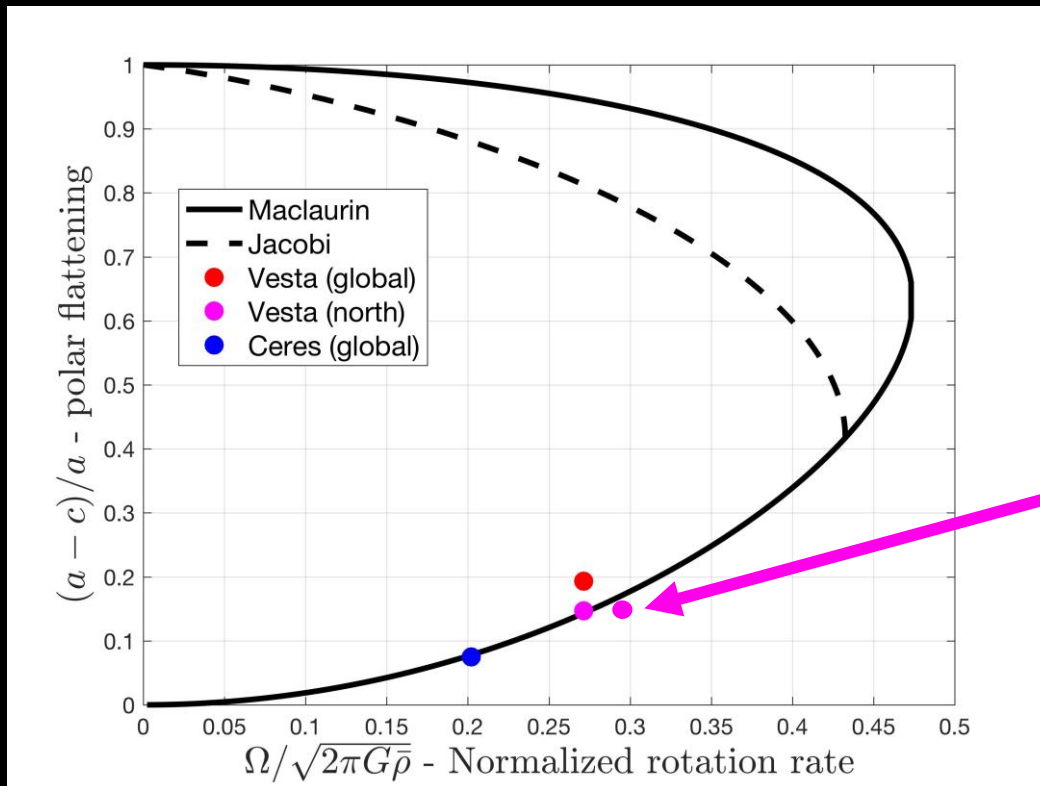
- Vesta was likely close to hydrostatic equilibrium in its early history (Fu et al., 2014).
- Vesta's northern terrains likely reflect its pre-impact equilibrium shape.
- Major impact occurred when Vesta was effectively non-relaxing leading to uncompensated Rheasilvia and Veneneia basins.



Early efficient viscous relaxation of Vesta

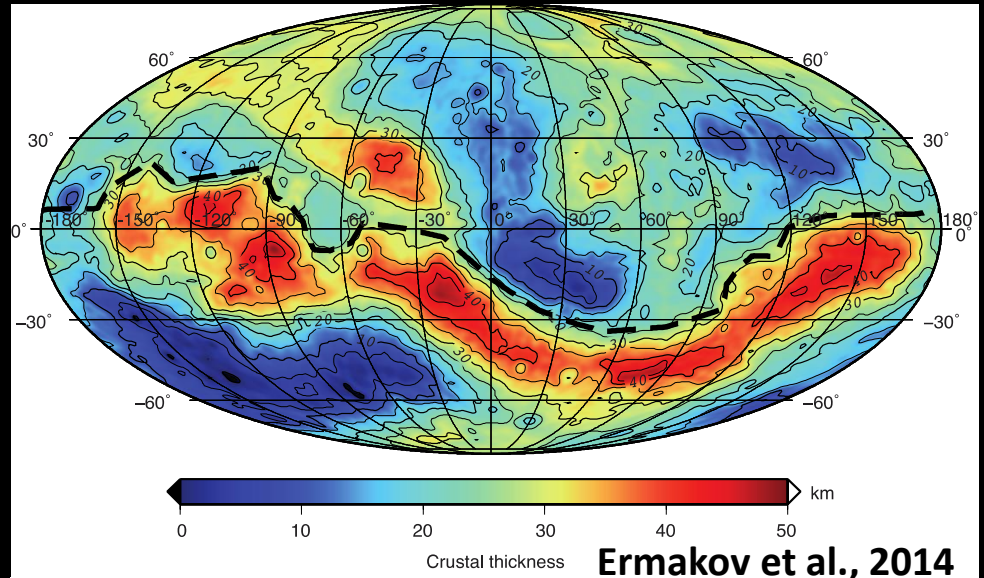


Early efficient viscous relaxation of Vesta

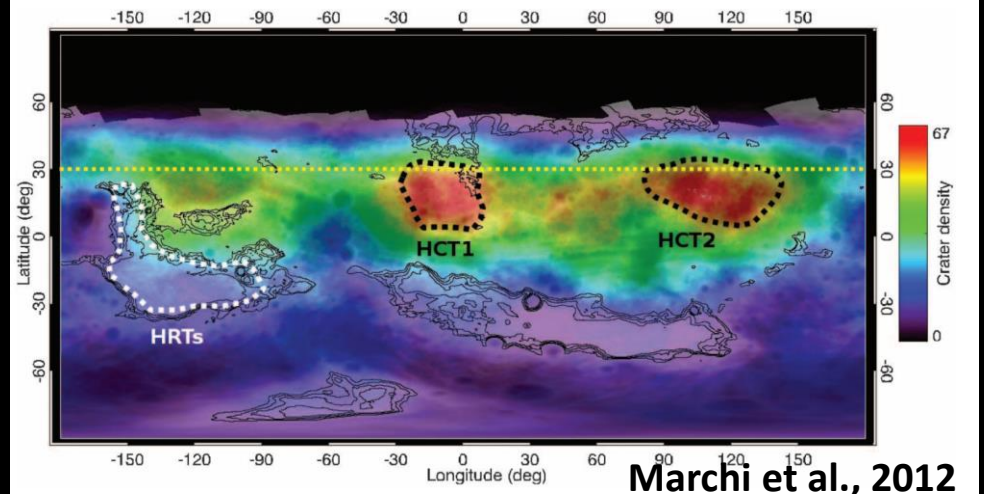


Vesta Crustal Thickness

- Crustal thickness inversion show a belt of thicker crust around the Southern Basins



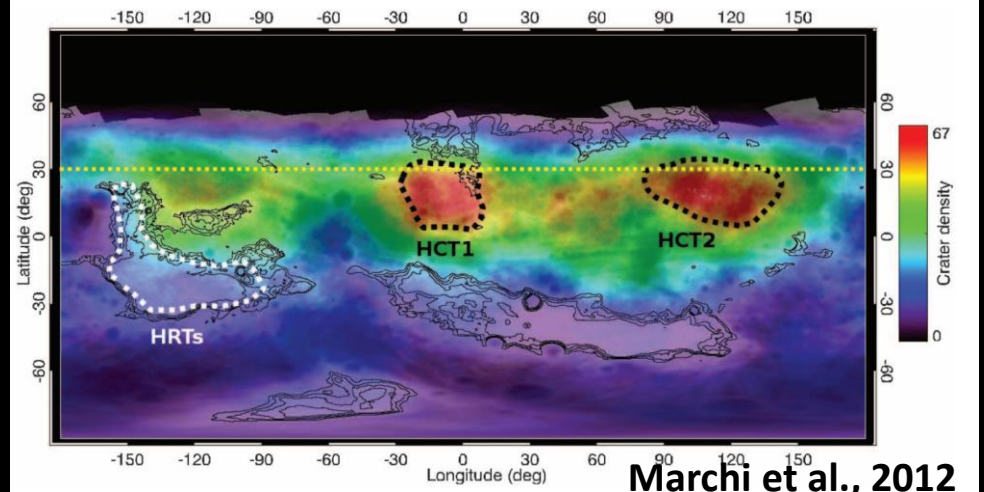
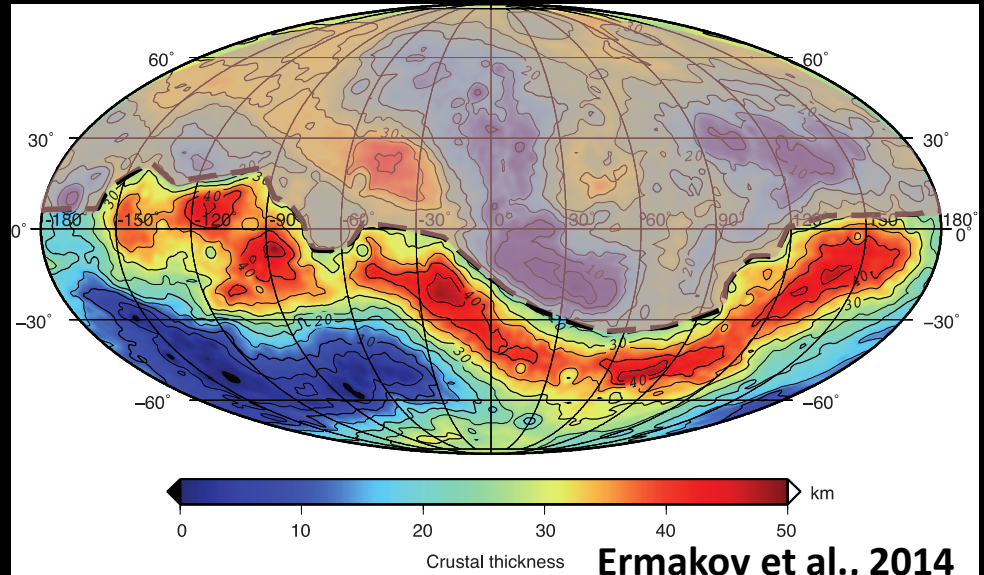
- Crater counting reveals that the northern Vesta terrains are old (>3Gy)



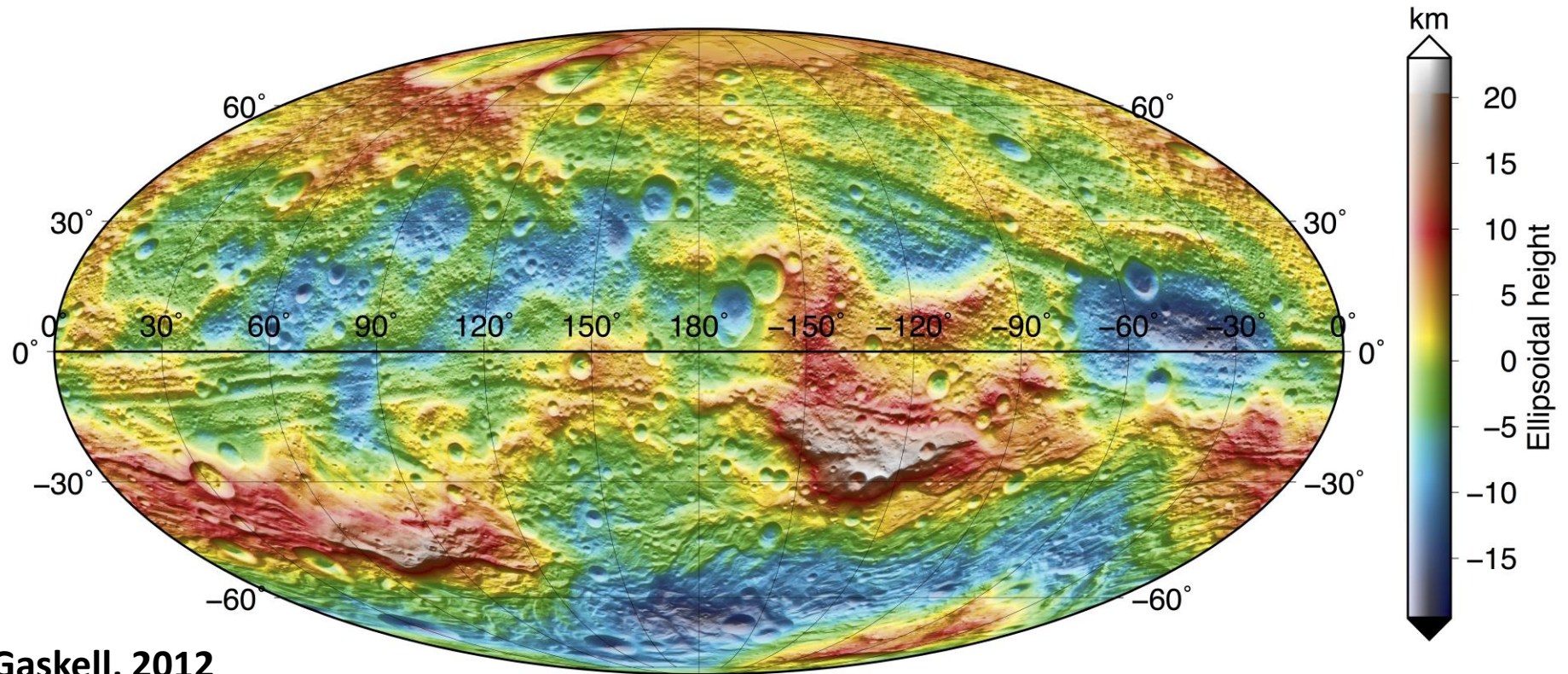
Vesta Crustal Thickness

- Crustal thickness inversion show a belt of thicker crust around the Southern Basins

- Crater counting reveals that the northern Vesta terrains are old ($>3\text{Gy}$)

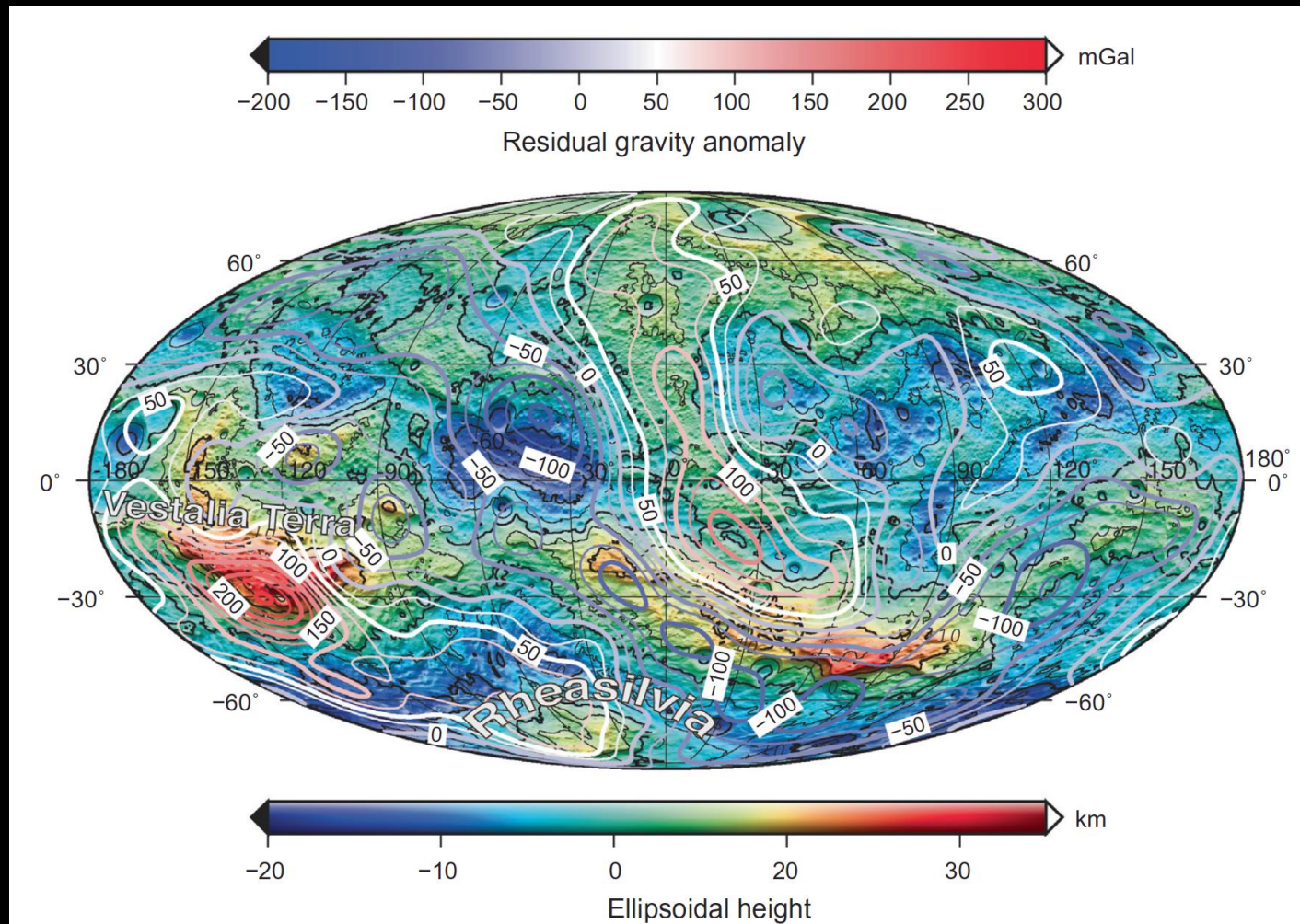


Local structures on Vesta



Ermakov et al., 2014

Vesta Bouguer Anomaly



Ermakov et al., 2014

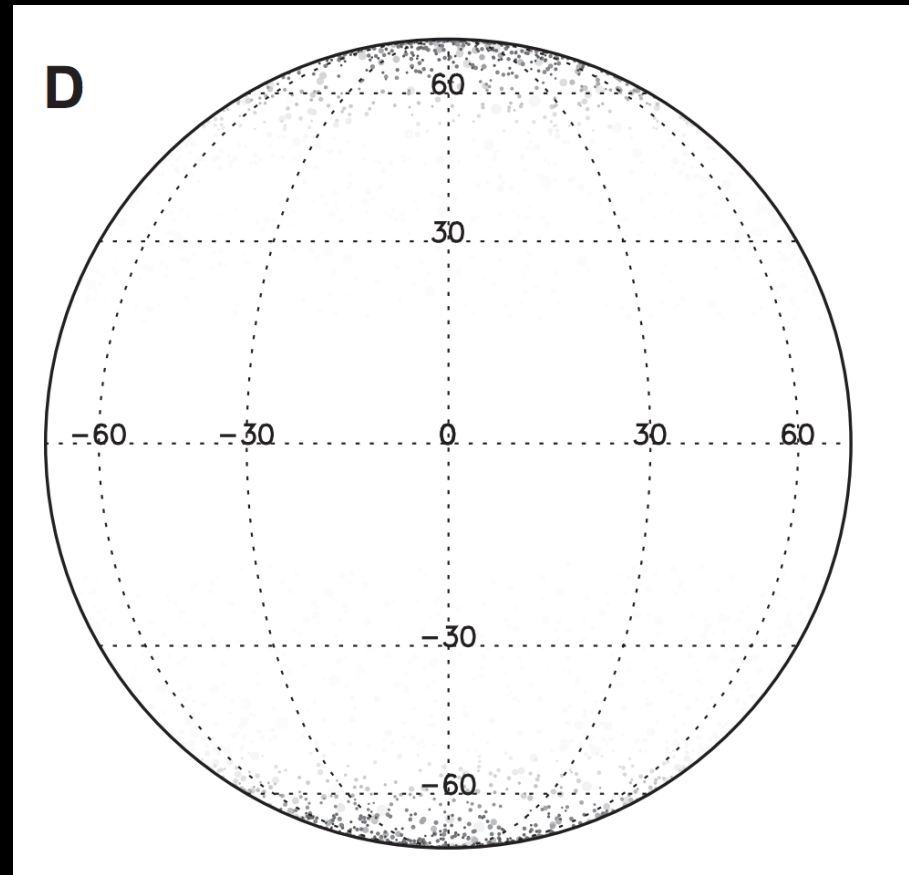
Summary on Vesta



- Formed early (< 5 My after CAI)
- Once hot and hydrostatic, **Vesta** is no longer either
- Differentiated interior
- Most of topography acquired when **Vesta** was already cool => uncompensated topography
- Combination of gravity/topography data with meteoritic geochemistry data provides constraints on the internal structure

Ceres Expectations

- Bland et al., 2013 predicted that craters on Ceres would quickly relax in an ice-dominated shell
 - Equatorial warmer craters would relax faster than colder polar craters
- Bland et al., 2016 did not find evidence for such relaxation pattern
 - No latitude dependence of crater depth

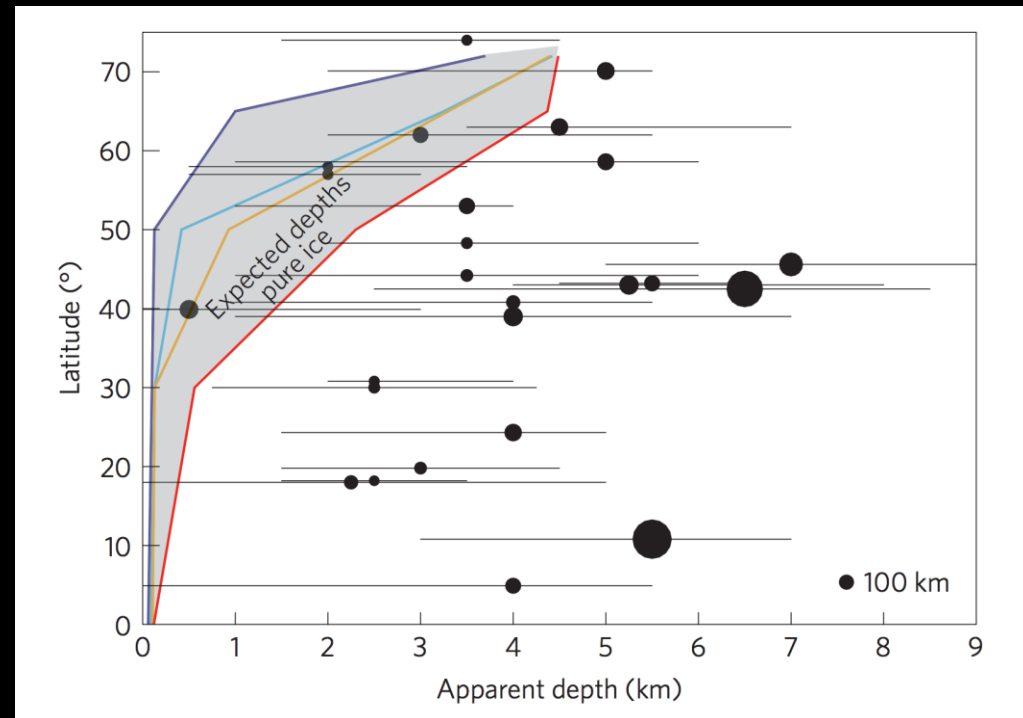


Bland, 2013

Ceres observation

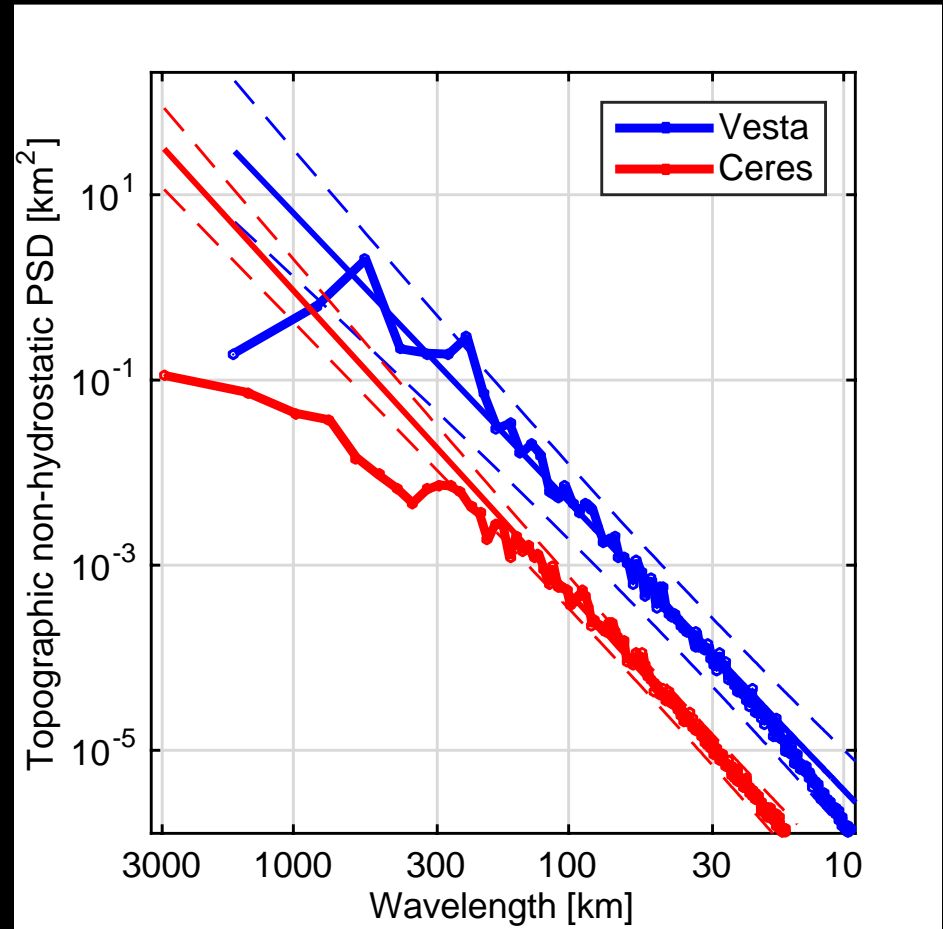
- Bland et al., 2013 predicted that craters on Ceres would quickly relax in an ice-dominated shell
 - Equatorial warmer craters would relax faster than colder polar craters
- Bland et al., 2016 did not find evidence for such relaxation pattern
 - No latitude dependence of crater depth

Crater depth study



Evidence for viscous relaxation

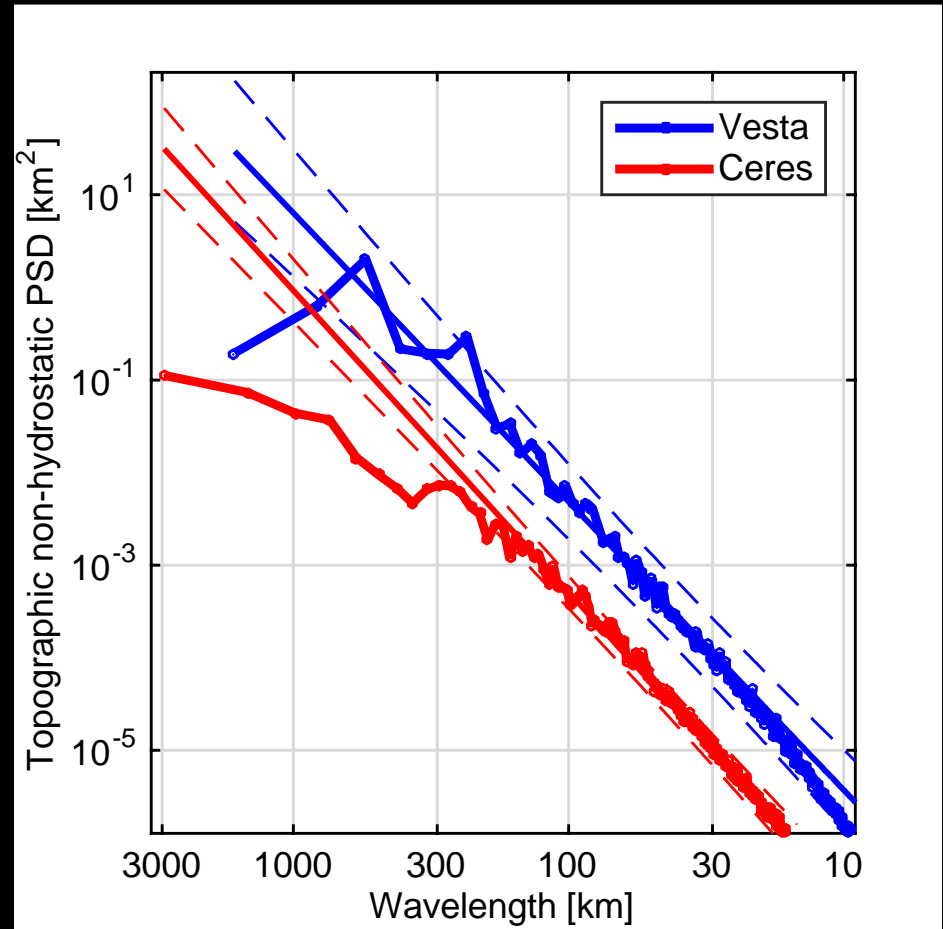
- **More general approach:**
study topography power spectrum
- Power spectra for Vesta closely fits with the power law to the lowest degrees ($\lambda < 750$ km)
- Ceres power spectrum deviates from the power law at $\lambda > 270$ km



Ermakov et al., 2017

Evidence for viscous relaxation

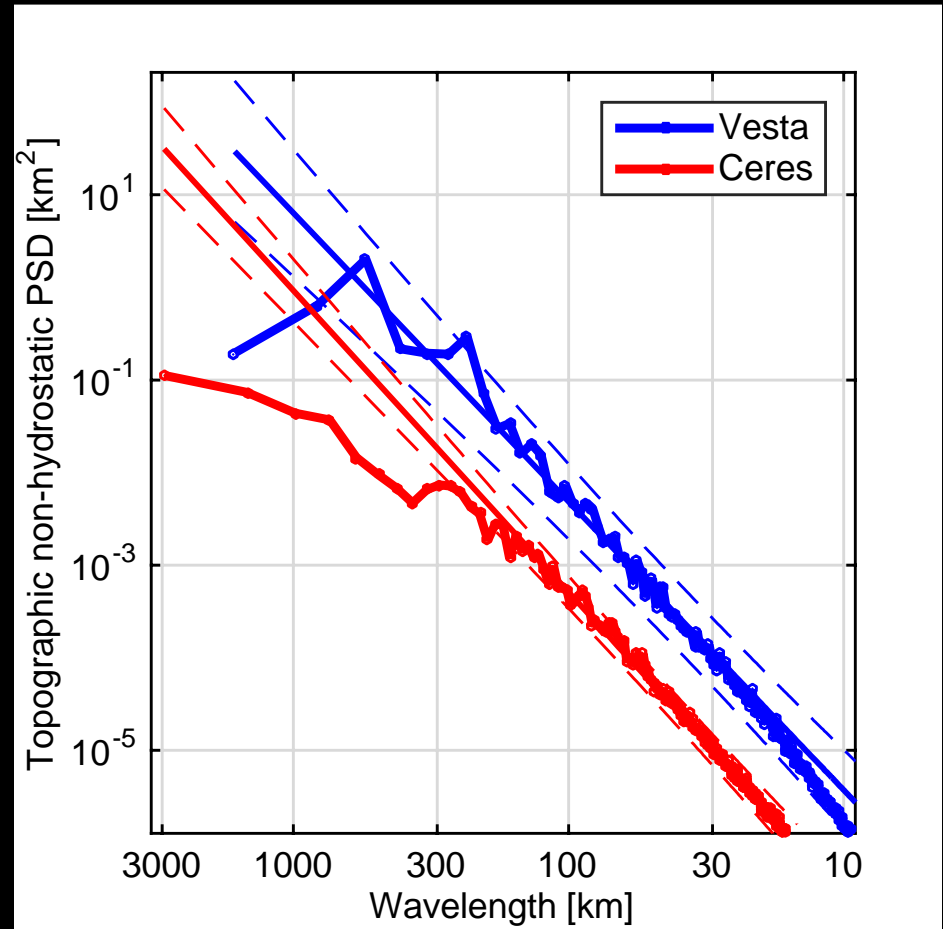
- More general approach: study topography power spectrum
- Power spectra for Vesta closely fits with the power law to the lowest degrees ($\lambda < 750$ km)
- Ceres power spectrum deviates from the power law at $\lambda > 270$ km



Ermakov et al., 2017

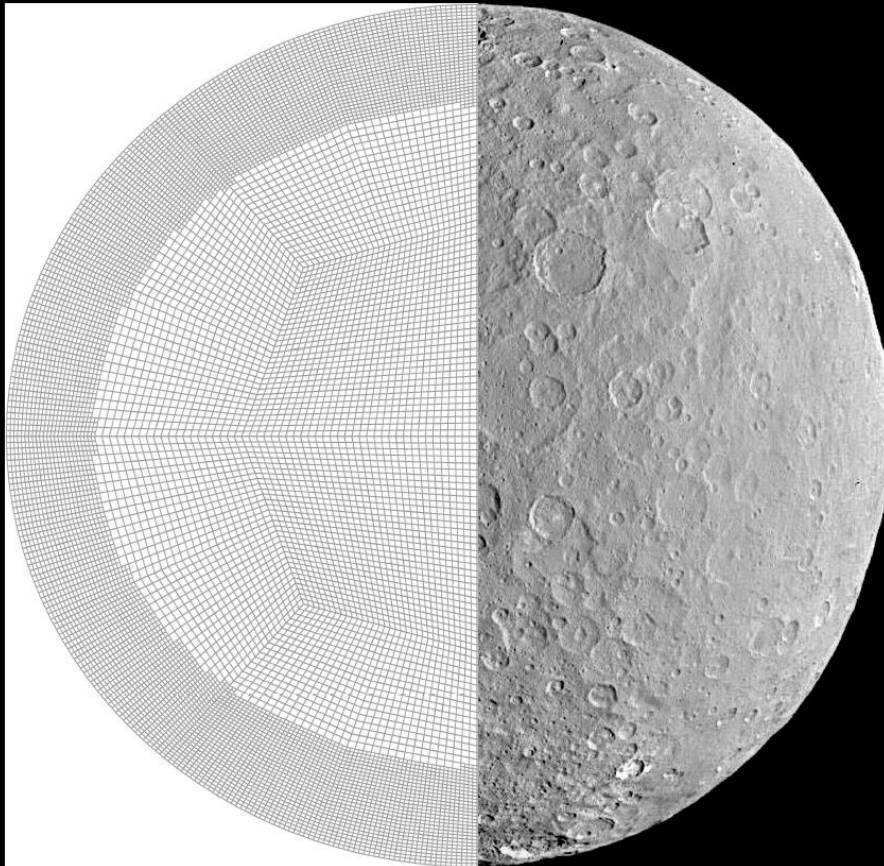
Evidence for viscous relaxation

- More general approach: study topography power spectrum
- Power spectra for Vesta closely fits with the power law to the lowest degrees ($\lambda < 750$ km)
- Ceres power spectrum deviates from the power law at $\lambda > 270$ km



Ermakov et al., 2017

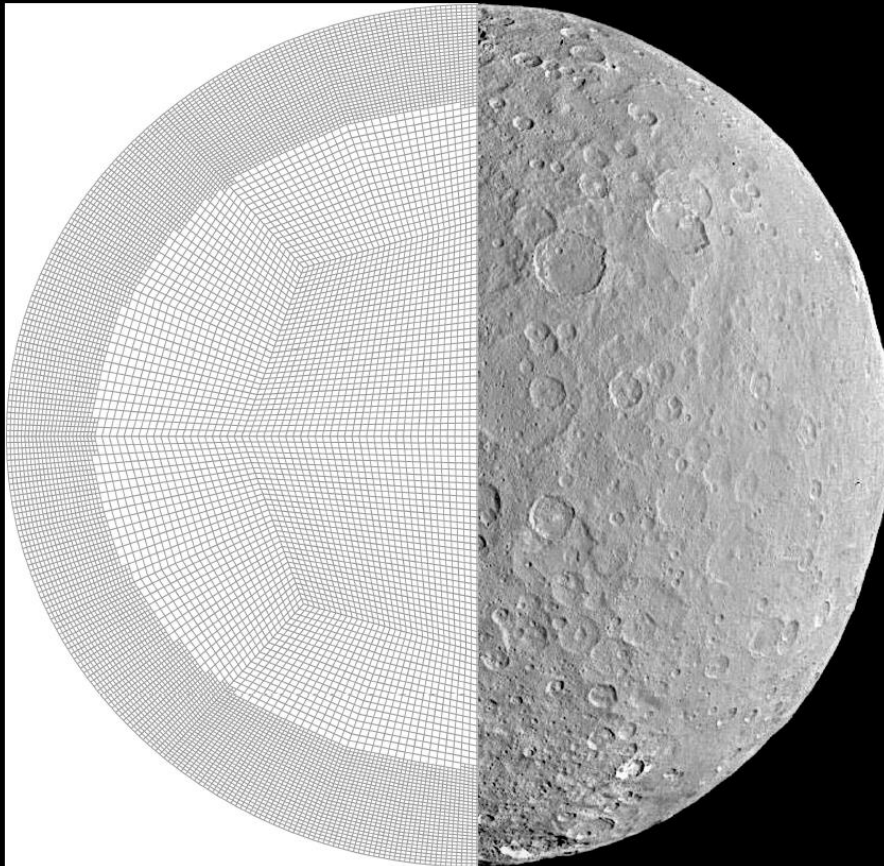
Finite element model



- Assume a density and rheology structure
- Solve Stokes equation for an incompressible flow using deal.ii library
- Compute the evolution of the outer surface power spectrum

Fu et al., 2014; Fu et al, 2017

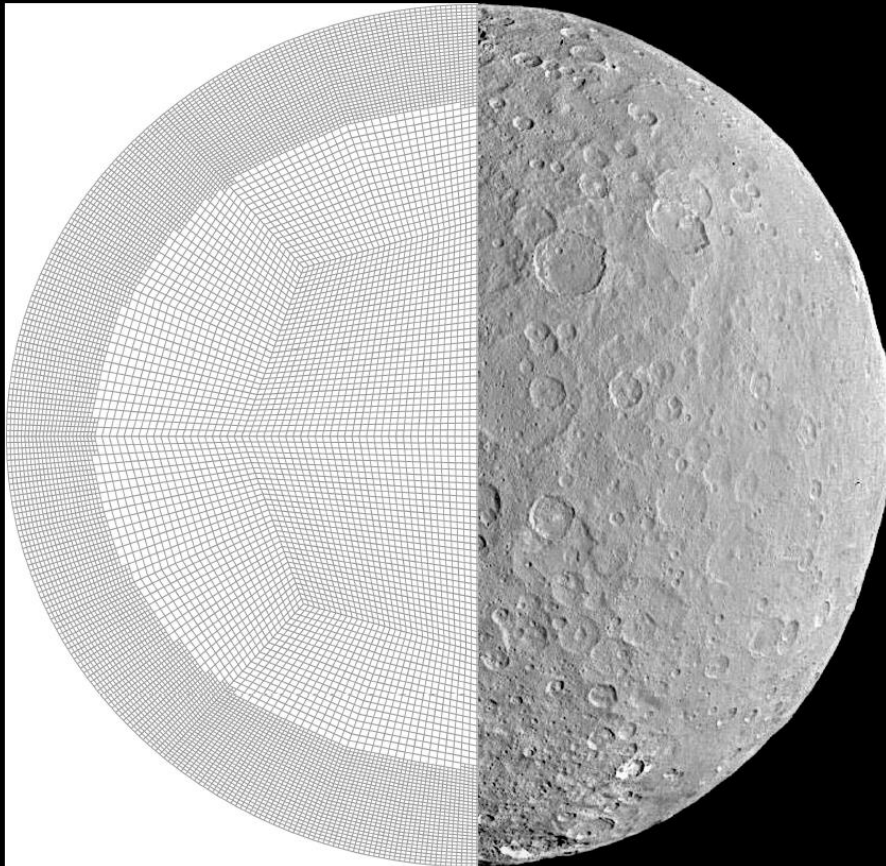
Finite element model



- Assume a density and rheology structure
- Solve Stokes equation for an incompressible flow using deal.ii library
- Compute the evolution of the outer surface power spectrum

Fu et al., 2014; Fu et al, 2017

Finite element model

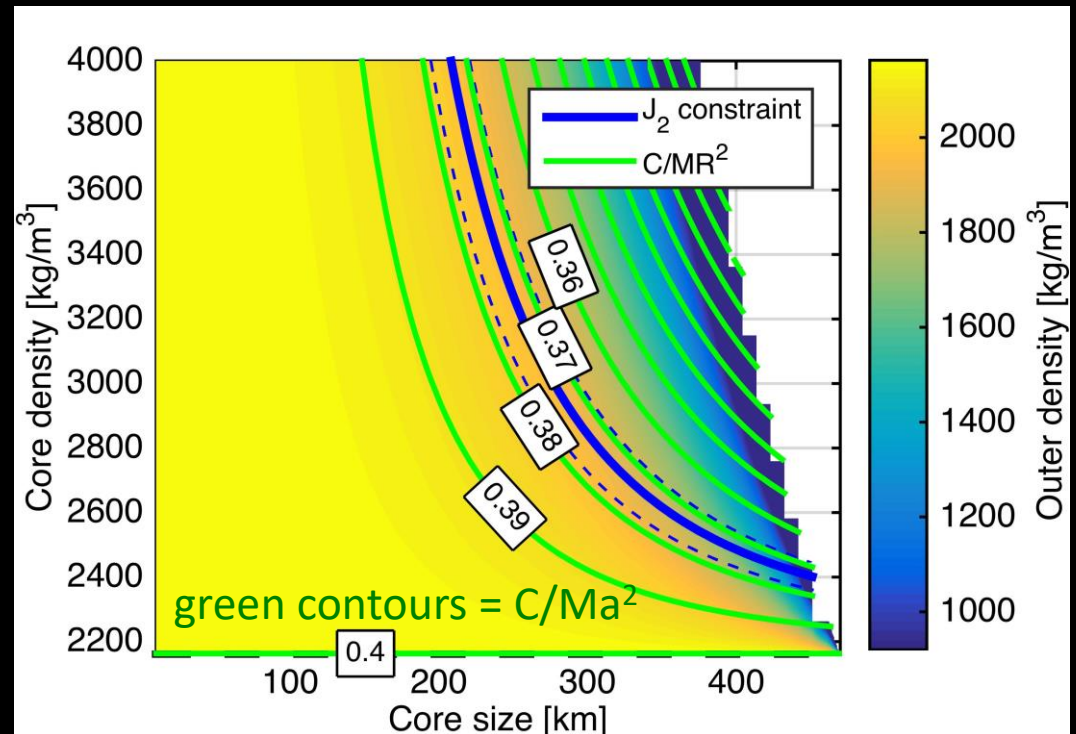


- Assume a density and rheology structure
- Solve Stokes equation for an incompressible flow using deal.ii library
- Compute the evolution of the outer surface power spectrum

Fu et al., 2014; Fu et al, 2017

Ceres internal structure

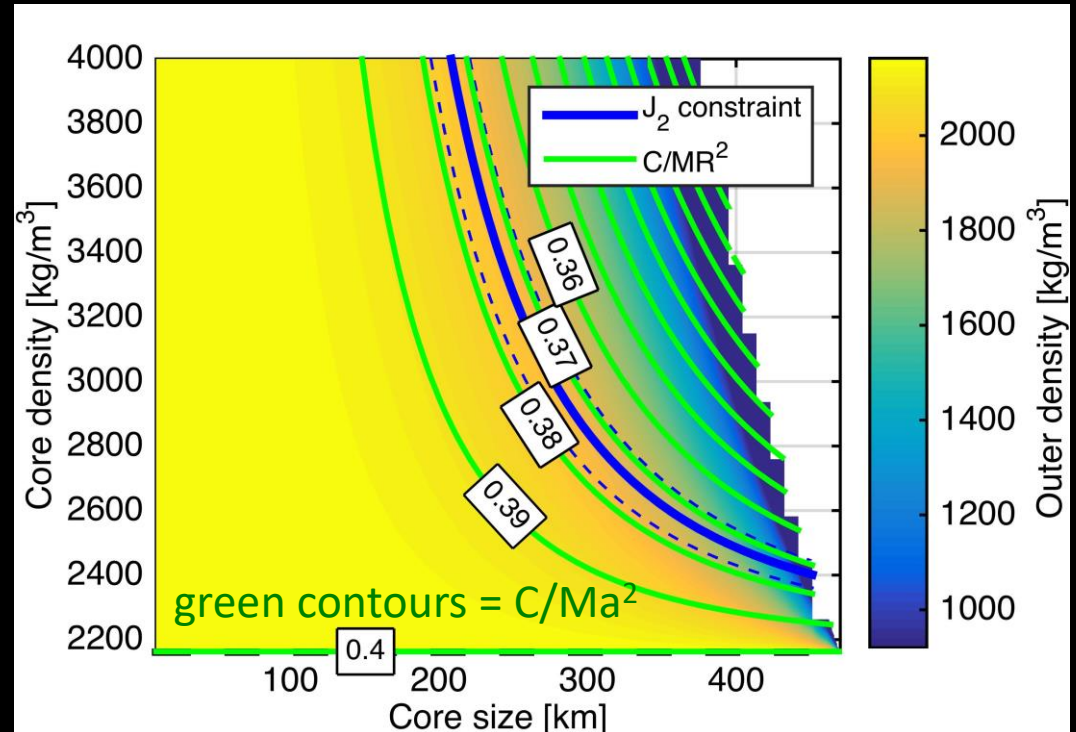
- Simplest model to interpret the gravity-topography data



Using Tricarico 2014 for computing hydrostatic equilibrium

Ceres internal structure

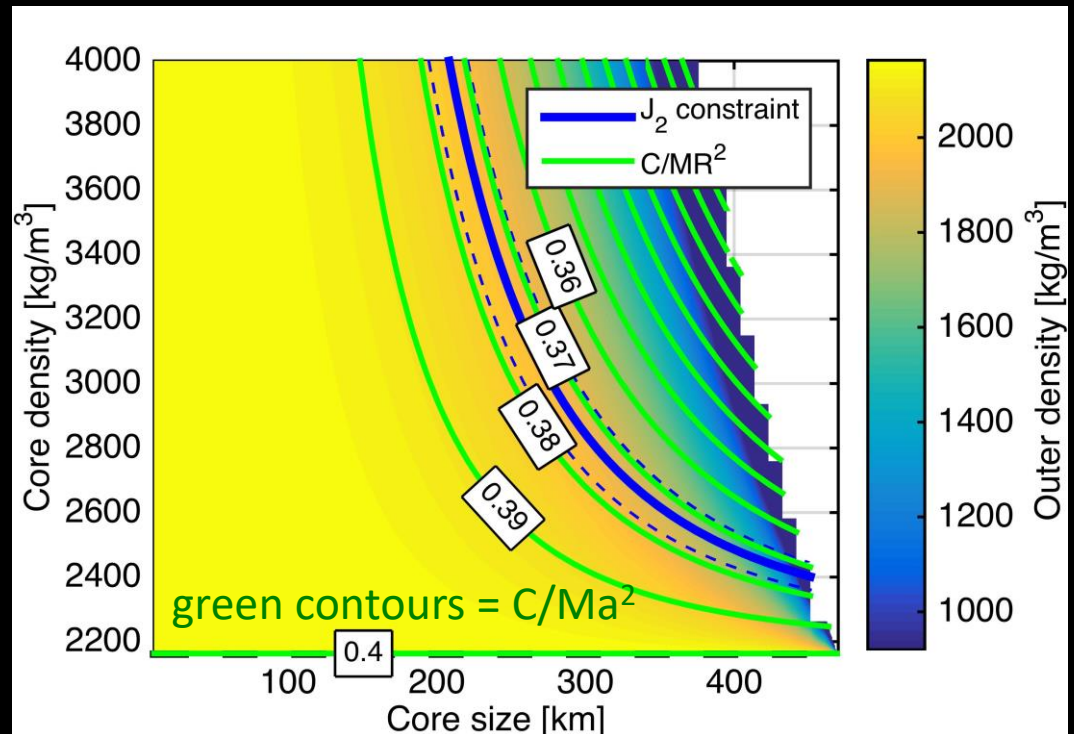
- Simplest model to interpret the gravity-topography data
- Only 5 parameters: two densities, two radii and rotation rate



Using Tricarico 2014 for computing hydrostatic equilibrium

Ceres internal structure

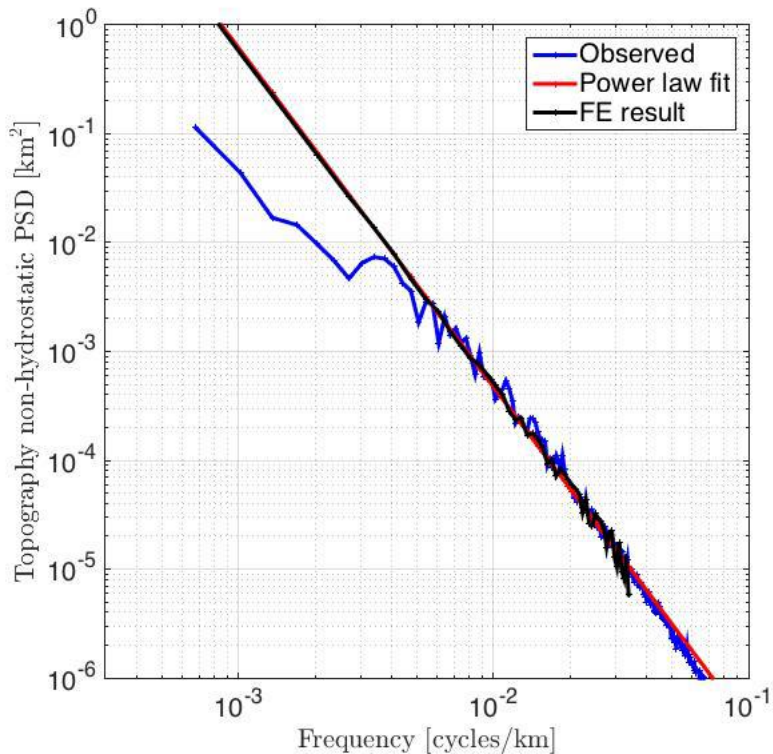
- Simplest model to interpret the gravity-topography data
- Only 5 parameters: two densities, two radii and rotation rate
- Yields $C/Ma^2 = 0.373$
 $C/M(R_{\text{vol}})^2 = 0.392$



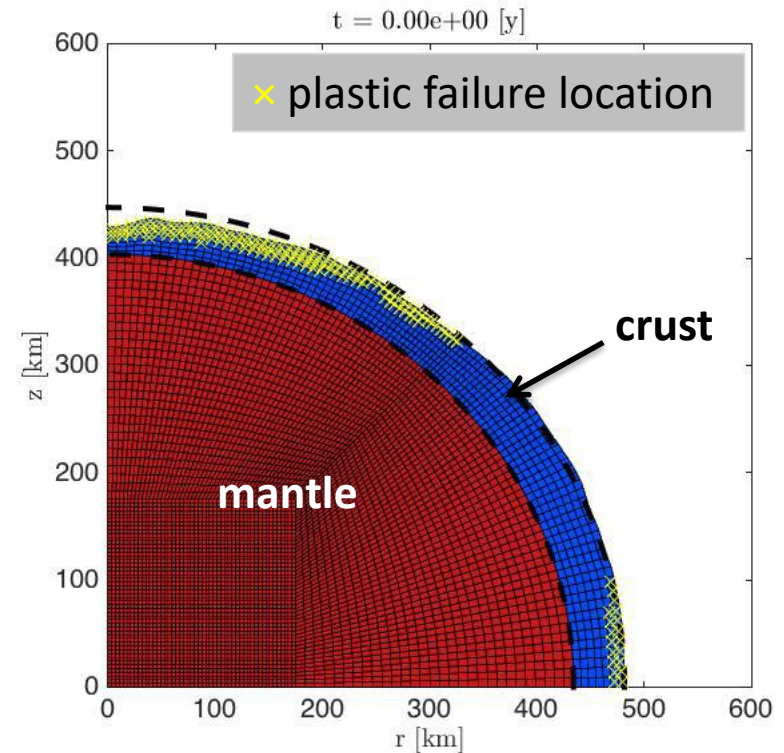
Using Tricarico 2014 for computing hydrostatic equilibrium

Example of a FE modeling run

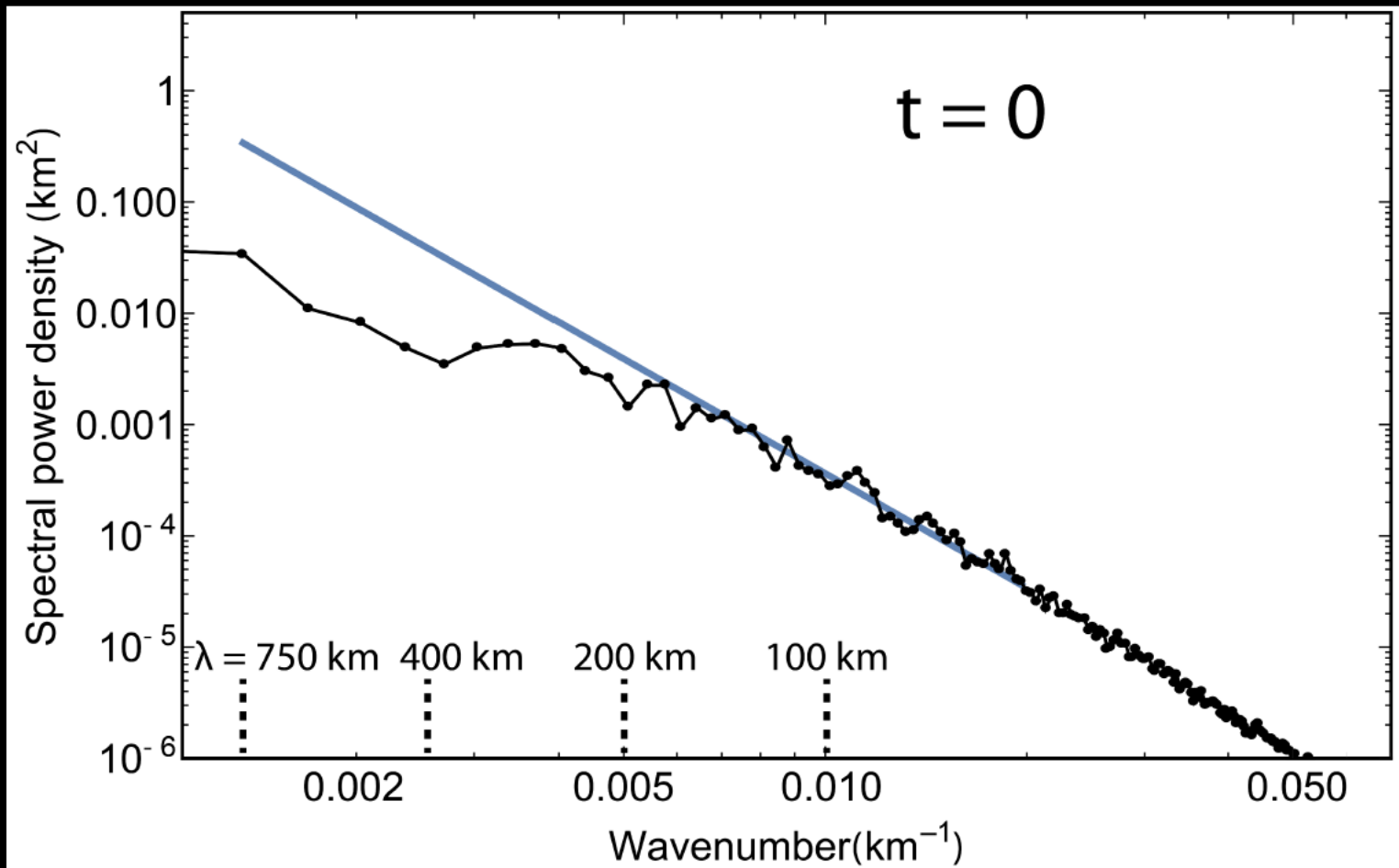
relaxation in the frequency domain



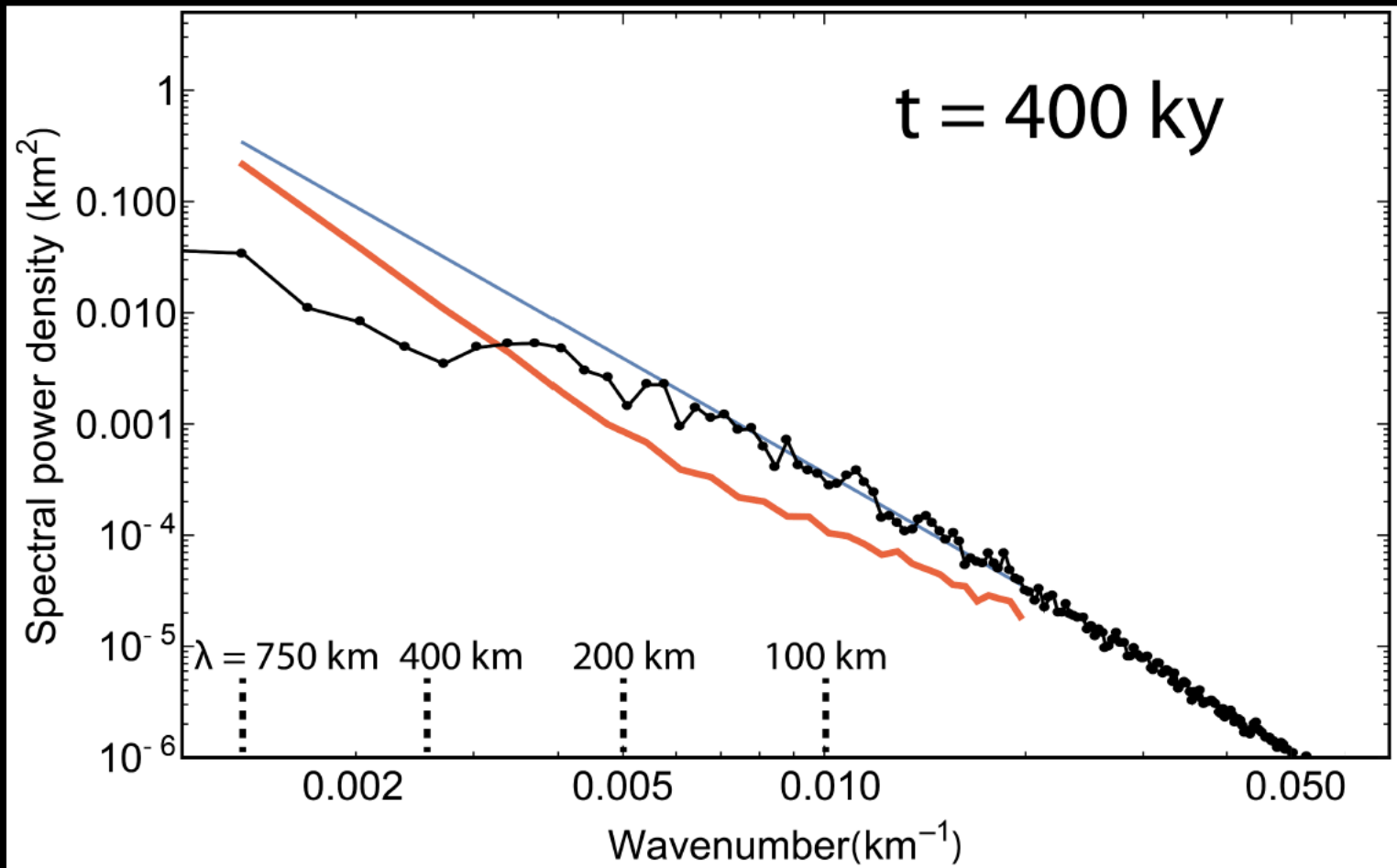
relaxation in the spatial domain



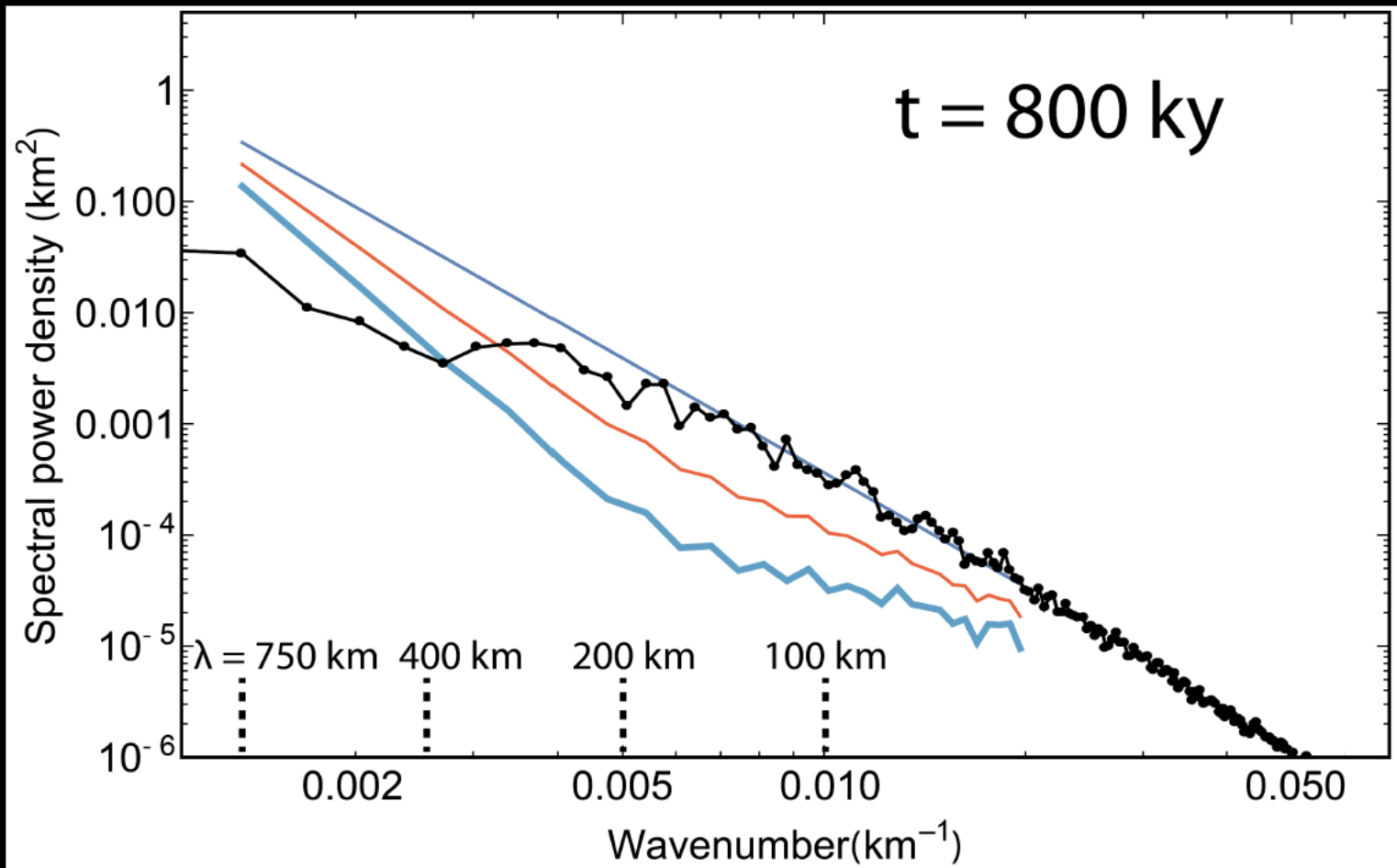
Ice shell, rocky interior



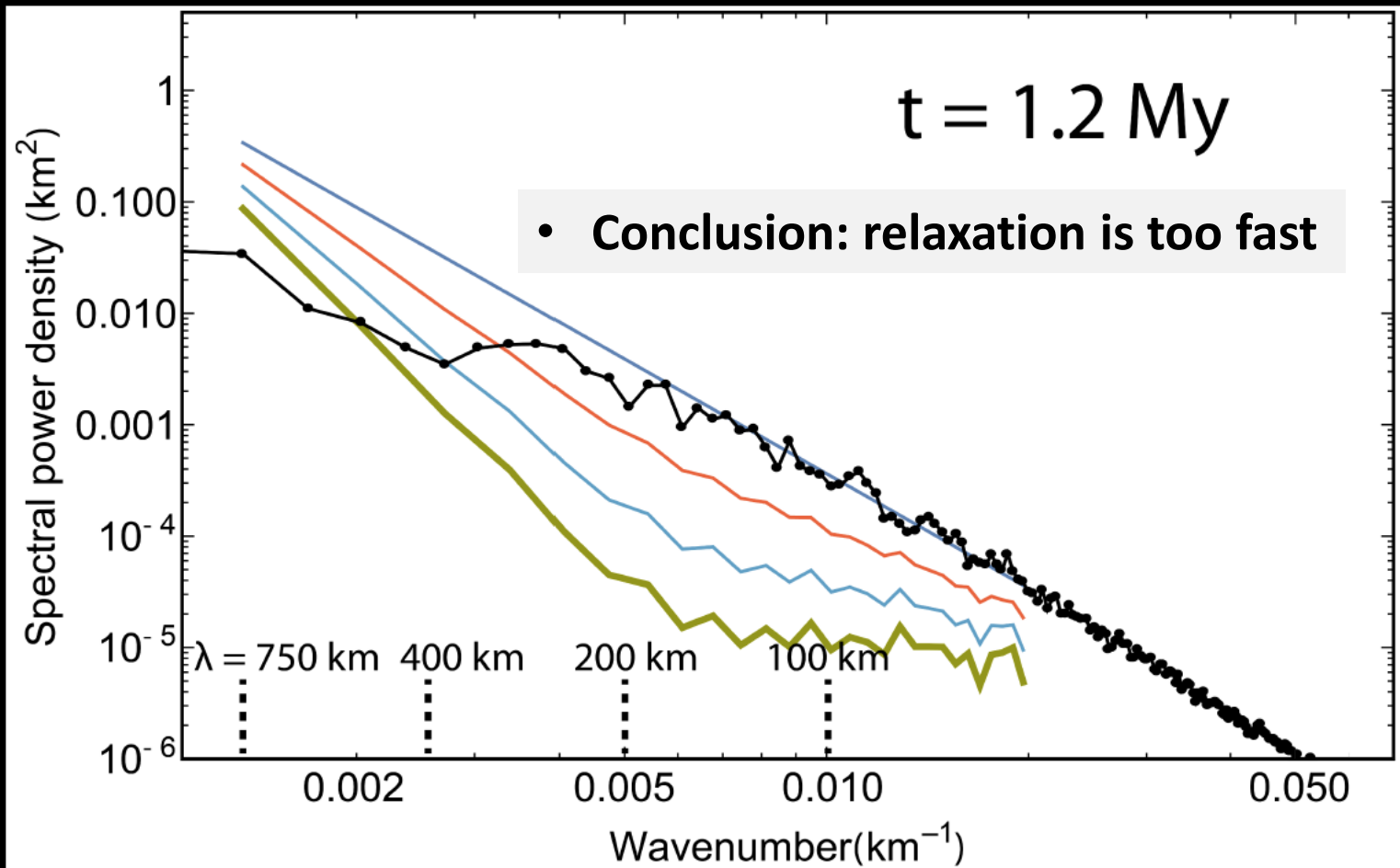
Ice shell, rocky interior



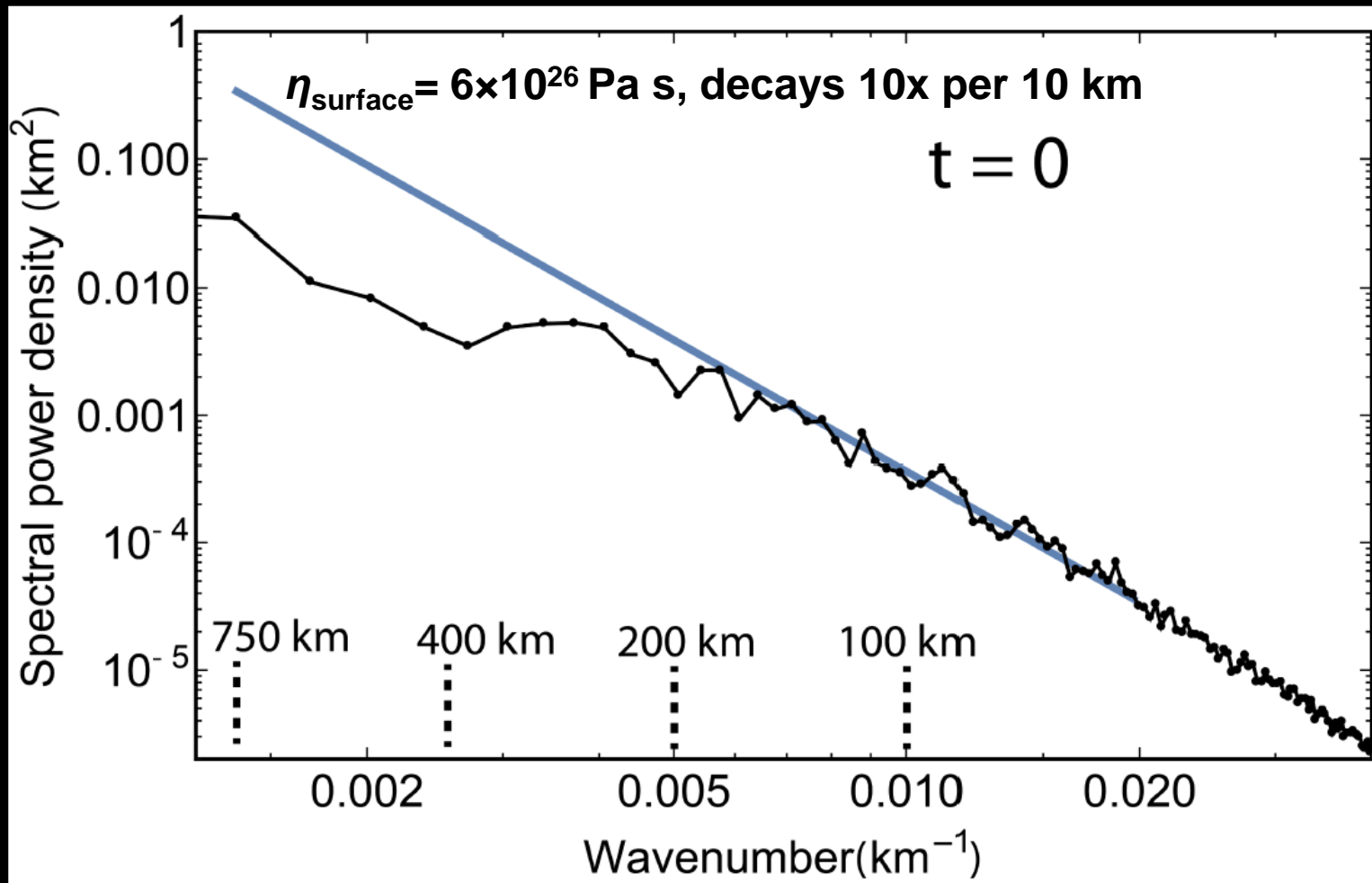
Ice shell, rocky interior



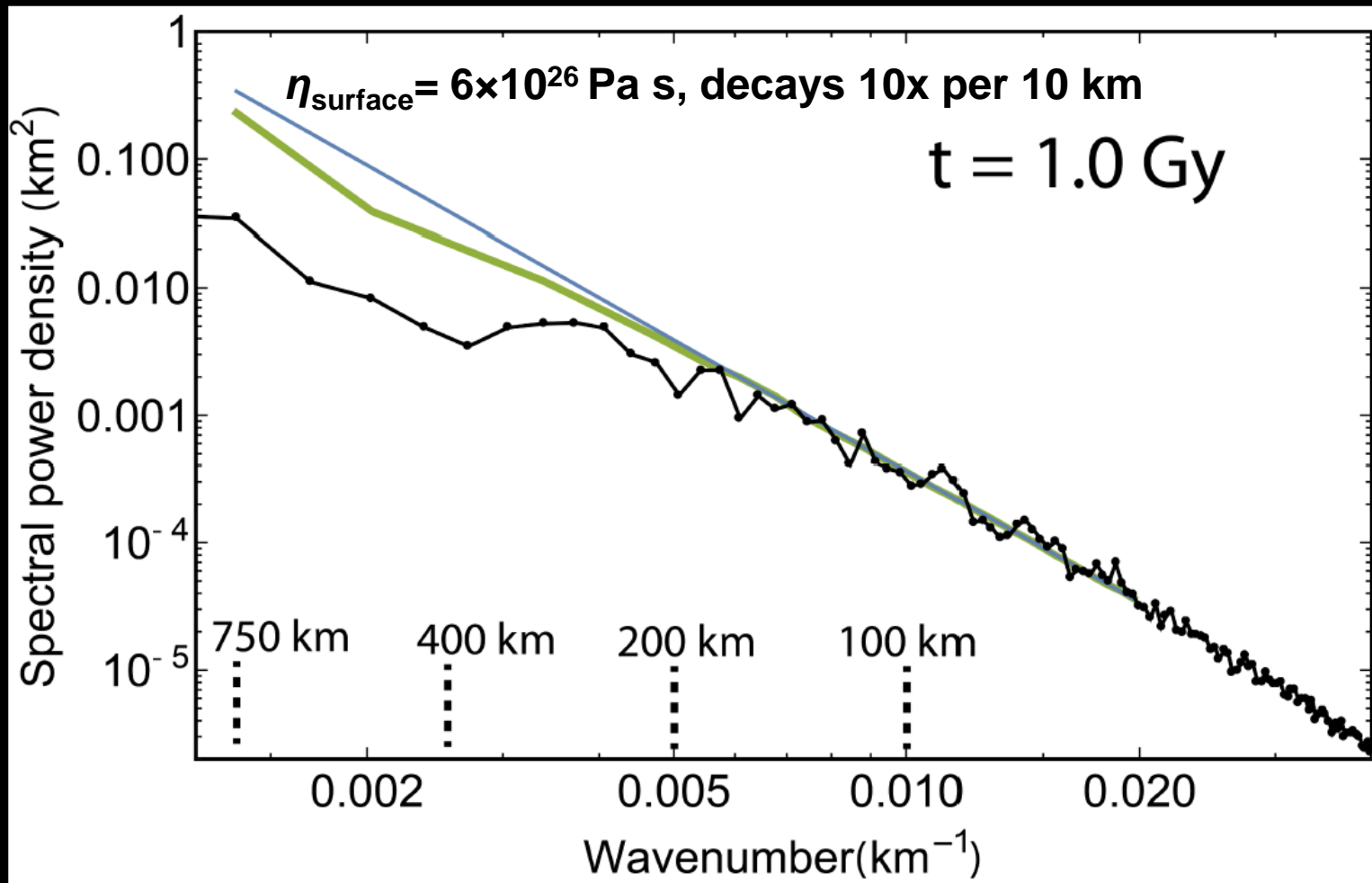
Ice shell, rocky interior



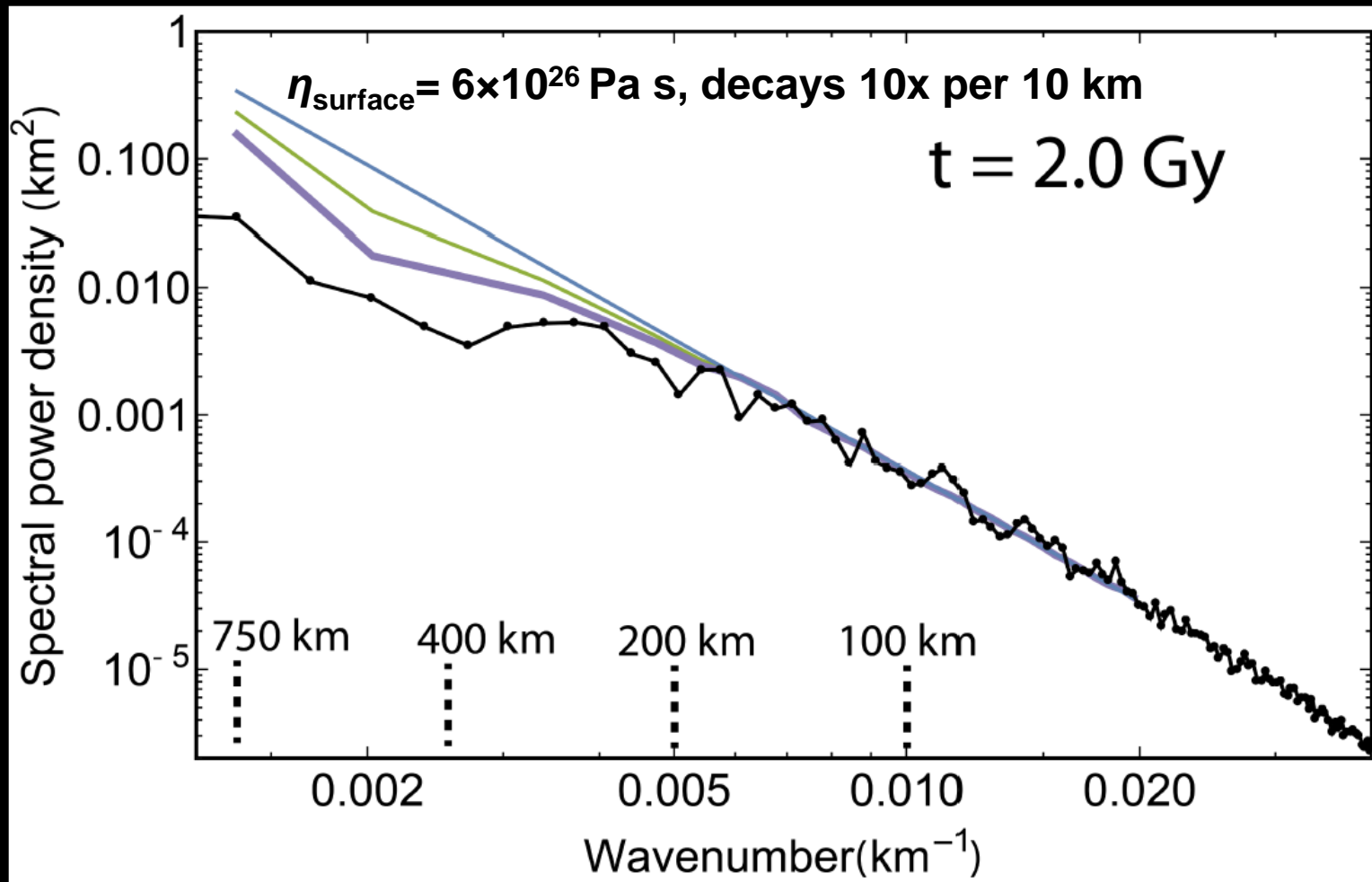
Stiff surface, weak interior



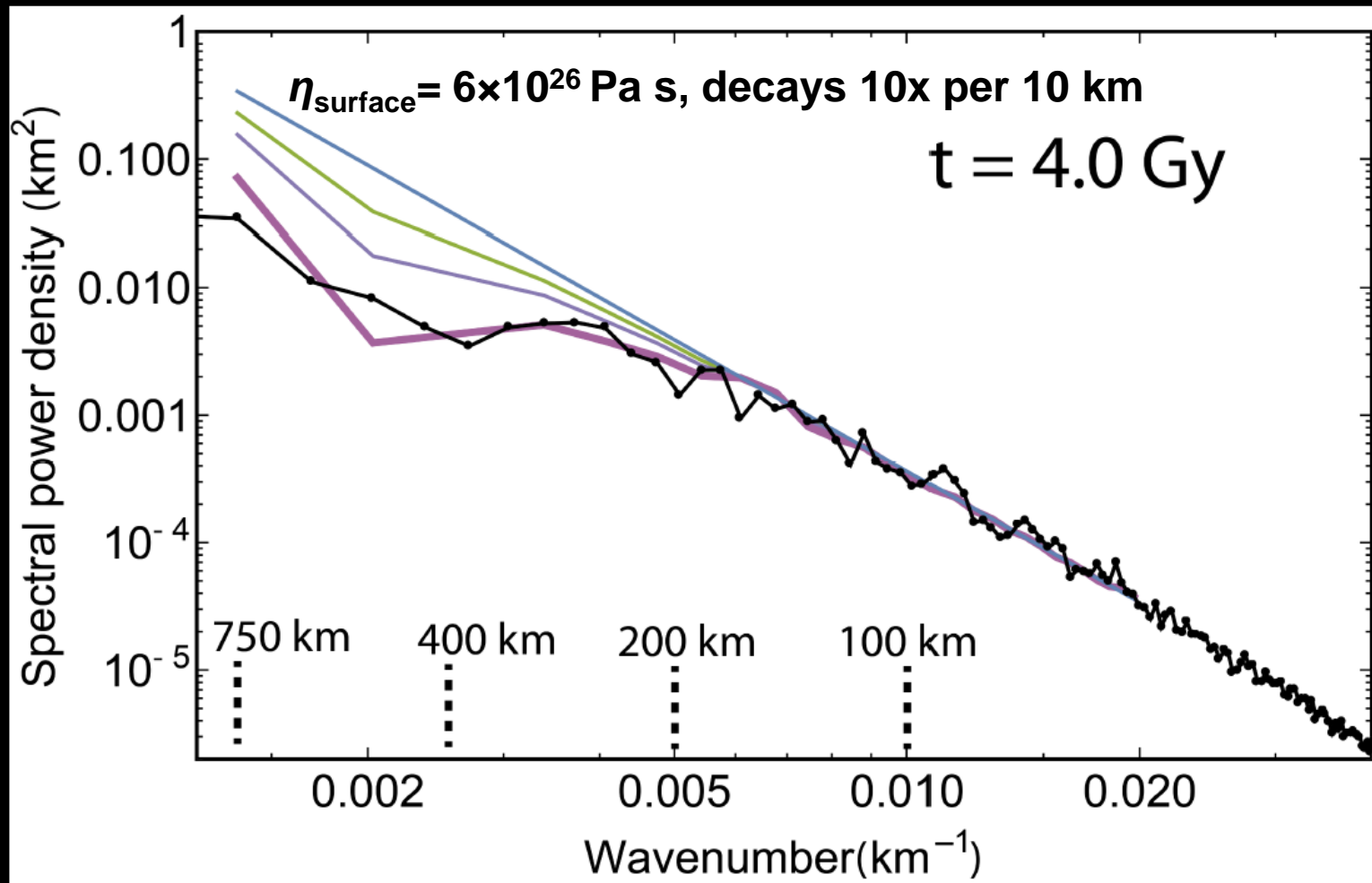
Stiff surface, weak interior



Stiff surface, weak interior

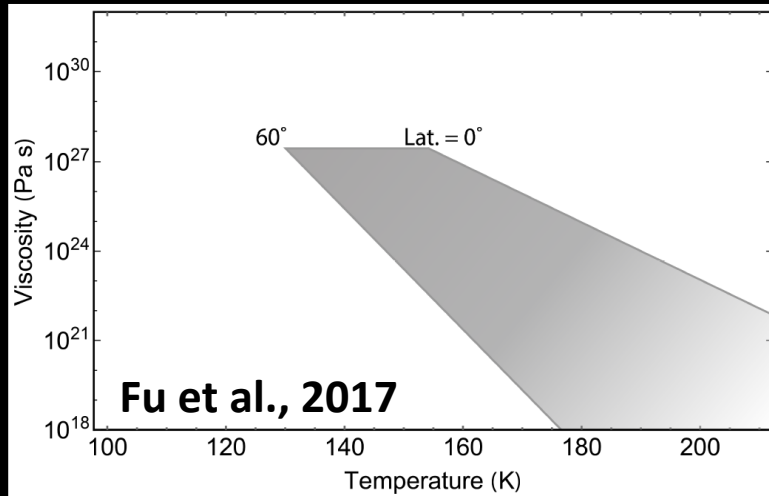


Stiff surface, weak interior

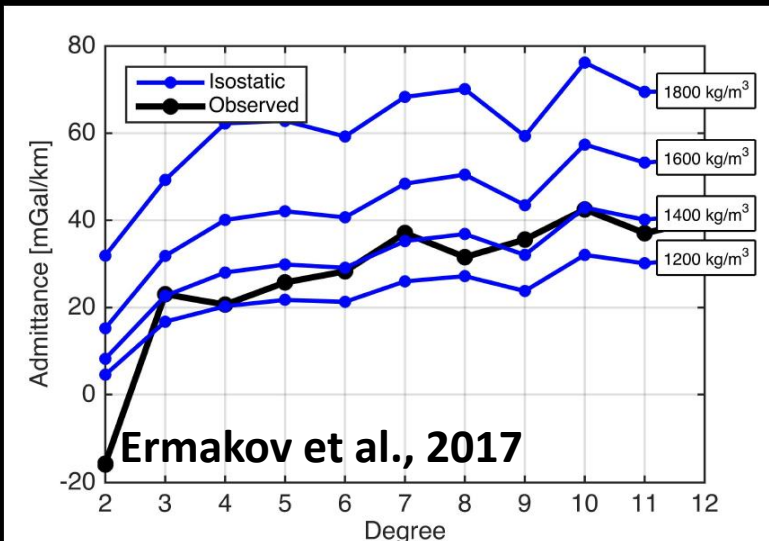


Rheology and density constraints

Rheology constraint
from FE modeling



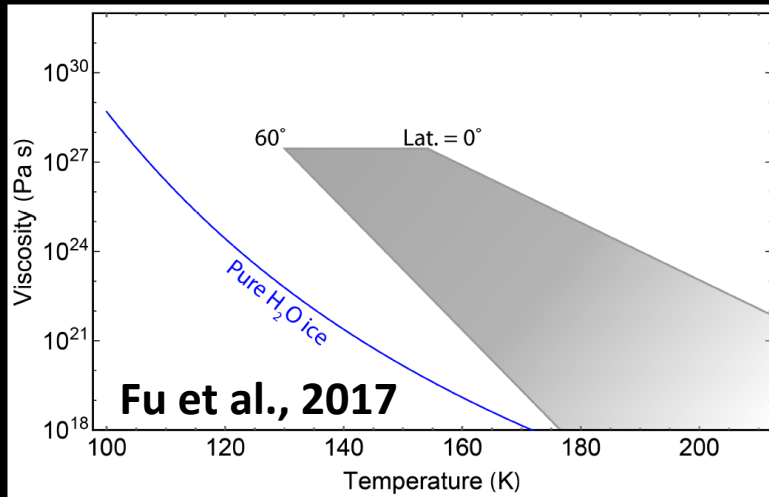
Density constraint from
admittance modeling



- Ceres crust is ~ 1000 times stronger than water ice
- Must be dominated by rock-like materials. Water ice in the Ceres' crust < 35 vol%
- Crust dominated salt and clathrates phases
- Low core density implies its hydrated state

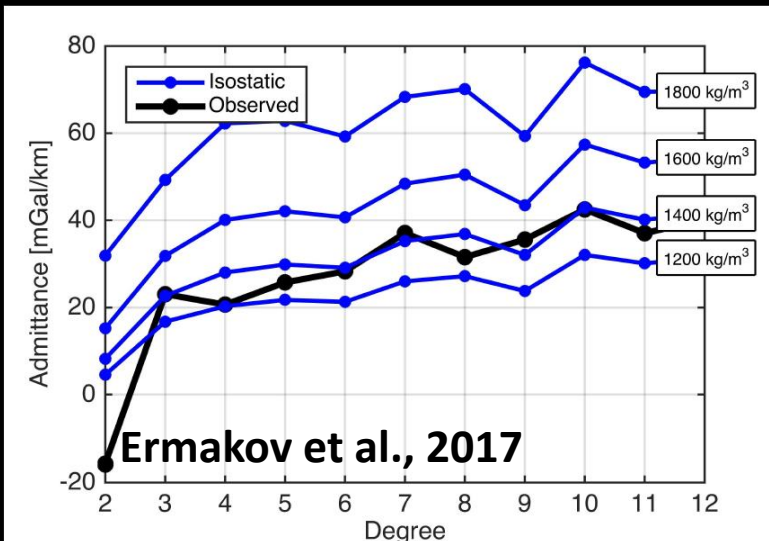
Rheology and density constraints

Rheology constraint
from FE modeling



- Ceres crust is ~ 1000 times stronger than water ice
- Must be dominated by rock-like materials. Water ice in the Ceres' crust < 35 vol%

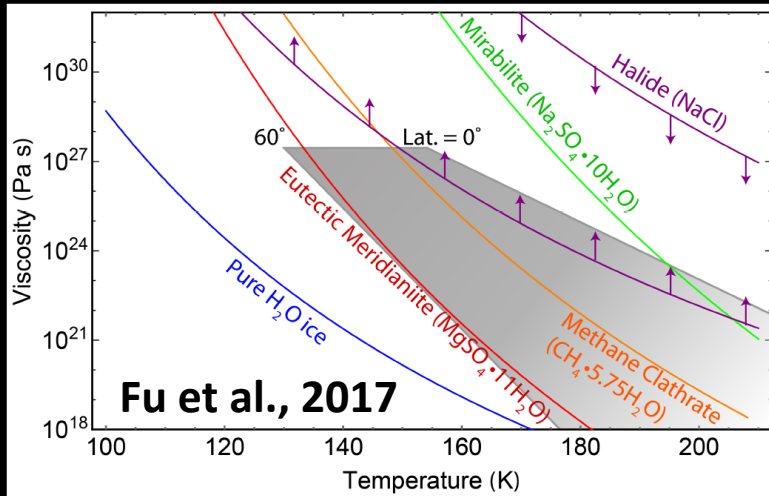
Density constraint from
admittance modeling



- Crust dominated salt and clathrates phases
- Low core density implies its hydrated state

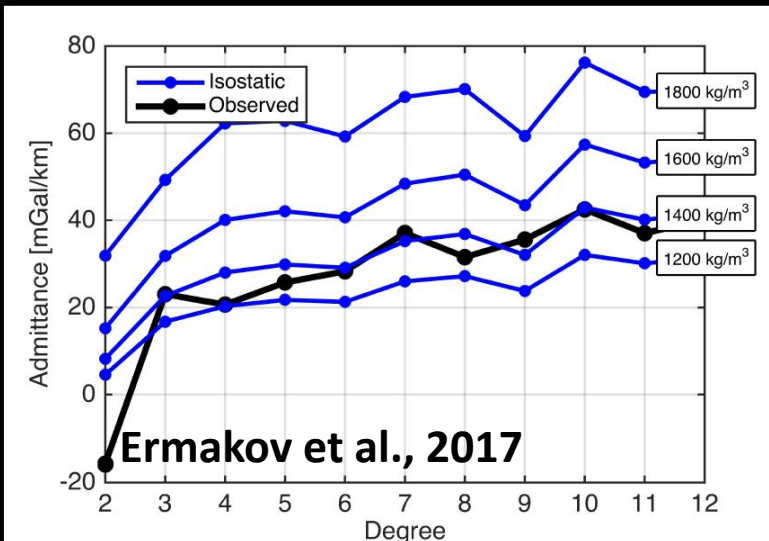
Rheology and density constraints

Rheology constraint
from FE modeling



- Ceres crust is ~ 1000 times stronger than water ice
- Must be dominated by rock-like materials. Water ice in the Ceres' crust < 35 vol%

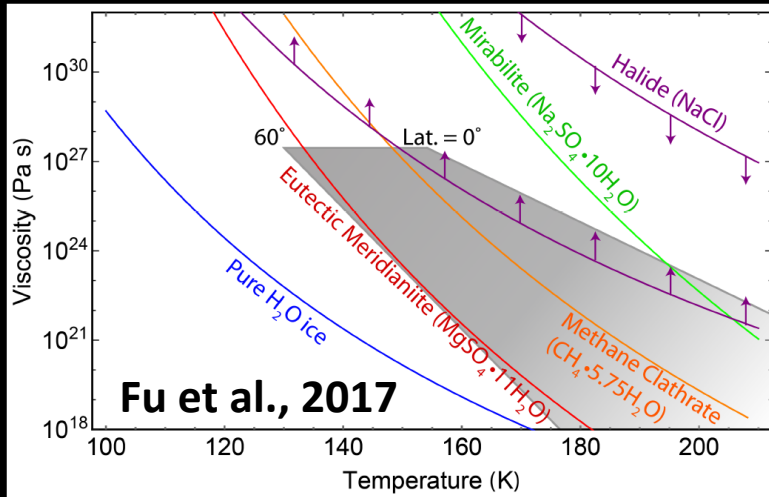
Density constraint from
admittance modeling



- Crust dominated salt and clathrates phases
- Low core density implies its hydrated state

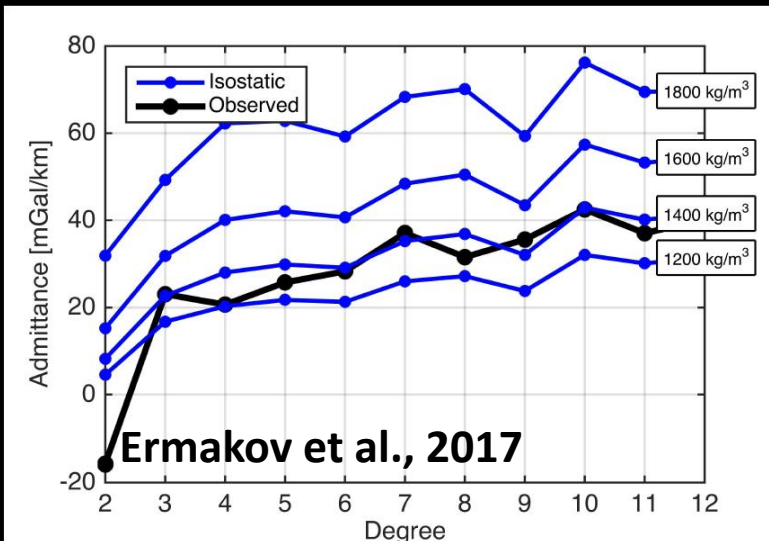
Rheology and density constraints

Rheology constraint
from FE modeling

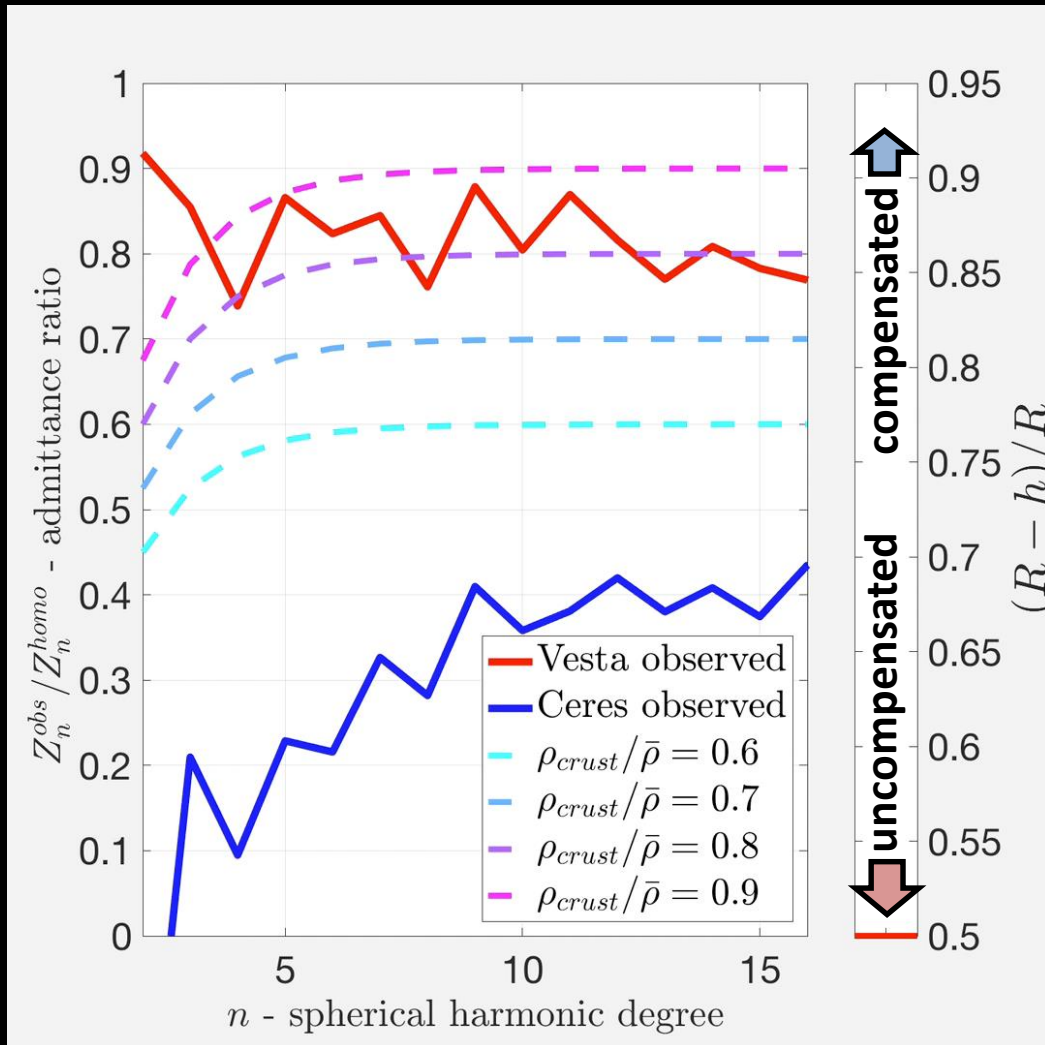


- Ceres crust is ~ 1000 times stronger than water ice
- Must be dominated by rock-like materials. Water ice in the Ceres' crust < 35 vol%
- Crust dominated salt and clathrates phases
- Low core density implies its hydrated state

Density constraint from
admittance modeling



Compensation: Vesta vs Ceres

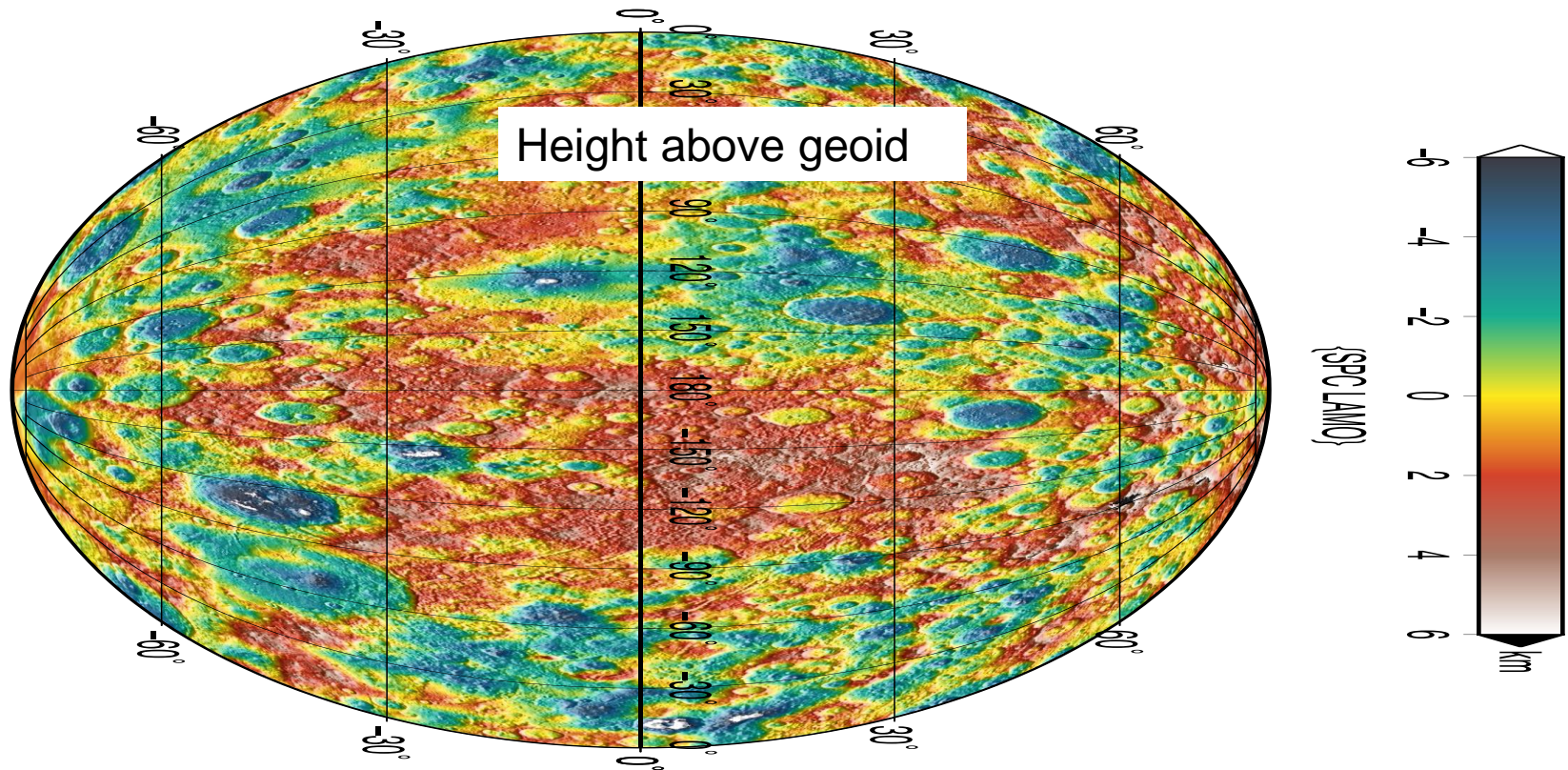




Compensation for **Vesta** and **Ceres**

- **Vesta** topography is uncompensated
- **Vesta** acquired most of its topography when the crust was already cool and not-relaxing
- **Ceres** topography is compensated
- Lower viscosities (compared to Vesta) enabled relaxation of topography to the isostatic state

Local structures on Ceres



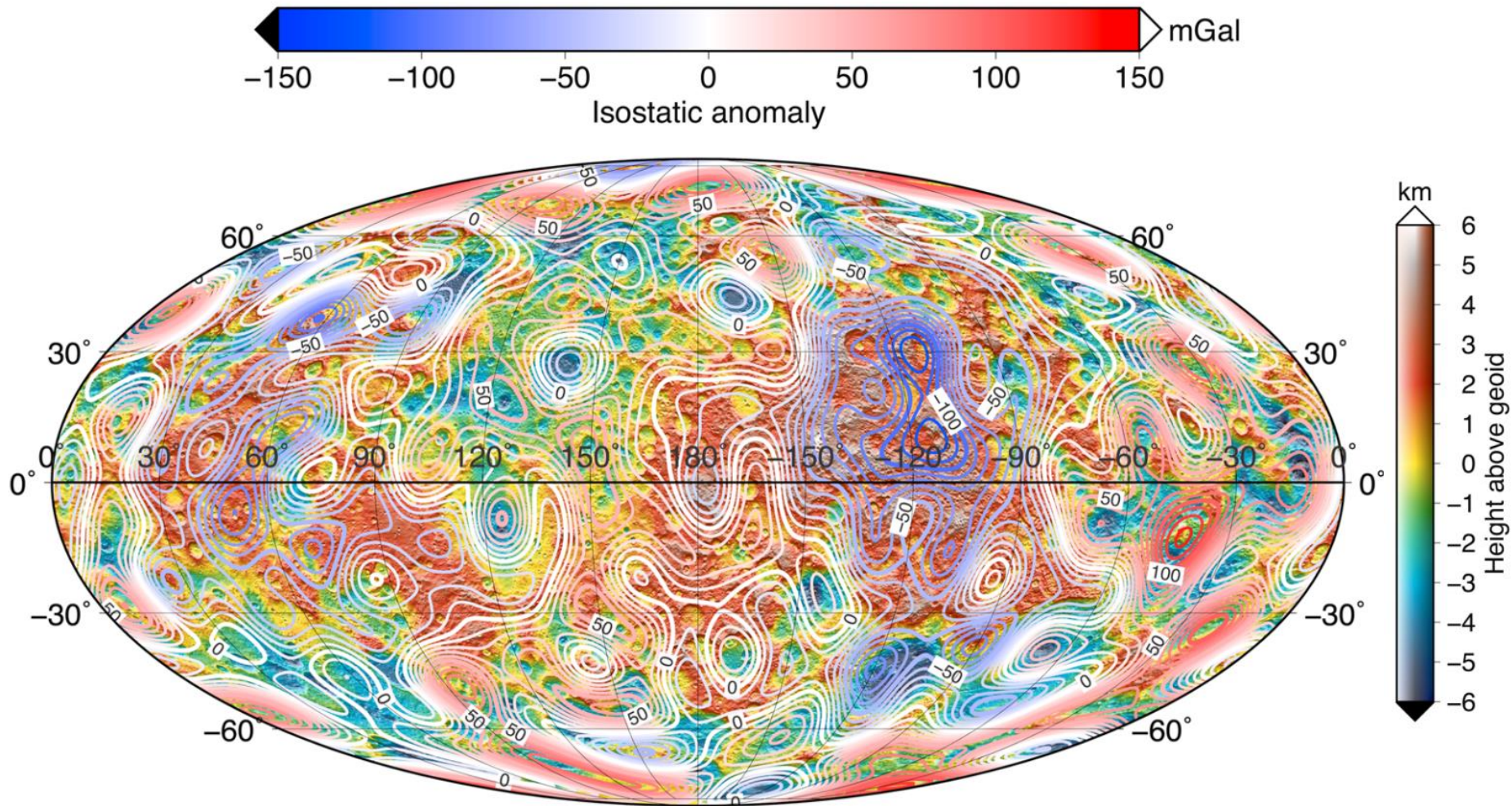
Park et al., 2016

Reference ellipsoid:

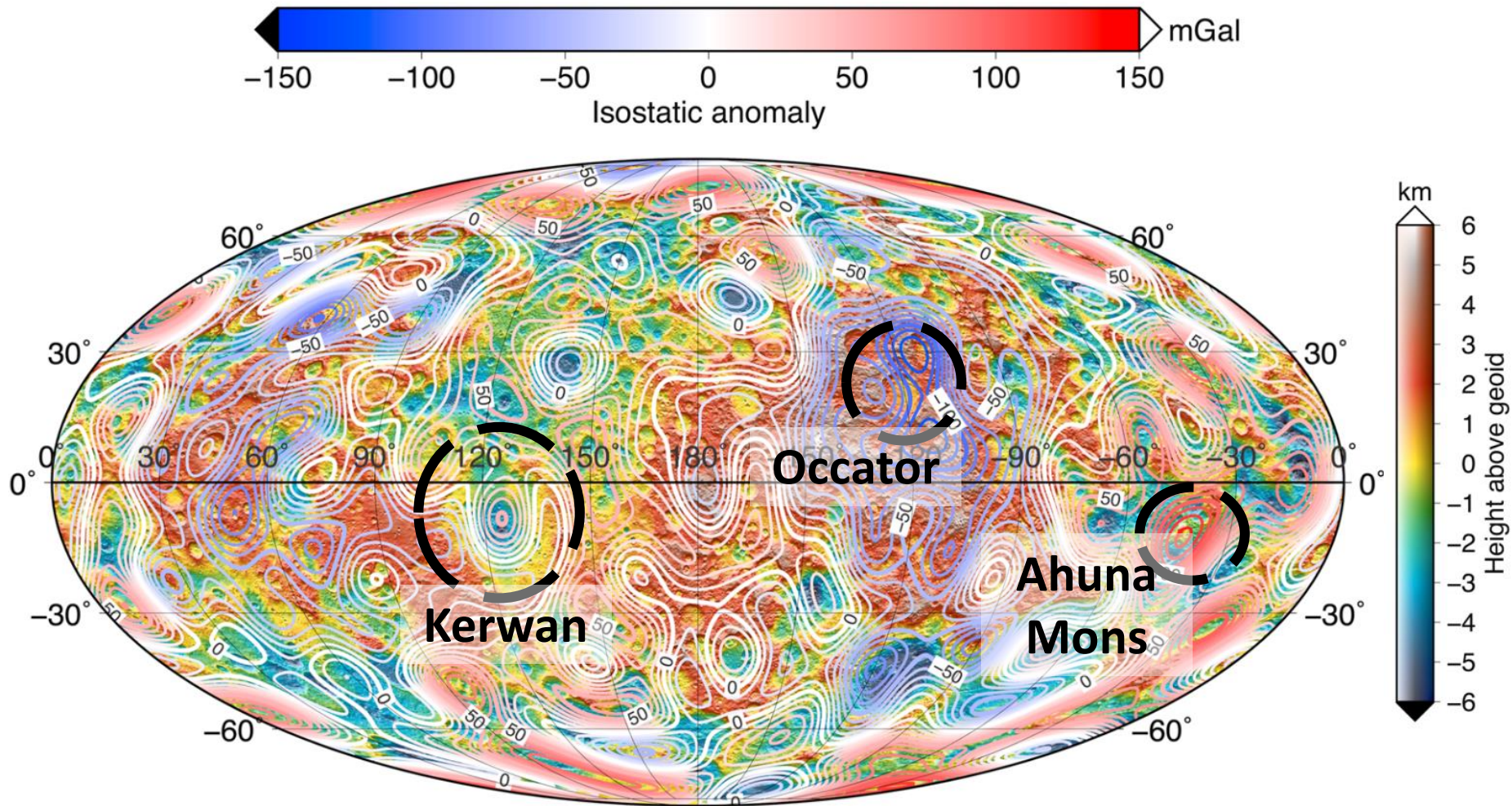
$a = 445.9$ km

$c = 482.0$ km

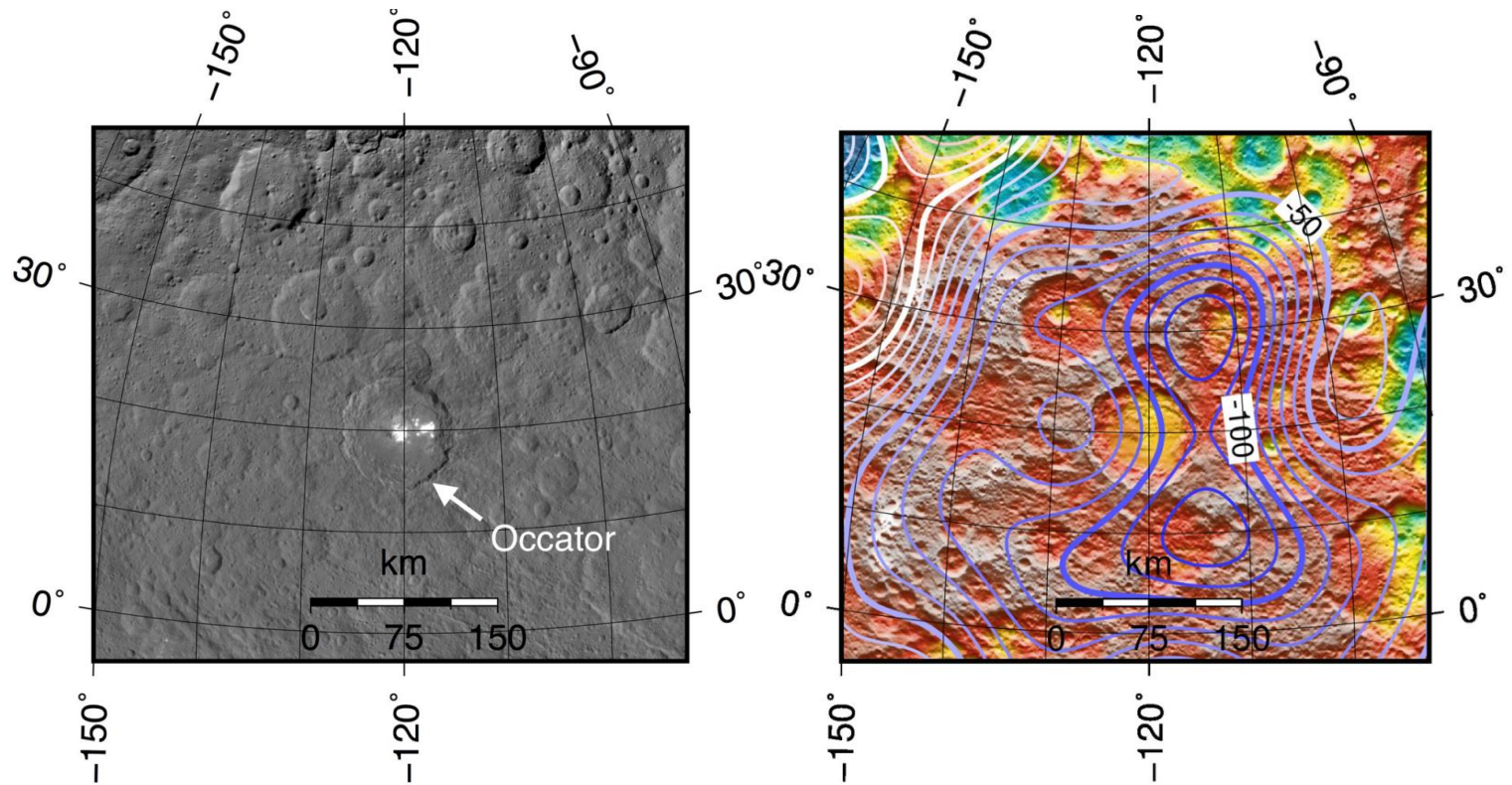
Isostatic anomaly



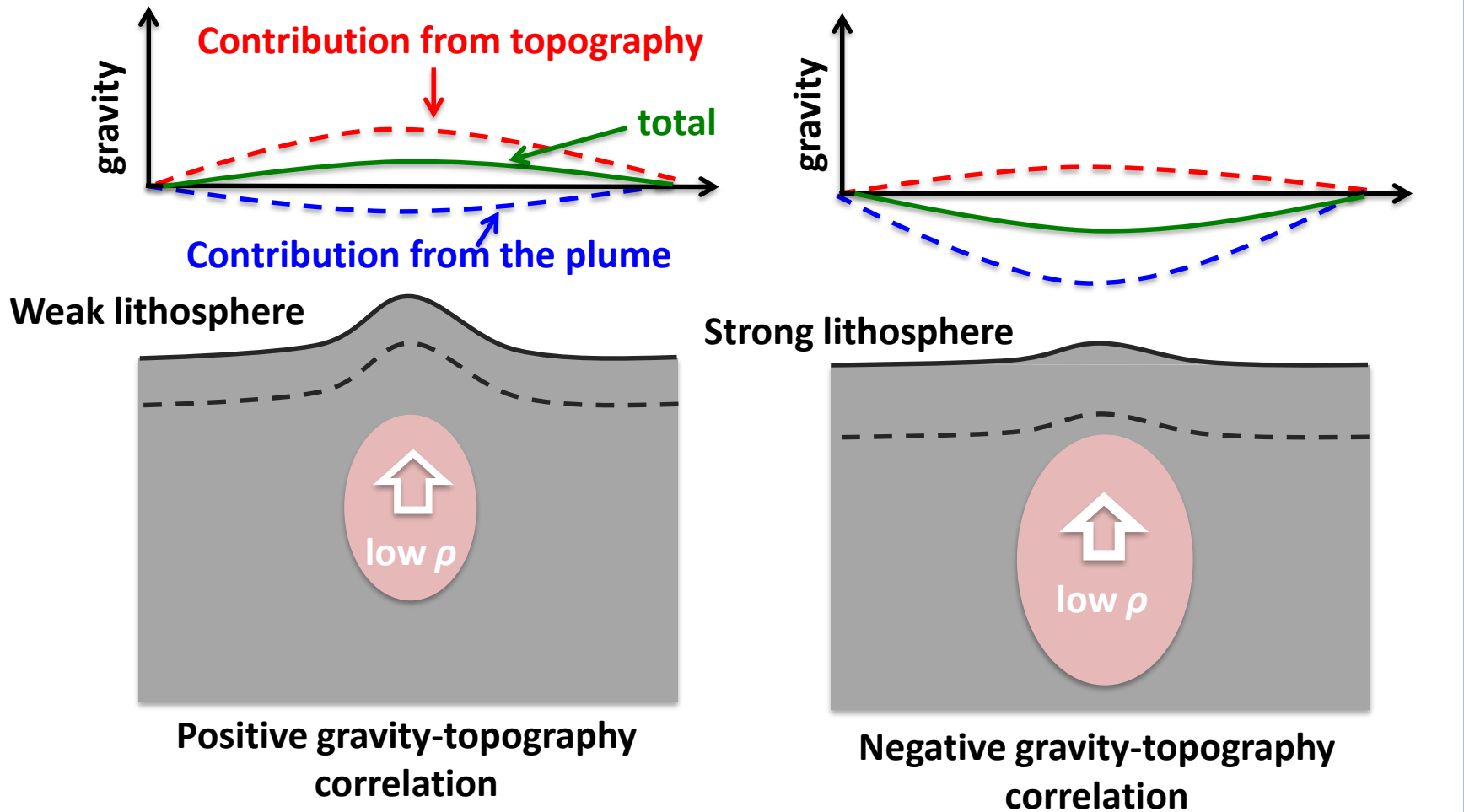
Isostatic anomaly



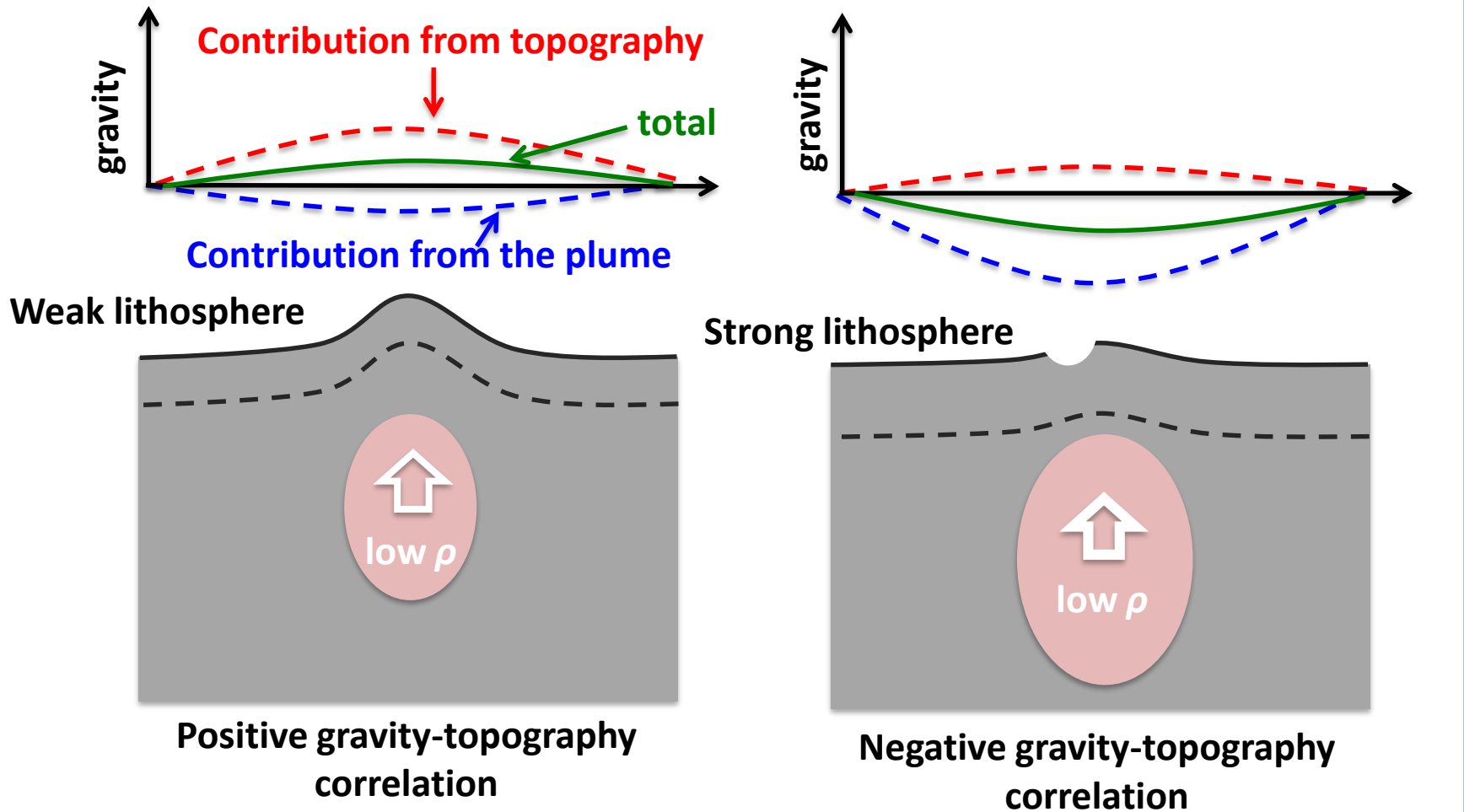
Occator isostatic anomaly



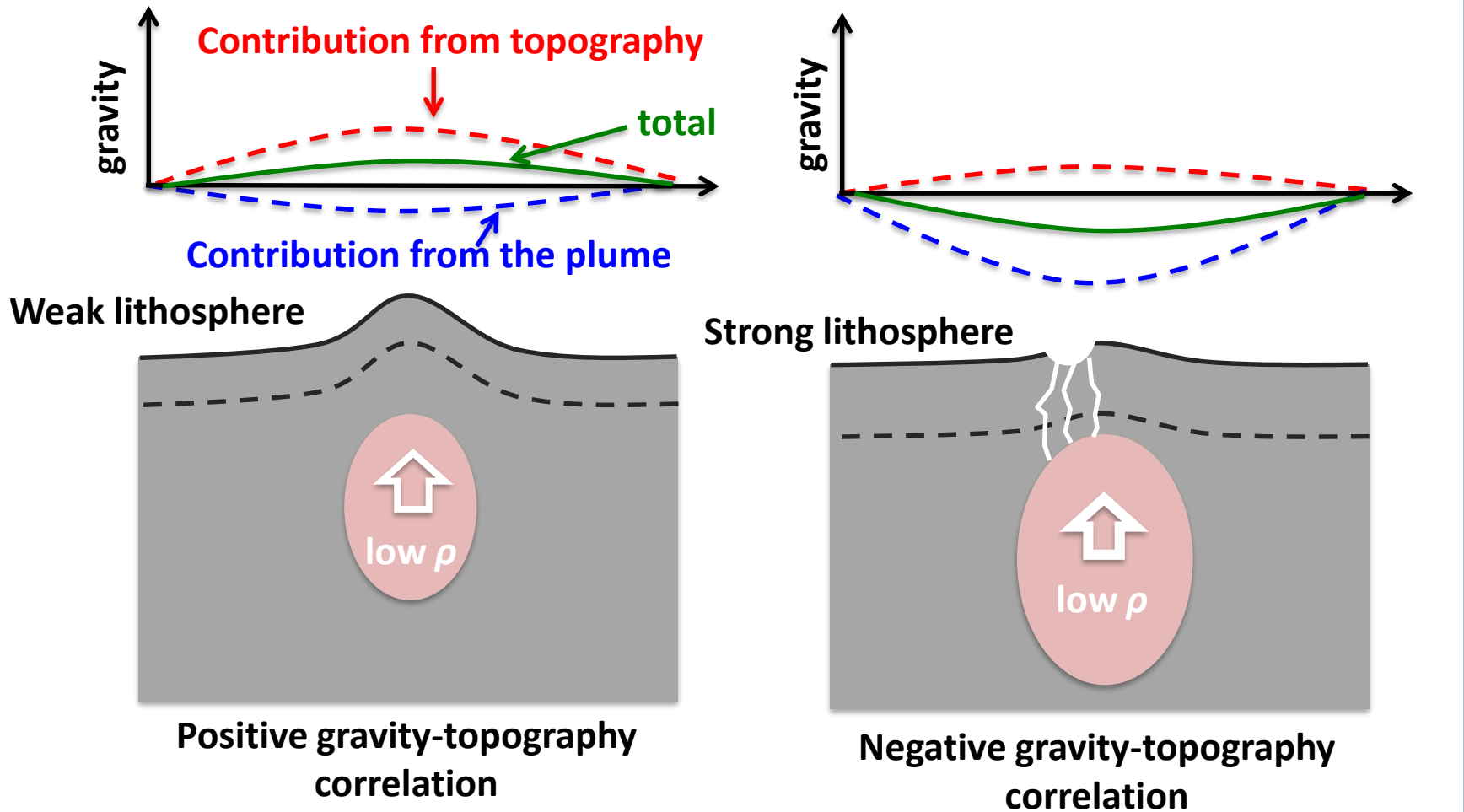
Buoyancy-driven anomaly



Buoyancy-driven anomaly

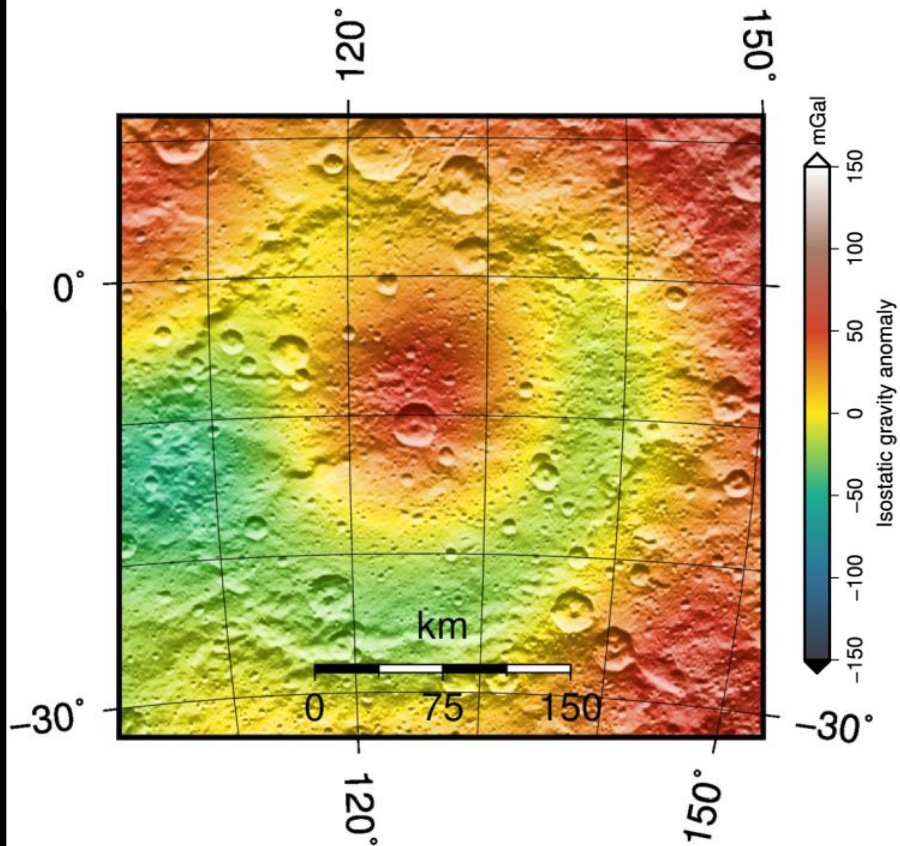


Buoyancy-driven anomaly



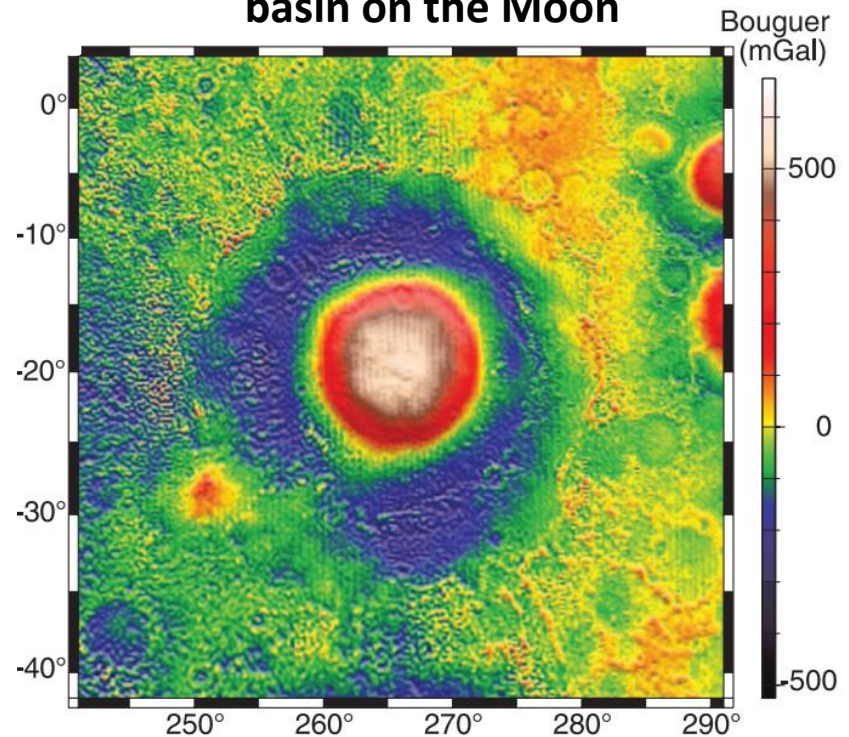
Mascons

Kerwan isostatic anomaly



Ermakov et al., 2017

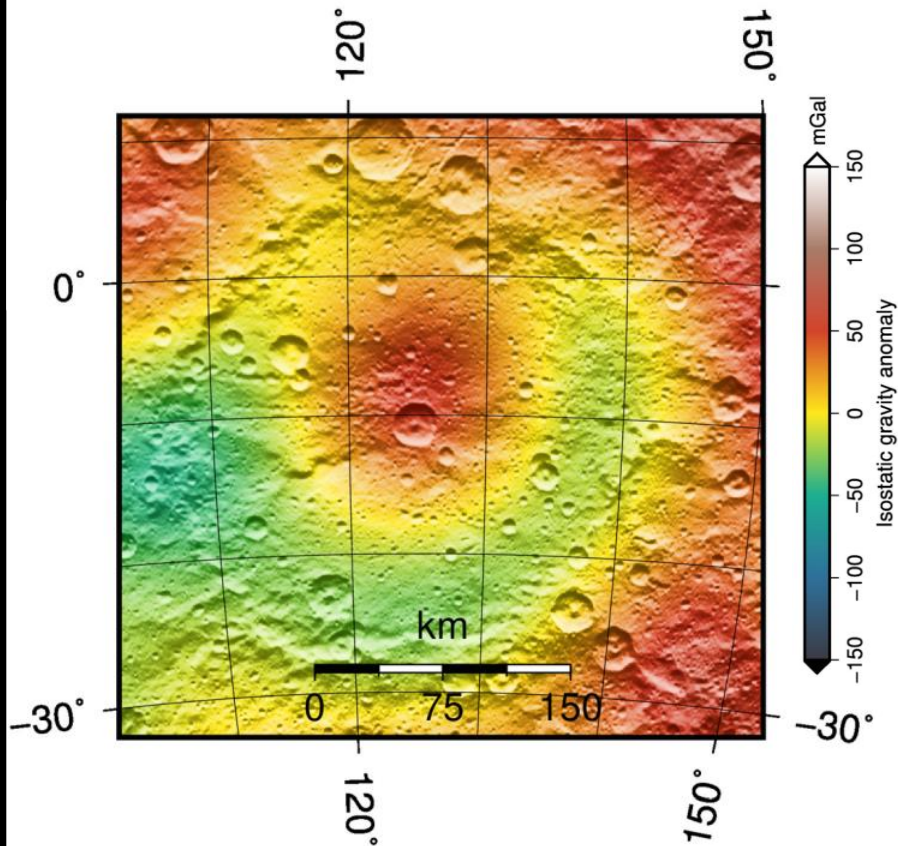
Bouguer anomaly in Orientale basin on the Moon



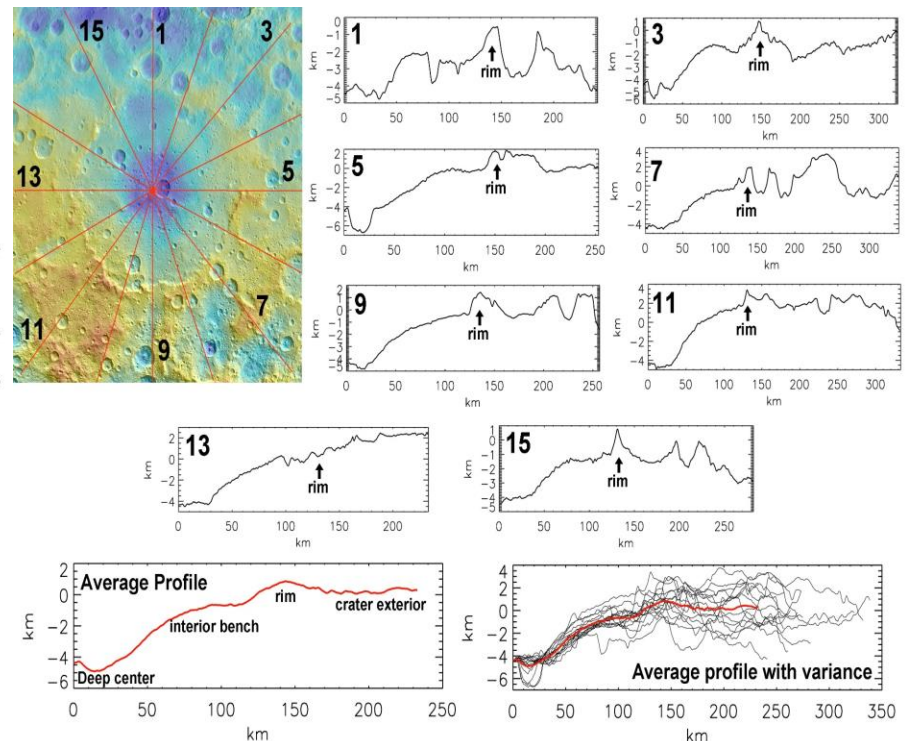
Zuber et al., 2016

Mascons

Kerwan isostatic anomaly



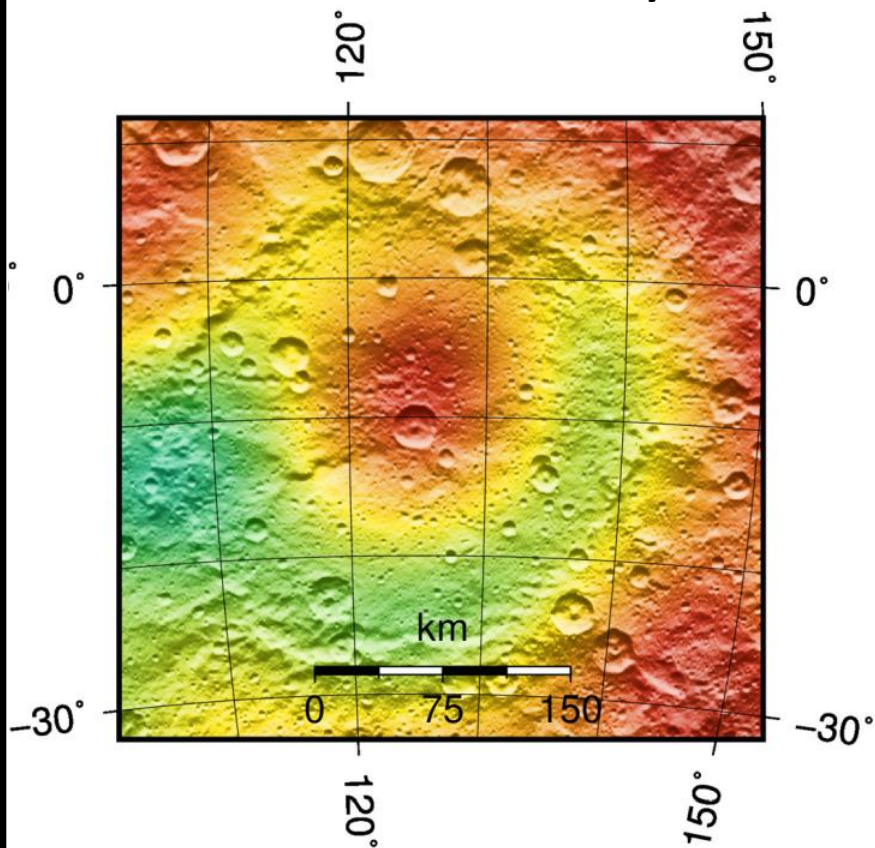
Ermakov et al., 2017



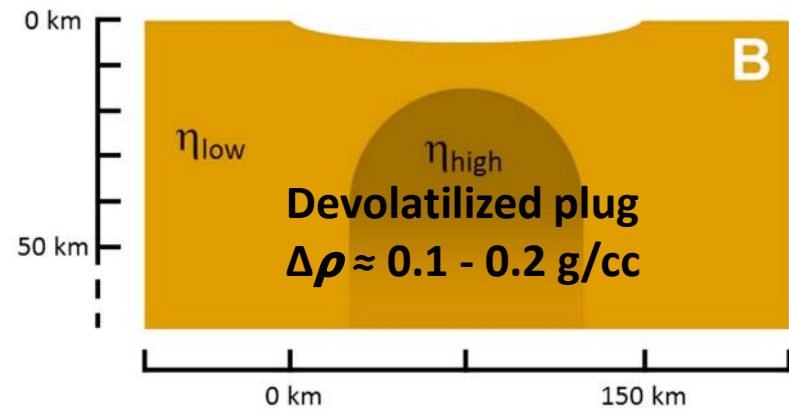
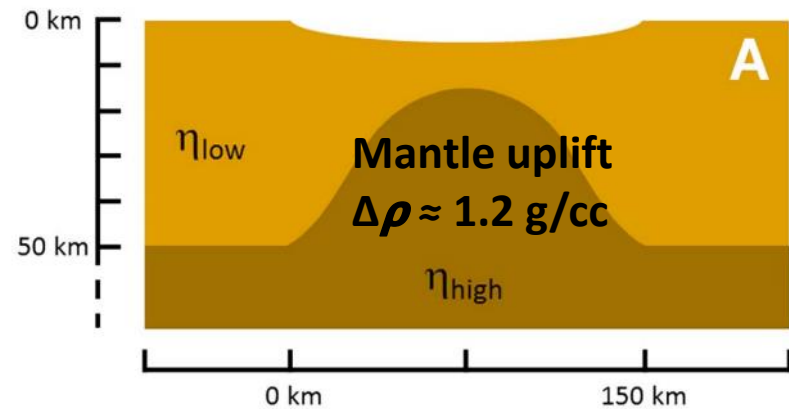
Bland et al., 2018

Mascons

Kerwan isostatic anomaly

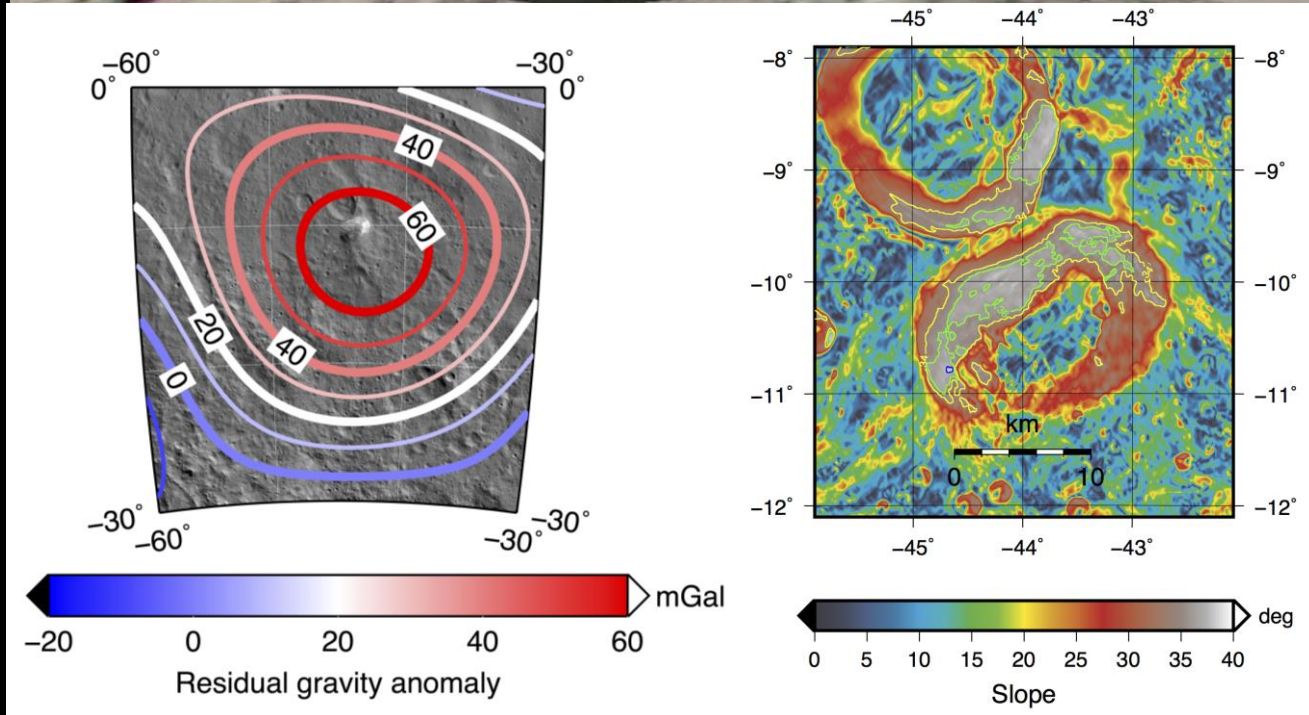
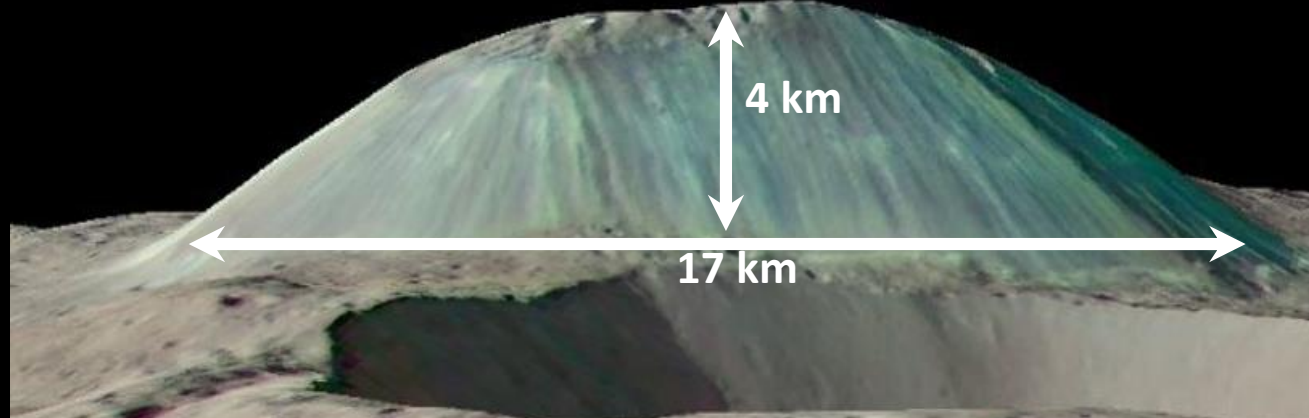


Ermakov et al., 2017



Bland et al., 2018

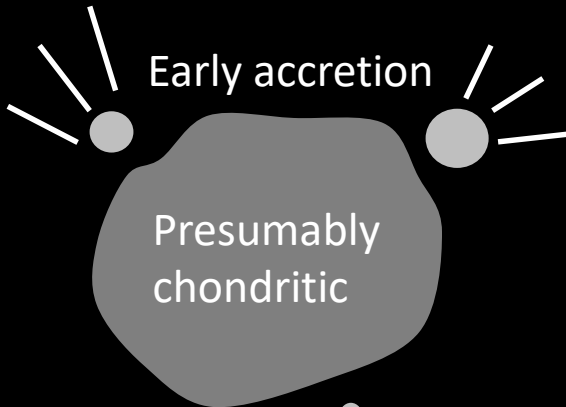
Ahuna Mons



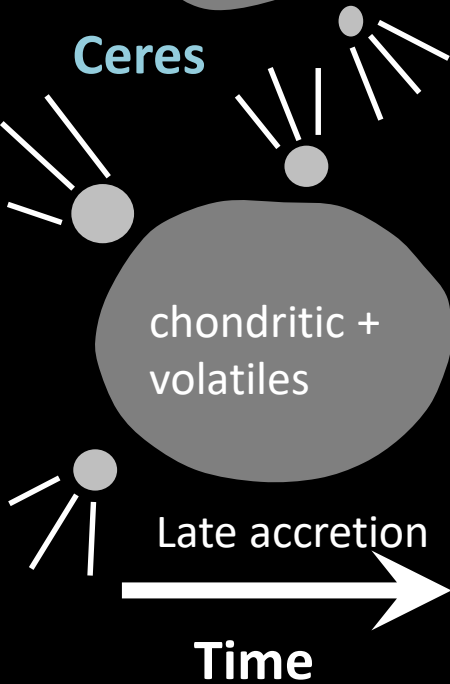


Vesta and Ceres comparative evolution

Vesta

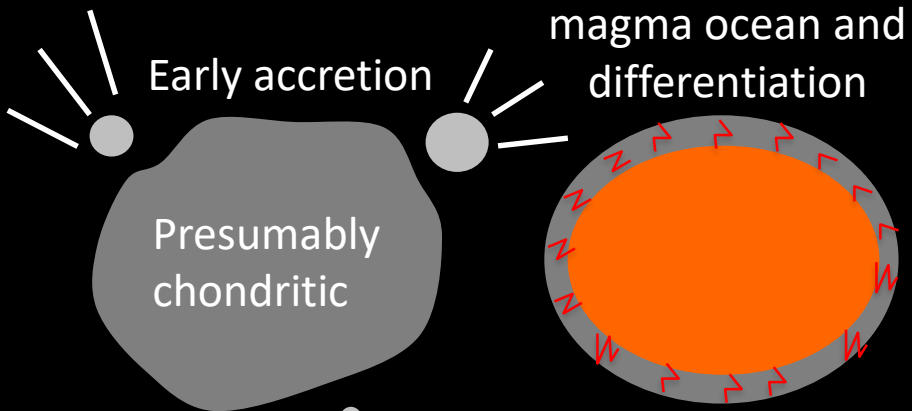


Ceres

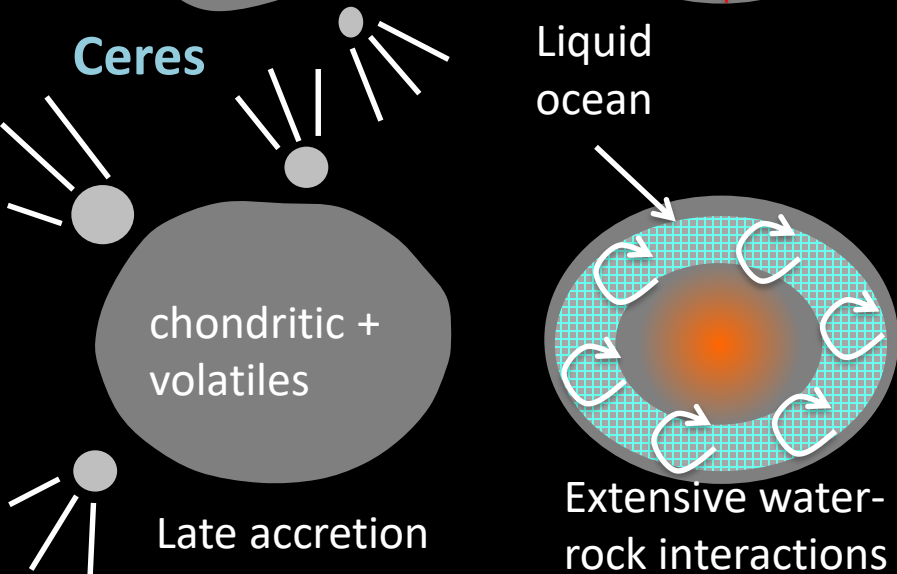


Vesta and Ceres comparative evolution

Vesta



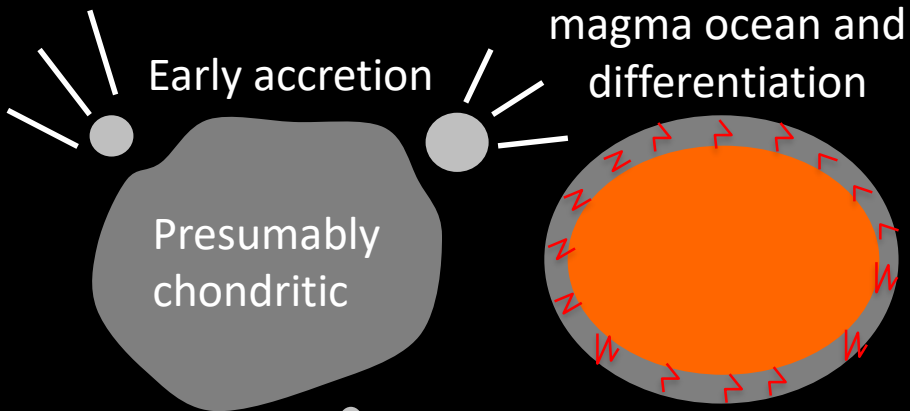
Ceres



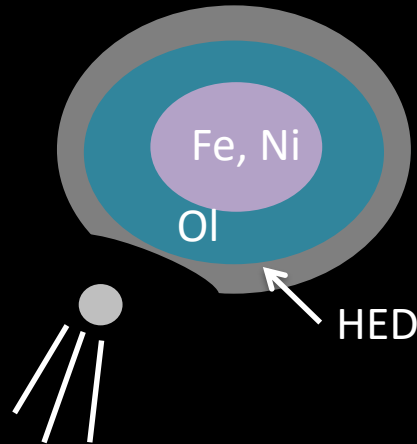
Time

Vesta and Ceres comparative evolution

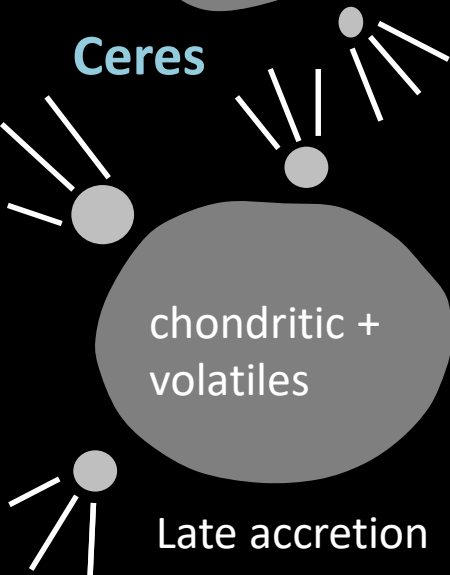
Vesta



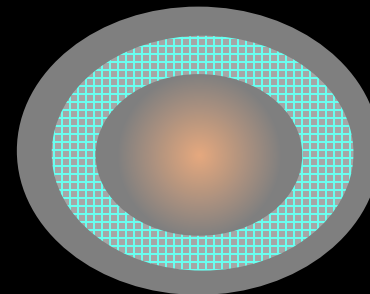
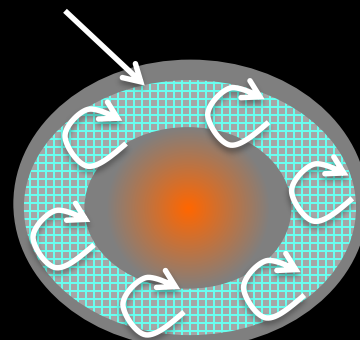
giant impact into cool Vesta



Ceres



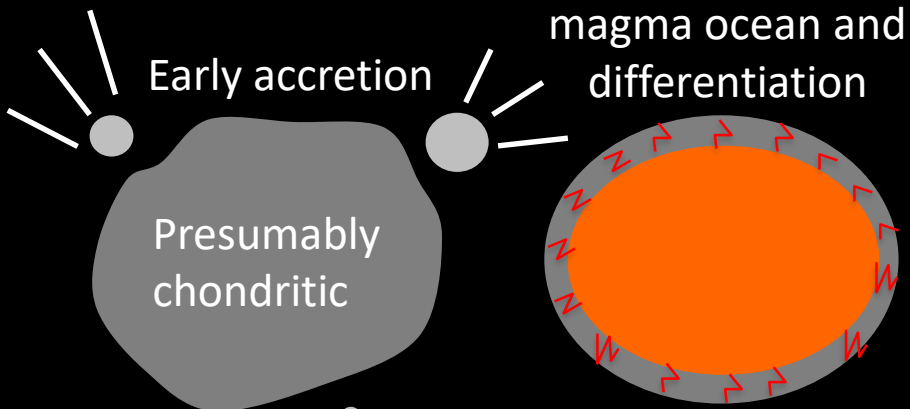
Liquid ocean



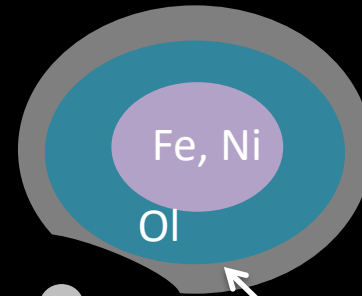
Time

Vesta and Ceres comparative evolution

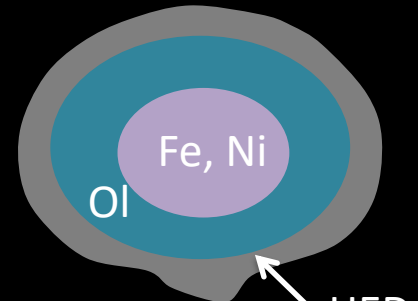
Vesta



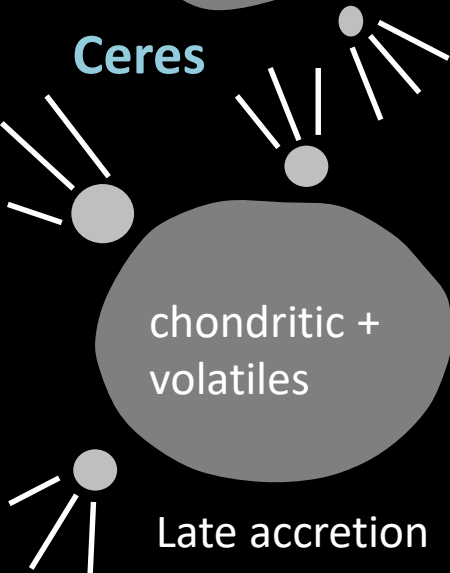
giant impact into cool Vesta



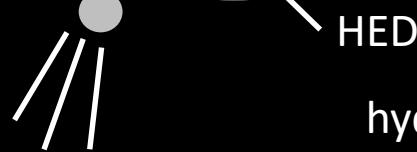
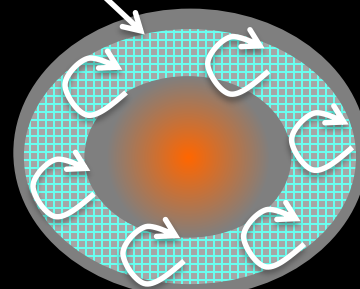
Present-state



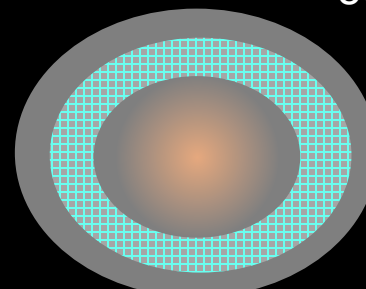
Ceres



Liquid ocean

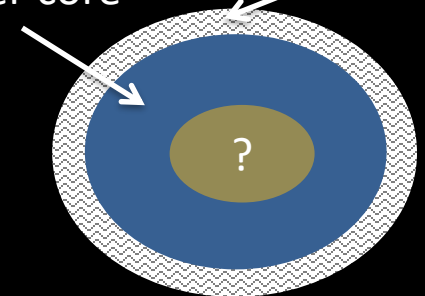


Ocean freezing
ice-rich crust erosion



hydrated
outer core

hydrated salts
water ice, rock

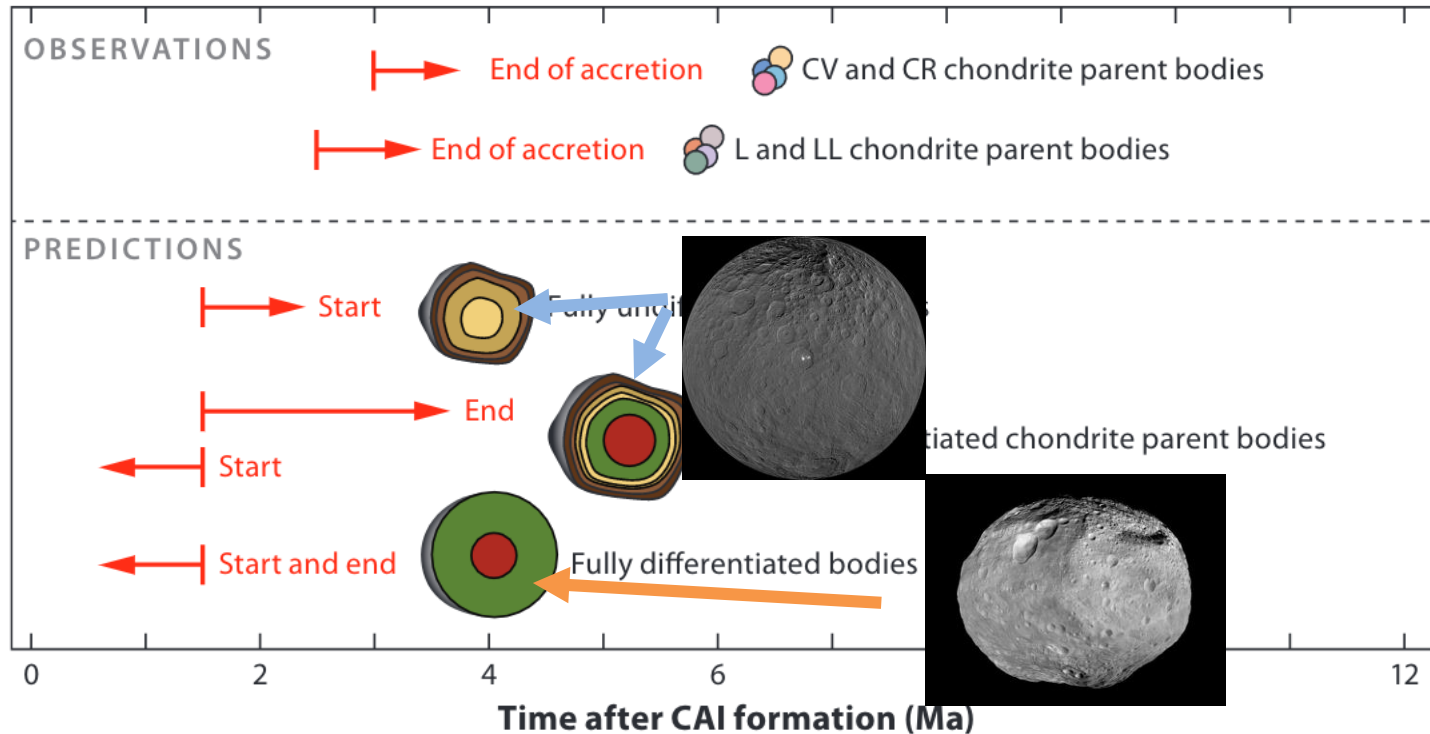


Present-state

Time

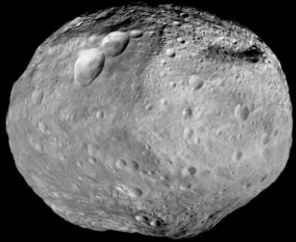
A spectrum of planetesimal differentiation

Accretion

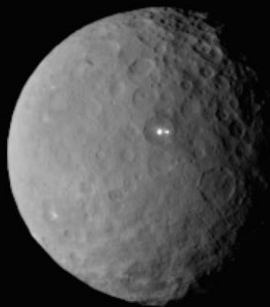


Weiss & Elkins-Tanton, 2013

Summary



- Formed early (< 5 My after CAI)
- Once hot and hydrostatic, **Vesta** is no longer either
- Differentiated interior
- Most of topography acquired when **Vesta** was already cool \Rightarrow uncompensated topography
- Combination of gravity/topography data with meteoritic geochemistry data provides constraints on the internal structure



- Cooler history
 - late formation
 - and/or heat transfer due to hydrothermal circulation
- Partially differentiated interior
- Experienced viscous relaxation
- Much lower surface viscosities (compared to Vesta) allowed compensated topography
- **Ceres'** crust is light (based on admittance analysis) and strong (based on FE relaxation modeling)
- Not much water ice in **Ceres** crust (< 35 vol%) now

Mascons on Ceres

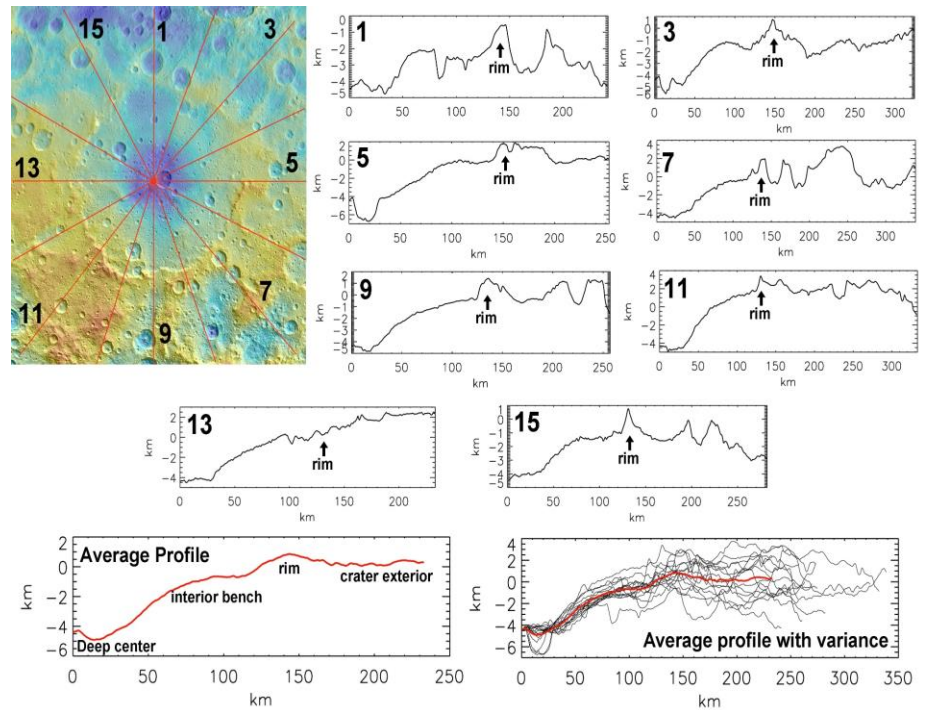
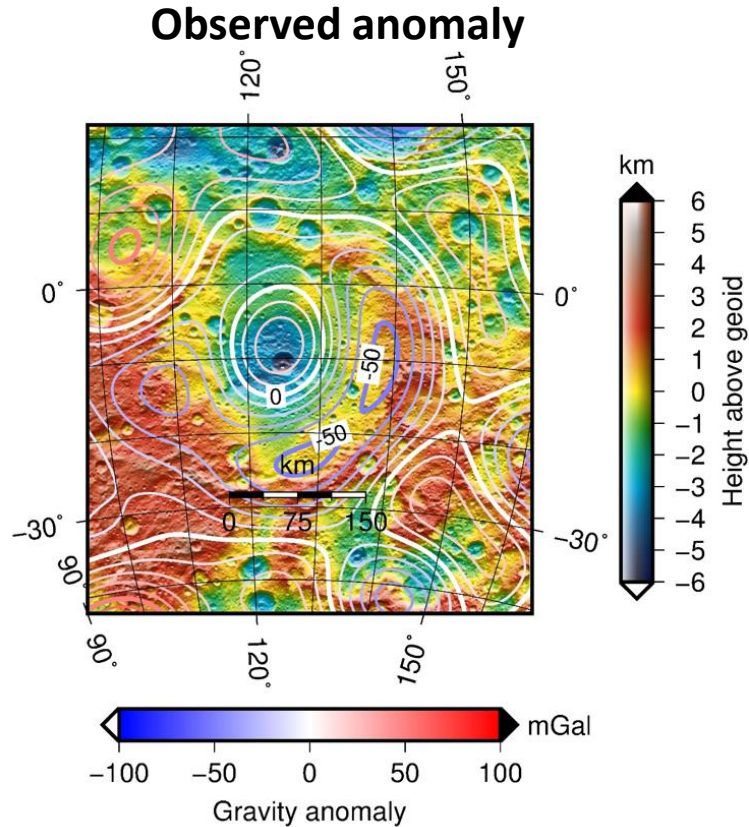


Figure S6. Isostatic gravity anomaly at Kerwan including gravity degree 3 to 16.

Contours are for gravity anomaly and the contour interval is 10 mGal. Colors show relative topography in the Kerwan region. After Ermakov et al. 2017.

Mascons on Ceres

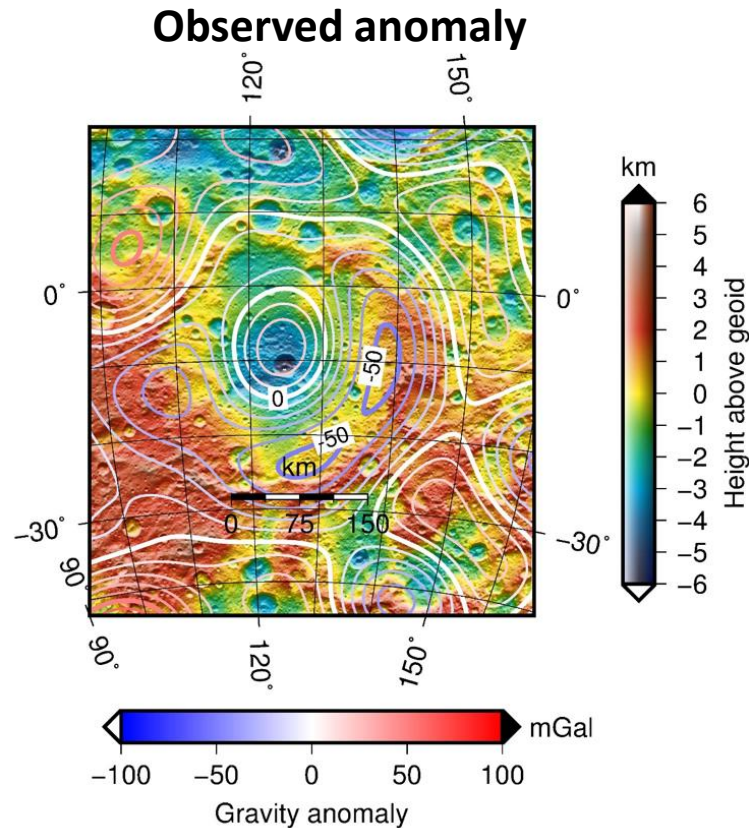


Figure S6. Isostatic gravity anomaly at Kerwan including gravity degree 3 to 16.

Contours are for gravity anomaly and the contour interval is 10 mGal. Colors show relative topography in the Kerwan region. After Ermakov et al. 2017.

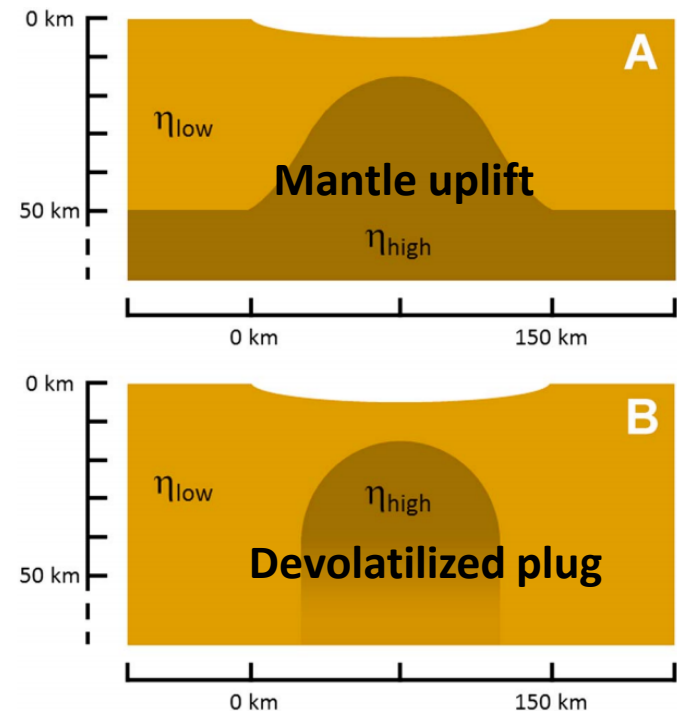


Figure 3. Two possible inferred subsurface structures beneath Kerwan. (a) Upward deflection of a high-viscosity (η) mantle beneath the crater. (b) Devolatilization of a plug of material beneath Kerwan, which increased the density and viscosity of the material. The details of the subsurface structure shown here have been selected to reproduce Kerwan's specific morphology. The latter case (b) is more consistent with other Dawn observations.

Mascons on Ceres

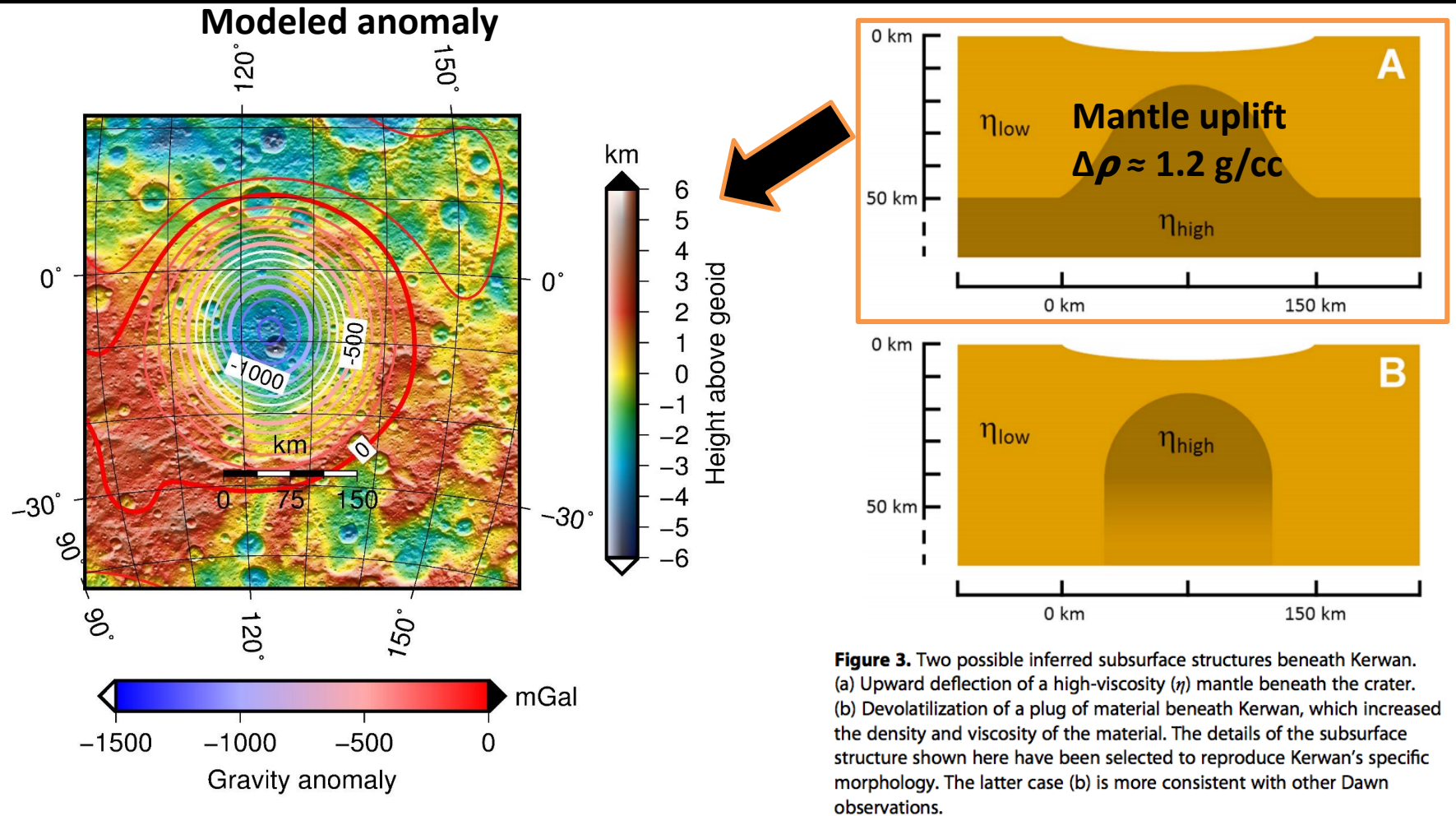
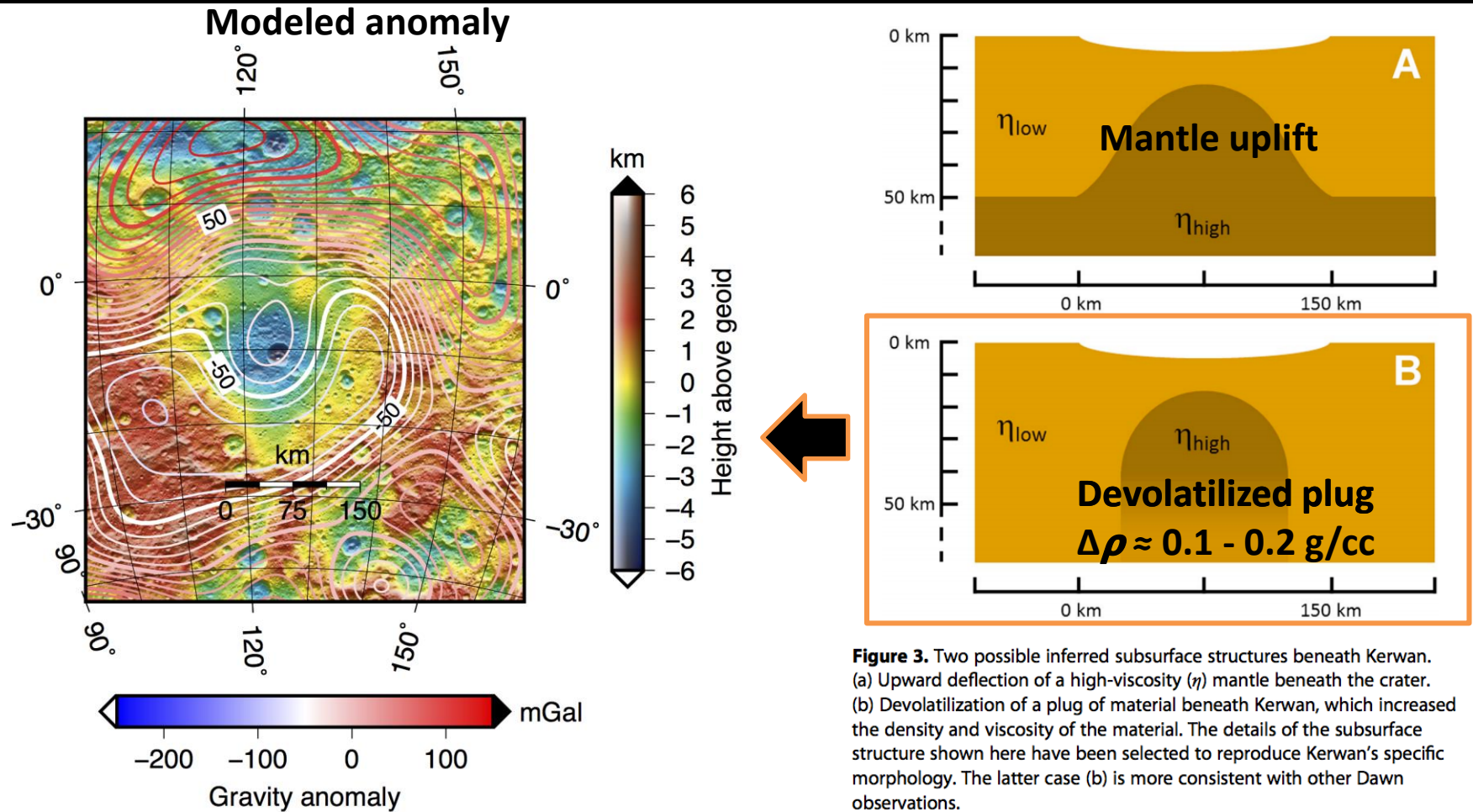
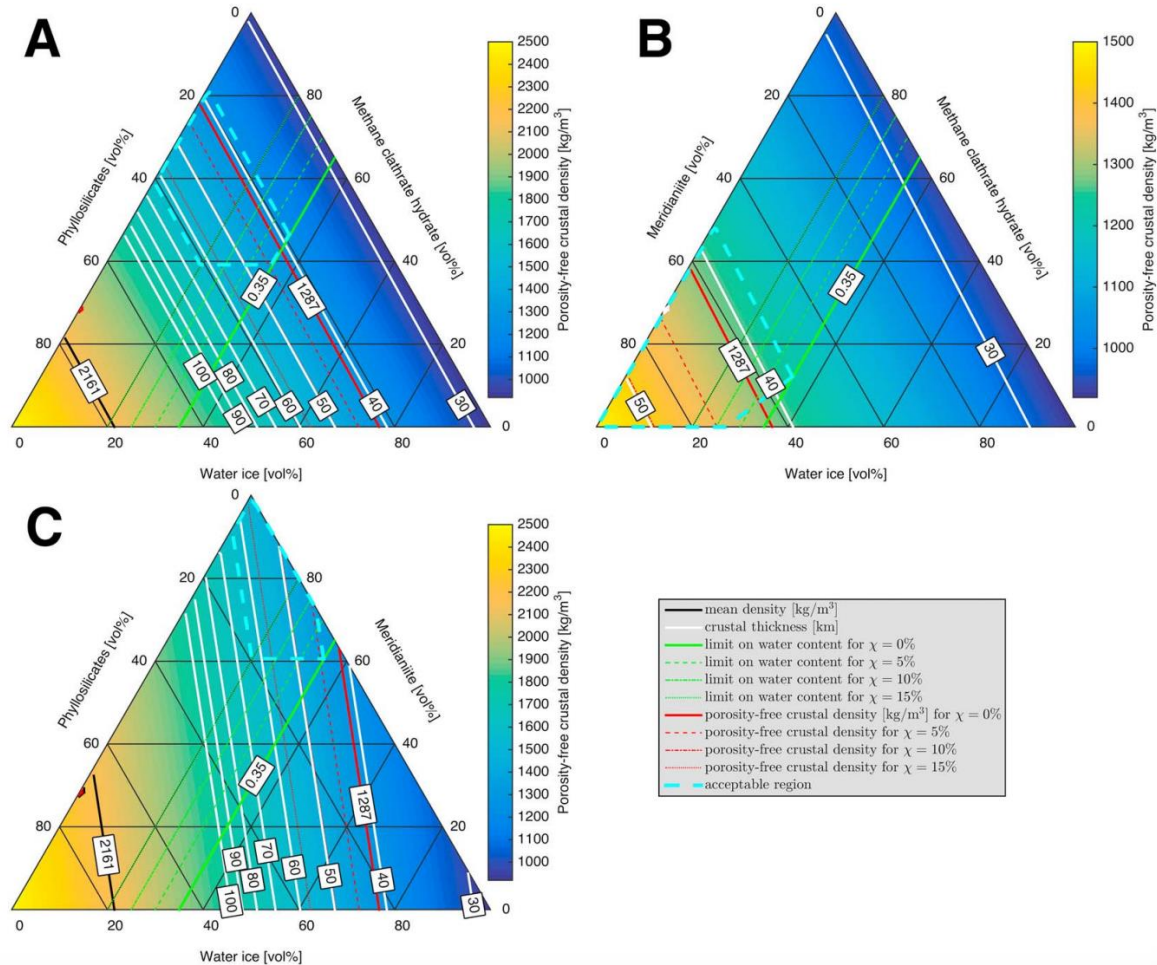


Figure 3. Two possible inferred subsurface structures beneath Kerwan. (a) Upward deflection of a high-viscosity (η) mantle beneath the crater. (b) Devolatilization of a plug of material beneath Kerwan, which increased the density and viscosity of the material. The details of the subsurface structure shown here have been selected to reproduce Kerwan's specific morphology. The latter case (b) is more consistent with other Dawn observations.

Mascons on Ceres



Crustal composition constraints

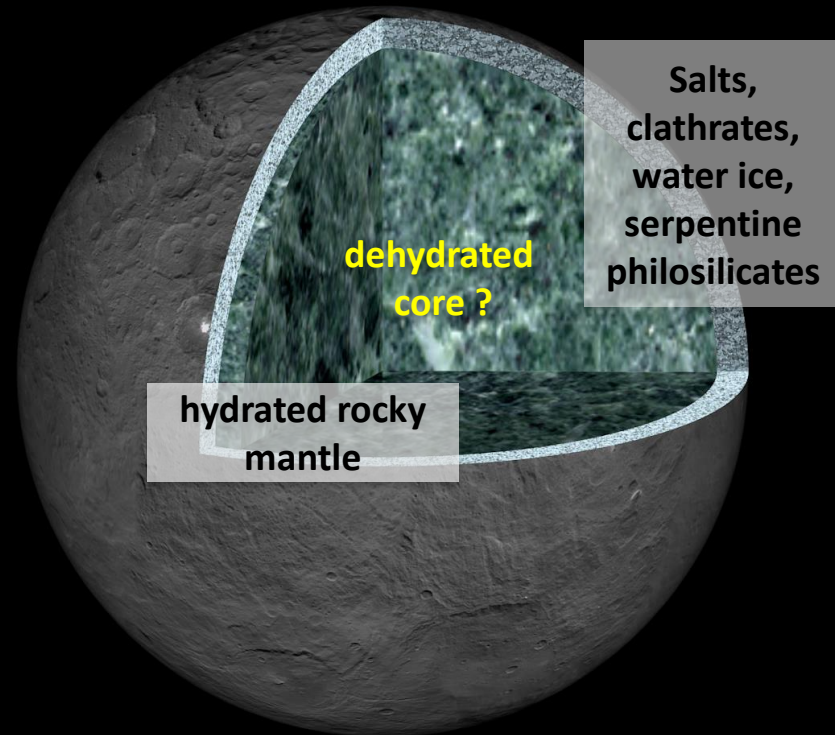
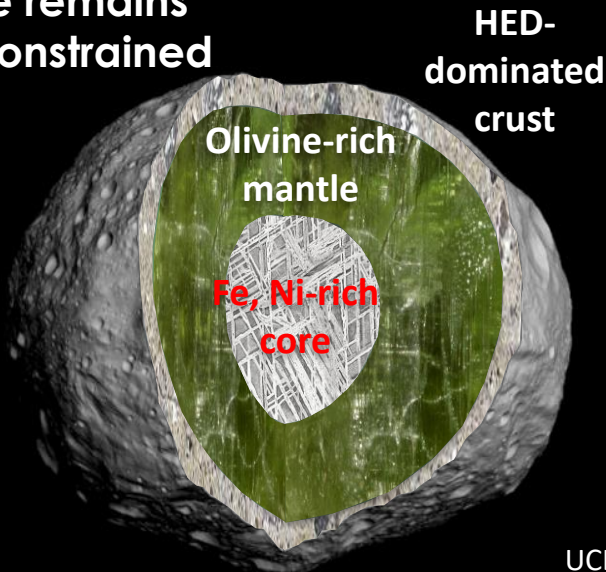


Ermakov et al., 2017

Internal structures of Vesta and Ceres

Ceres →

- Crust is light (1.1-1.4 g/cc) and mechanically rock-like w
- Mantle density ~2.4 g/cc and unlithified at least to a depth of 100 km
- Possible dehydrated rocky core remains unconstrained

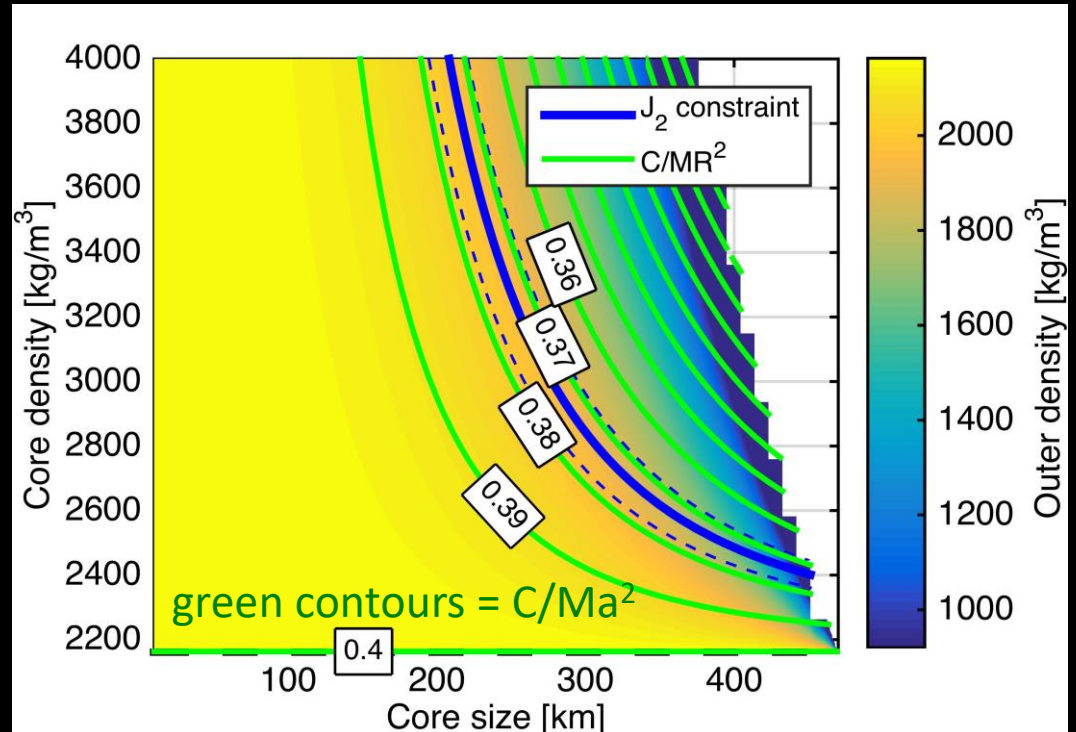


← Vesta

- Crustal density constrained by HEDs and admittance (2.8 g/cc)
- Assuming density of iron meteorites (5-8 g/cc), the core radius is 110 – 155 km

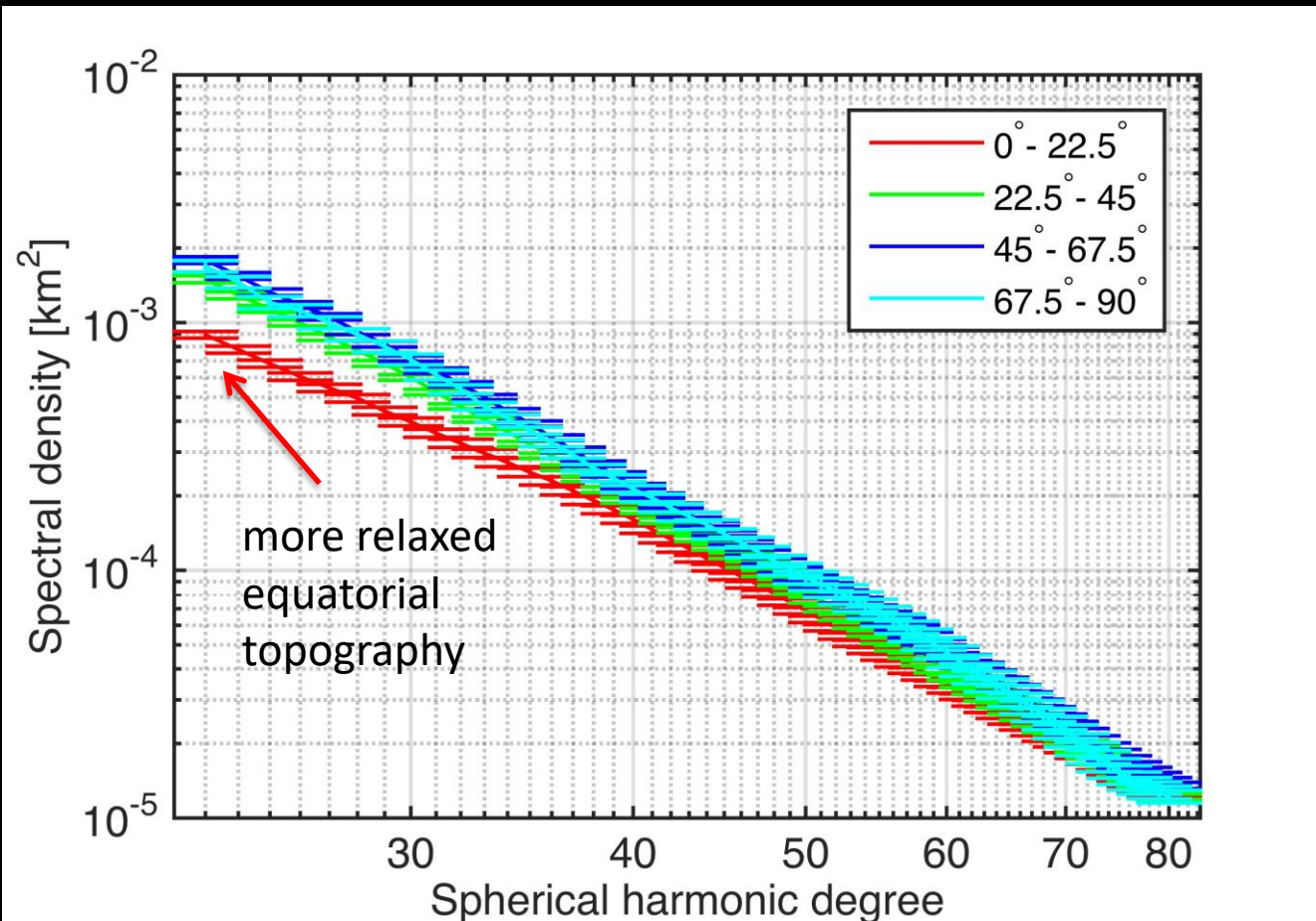
Two-layer model

- Simplest model to interpret the gravity-topography data
- Only 5 parameters: two densities, two radii and rotation rate
- Yields $C/Ma^2 = 0.373$
 $C/M(R_{\text{vol}})^2 = 0.392$



Using Tricarico 2014 for computing hydrostatic equilibrium

Latitude dependence of relaxation



Ermakov et al., in prep

Gravity and topography in spherical harmonics

- Shape radius vector

$$r(f, l) = R_0 \sum_{n=1}^{\infty} \sum_{m=0}^n (A_{nm} \cos(m l) + B_{nm} \sin(m l)) P_{nm}(\sin f)$$

- Gravitational potential

$$U(r, f, l) = \frac{GM}{R} + \sum_{n=2}^{\infty} \sum_{m=0}^n \frac{R_0^n}{r^{n+1}} (C_{nm} \cos(m l) + S_{nm} \sin(m l)) P_{nm}(\sin f)$$

- Power Spectral Density

$$S_n^{gg} = \sum_{m=0}^n \frac{C_{nm}^2 + S_{nm}^2}{2n+1}$$

gravity

$$S_n^{tt} = \sum_{m=0}^n \frac{A_{nm}^2 + B_{nm}^2}{2n+1}$$

topography

$$S_n^{gt} = \sum_{m=0}^n \frac{A_{nm} C_{nm} + B_{nm} S_{nm}}{2n+1}$$

gravity-topography
cross power

Isostatic model

Z_n - gravity-topography admittance

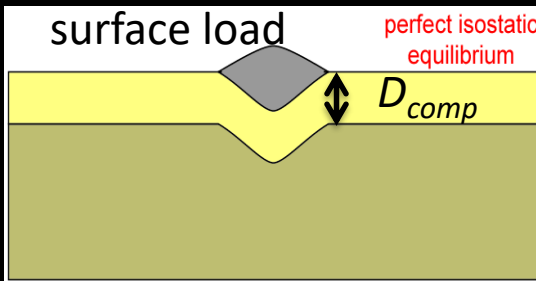
$$Z_n = \frac{S_{gt}}{S_{tt}}$$

➤ Linear two-layer hydrostatic model

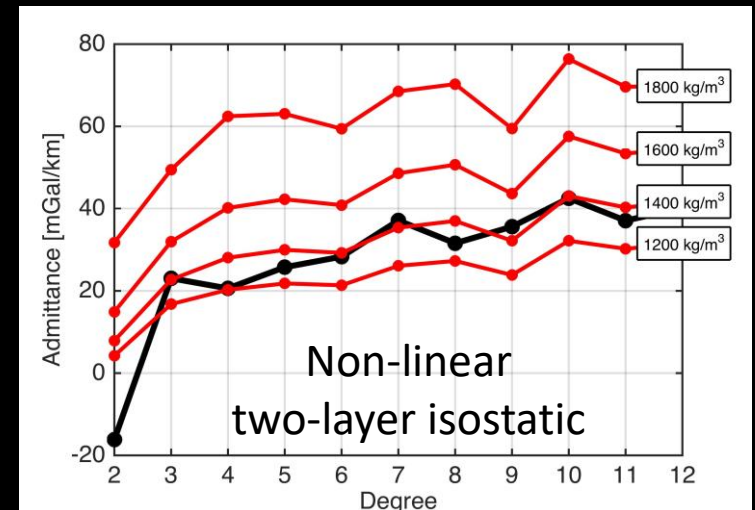
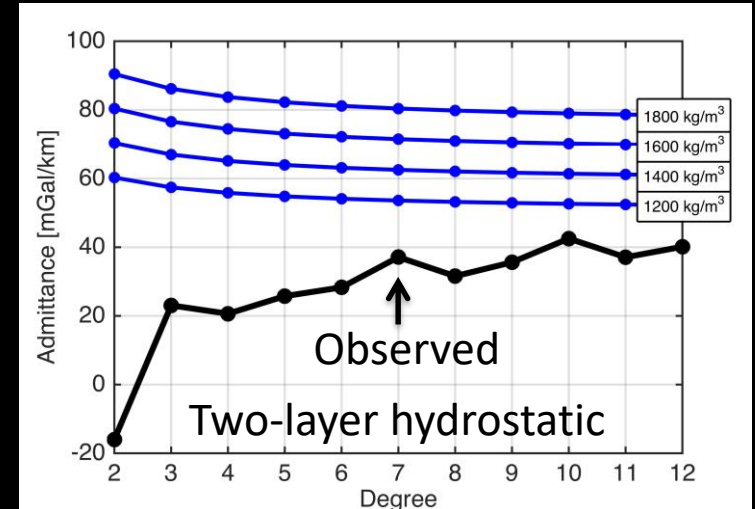
$$Z_n = \frac{GM}{R^3} \frac{3(n+1)}{2n+1} \frac{r_{crust}}{r_{mean}}$$

➤ Linear isostatic model

$$Z_n = \frac{GM}{R^3} \frac{3(n+1)}{2n+1} \frac{r_{crust}}{r_{mean}} \left(1 - \frac{D_{comp}}{R} \right)$$

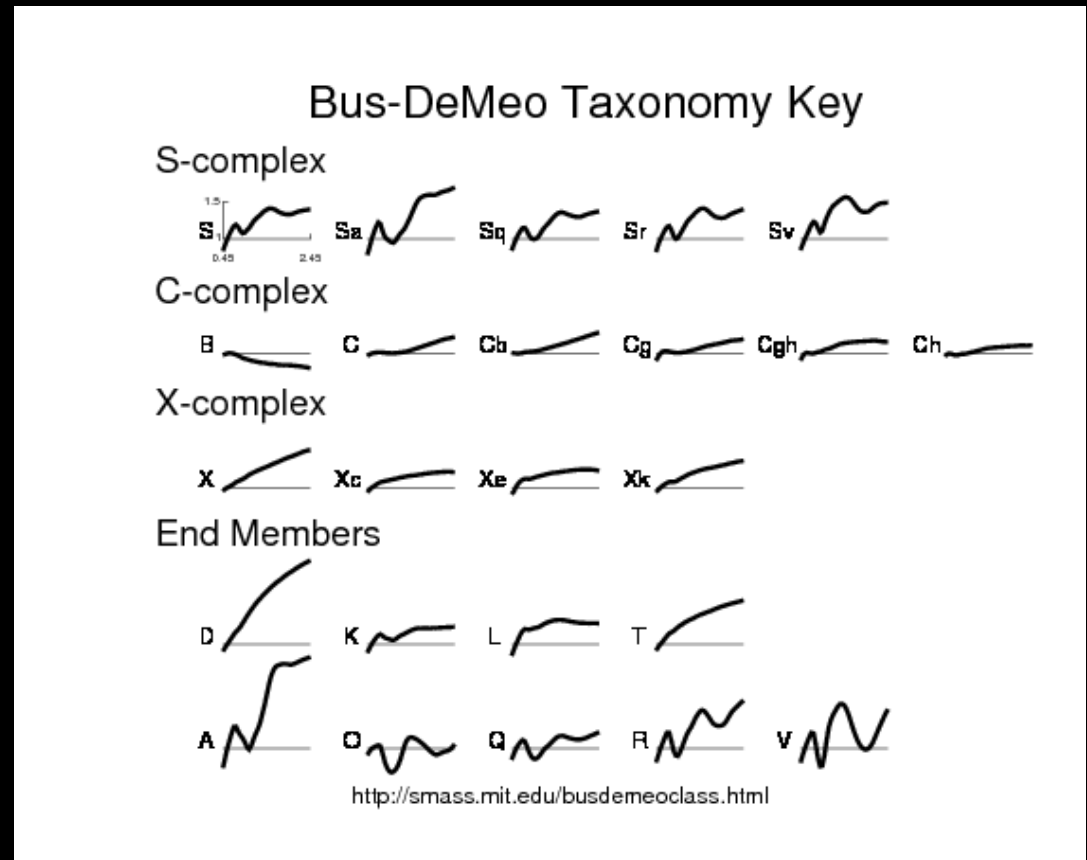


D_{comp} - depth of compensation



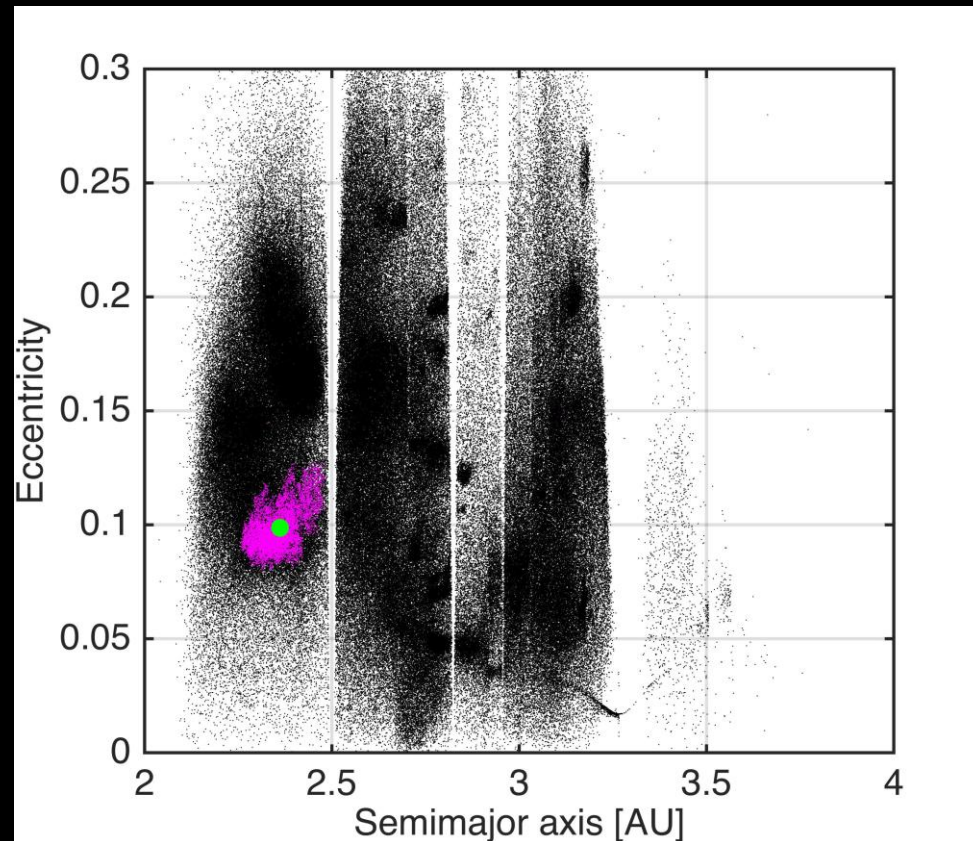
Why Vesta?

- Unique basaltic spectrum



Why Vesta?

- Unique basaltic spectrum
- A group of asteroids in the dynamical vicinity of Vesta with similar spectra



Why Vesta?

- Unique basaltic spectrum
- A group of asteroids in the dynamical vicinity of Vesta with similar spectra
- Large depression in the southern hemisphere of Vesta

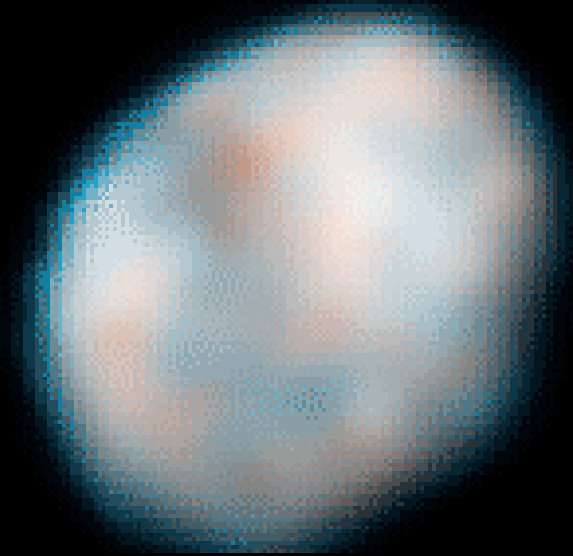
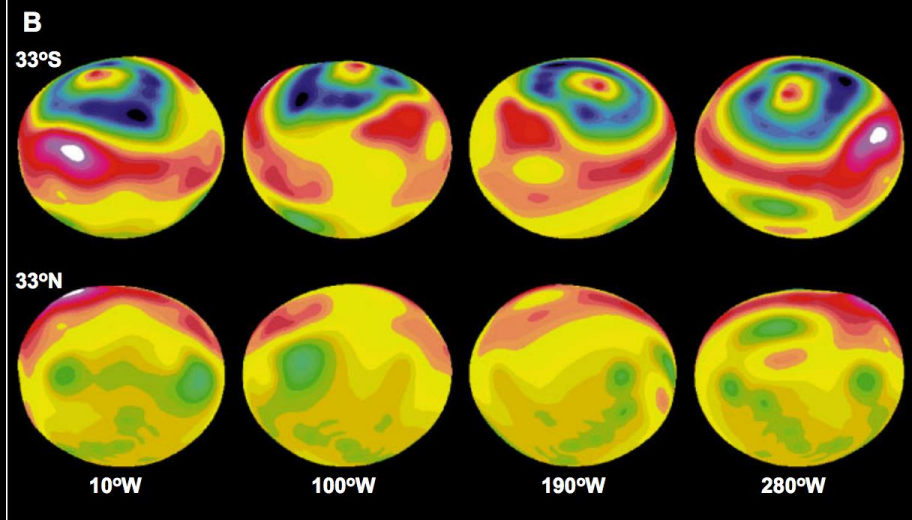


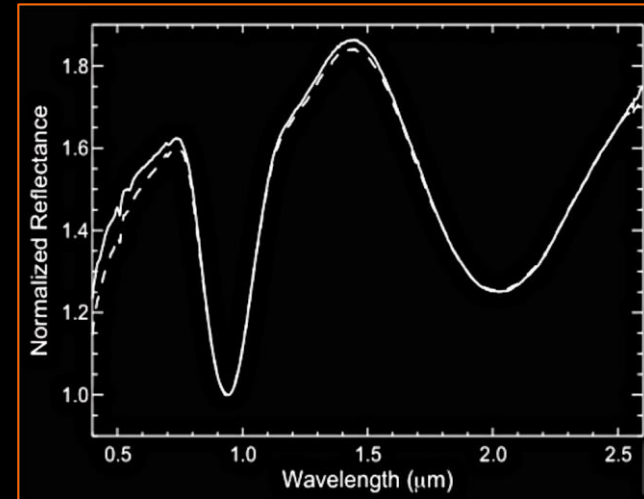
Image credit: NASA/HST



UCLA planetary seminar Thomas et al., 1997

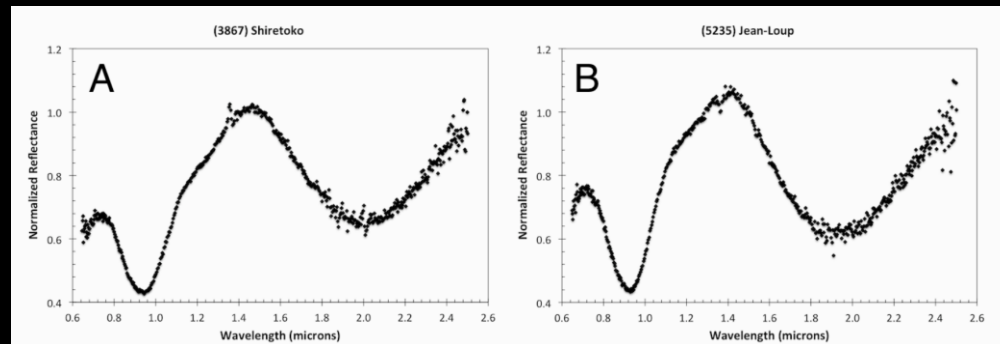
Why Vesta?

- Unique basaltic spectrum
- A group of asteroids in the dynamical vicinity of Vesta with similar spectra
- Large depression in the southern hemisphere of Vesta
- A group of Howardite-Eucrite-Diogenite (HED) meteorites, with similar reflectance spectra



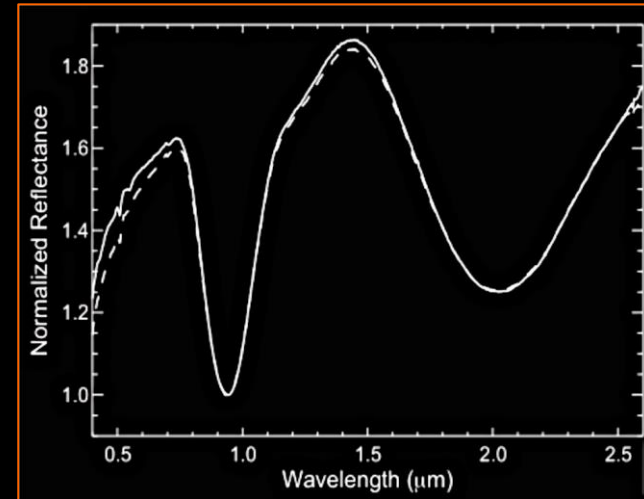
↑ Reflectance spectra of eucrite Millbillillie from Wasson et al. (1998)

↓ V-type asteroids spectra from Hardensen et al., (2014)



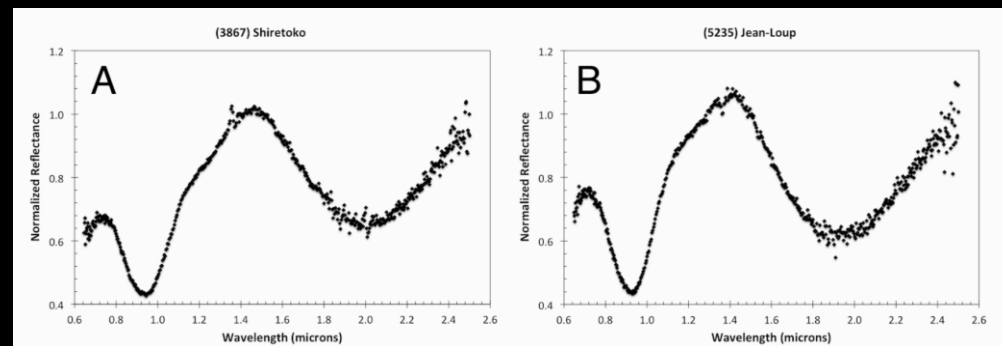
Why Vesta?

- Unique basaltic spectrum
- A group of asteroids in the dynamical vicinity of Vesta with similar spectra
- Large depression in the southern hemisphere of Vesta
- A group of Howardite-Eucrite-Diogenite (HED) meteorites, with similar reflectance spectra
- Strongest connection between a class of meteorites and an asteroidal family



↑ Reflectance spectra of eucrite Millbillillie from Wasson et al. (1998)

↓ V-type asteroids spectra from Hardensen et al., (2014)



Note on Vening-Meinesz and Kaula rules

- Vening-Meinesz rule for variance of topography (Vening-Meinesz, 1951)

$$V_t \sim 1/n^2$$

- Kaula law for RMS of gravity (Kaula, 1963)

$$M_g \sim 1/n^2$$

- Are these two rules consistent assuming uncompensated topography?

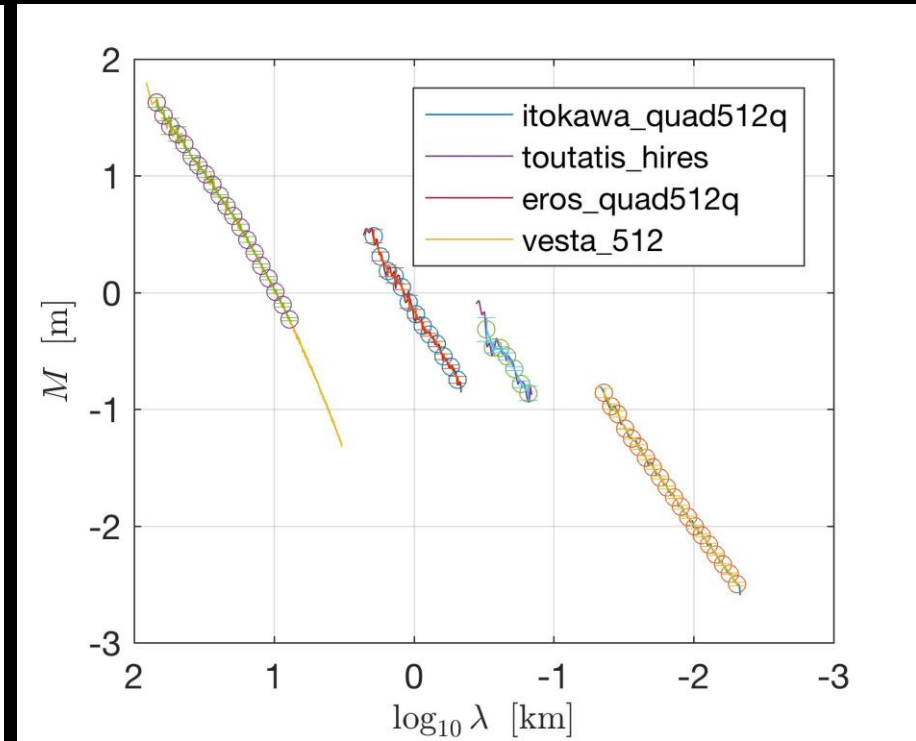
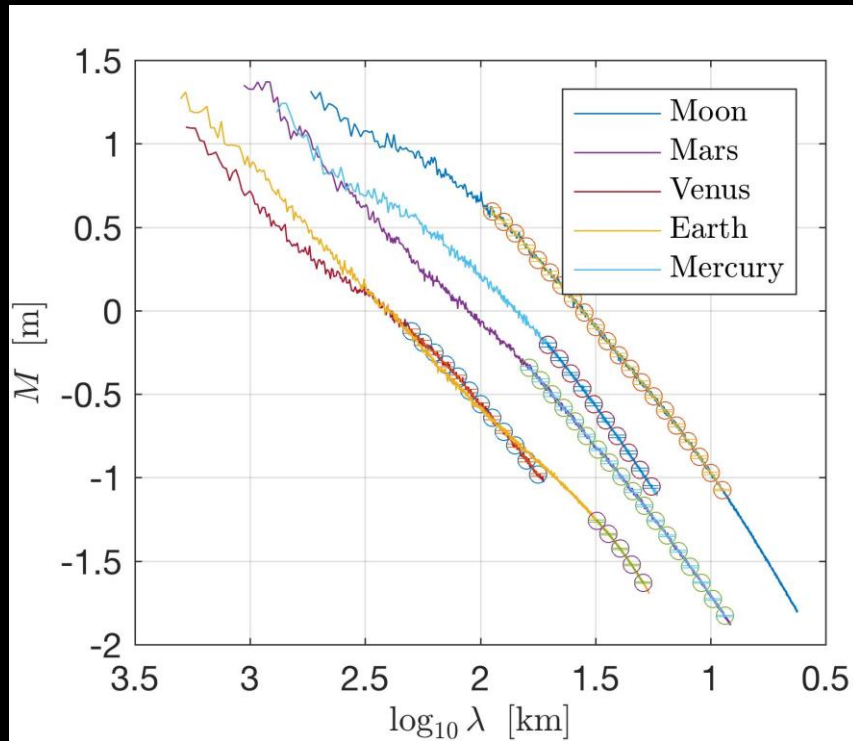
$$V_t \sim 1/n^2 \Rightarrow M_t \sim 1/n^{1.5} \Rightarrow M_g \sim 1/n^{2.5}$$

- But Kaula rule says $M_g \sim 1/n^2$ NOT $M_g \sim 1/n^{2.5}$



- Typically assumed in the literature Kaula and Vening-Meinesz rules are not mutually consistent assuming uncompensated topography

RMS spectra



Power laws

- General form of a power law

$$M = AR^{\alpha_1} \varrho^{\alpha_2} \lambda^{\alpha_3}$$

- Power law assuming (inverse) surface gravity scaling ($g \sim R^* \rho$)

$$M = AR^{-1} \varrho^{-1} \lambda^{\alpha_3}$$

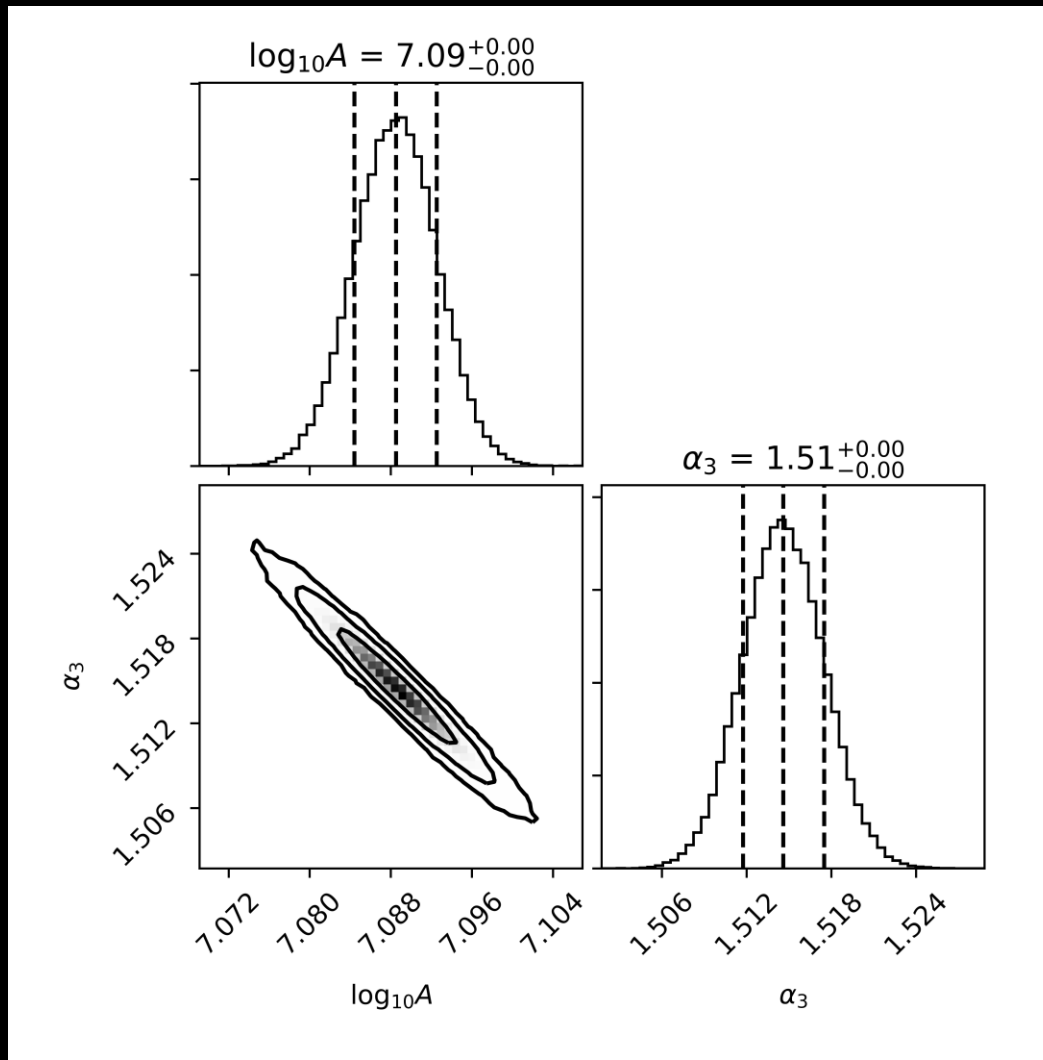
- If we take a \log_{10} of M , we get an equation of a hyperplane

$$\log_{10} M = \log_{10} A + \alpha_1 \log_{10} R + \alpha_2 \log_{10} \varrho + \alpha_3 \log_{10} \lambda$$

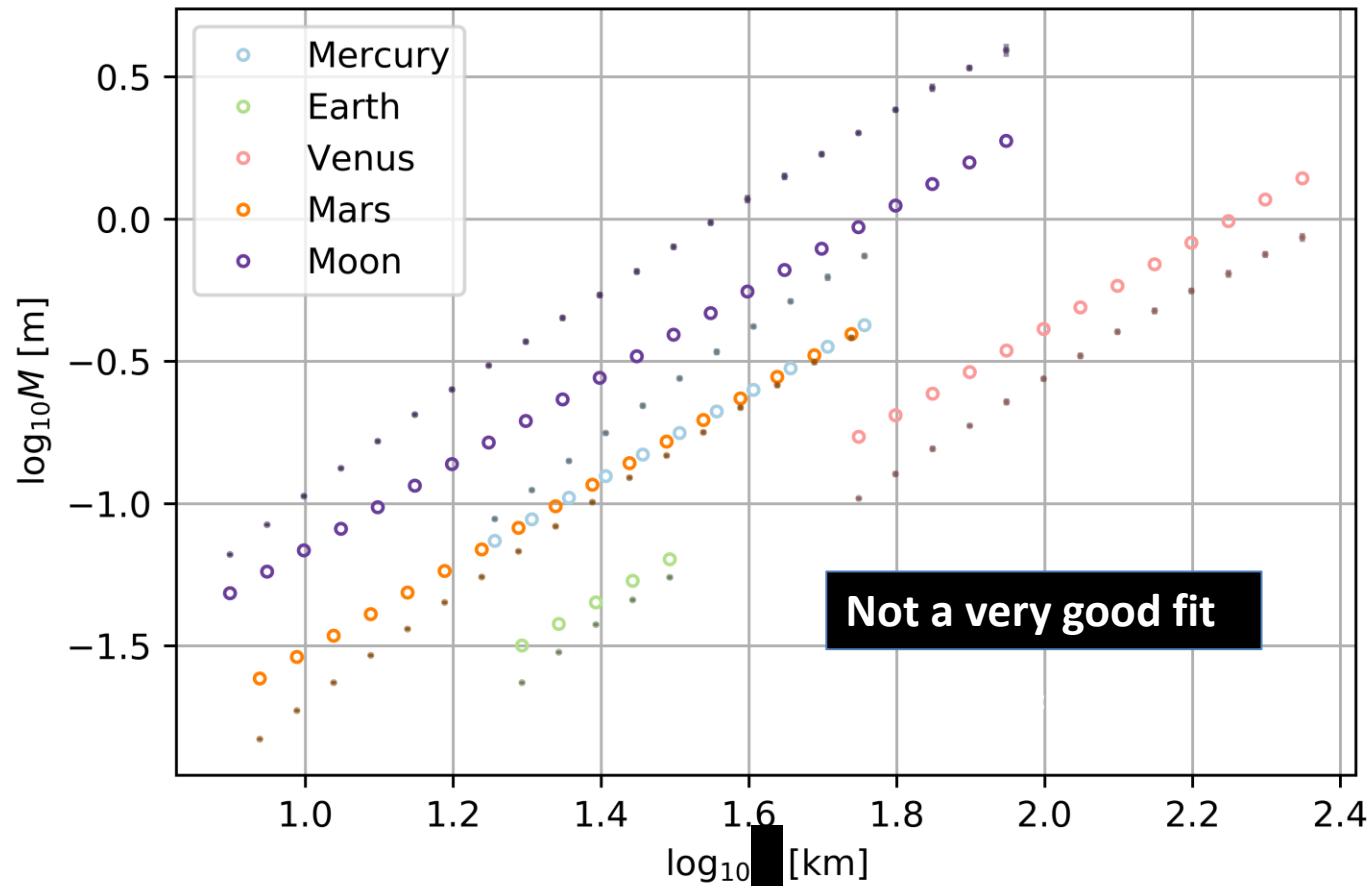
- In our data set, we have a lot of points along the λ direction and not as many points on the other two (R and ρ) directions.
 - In the R and ρ directions, we have as many data points as we have bodies
 - In the λ direction, we have as many data points as many we have λ bins.

Results of the MCMC runs

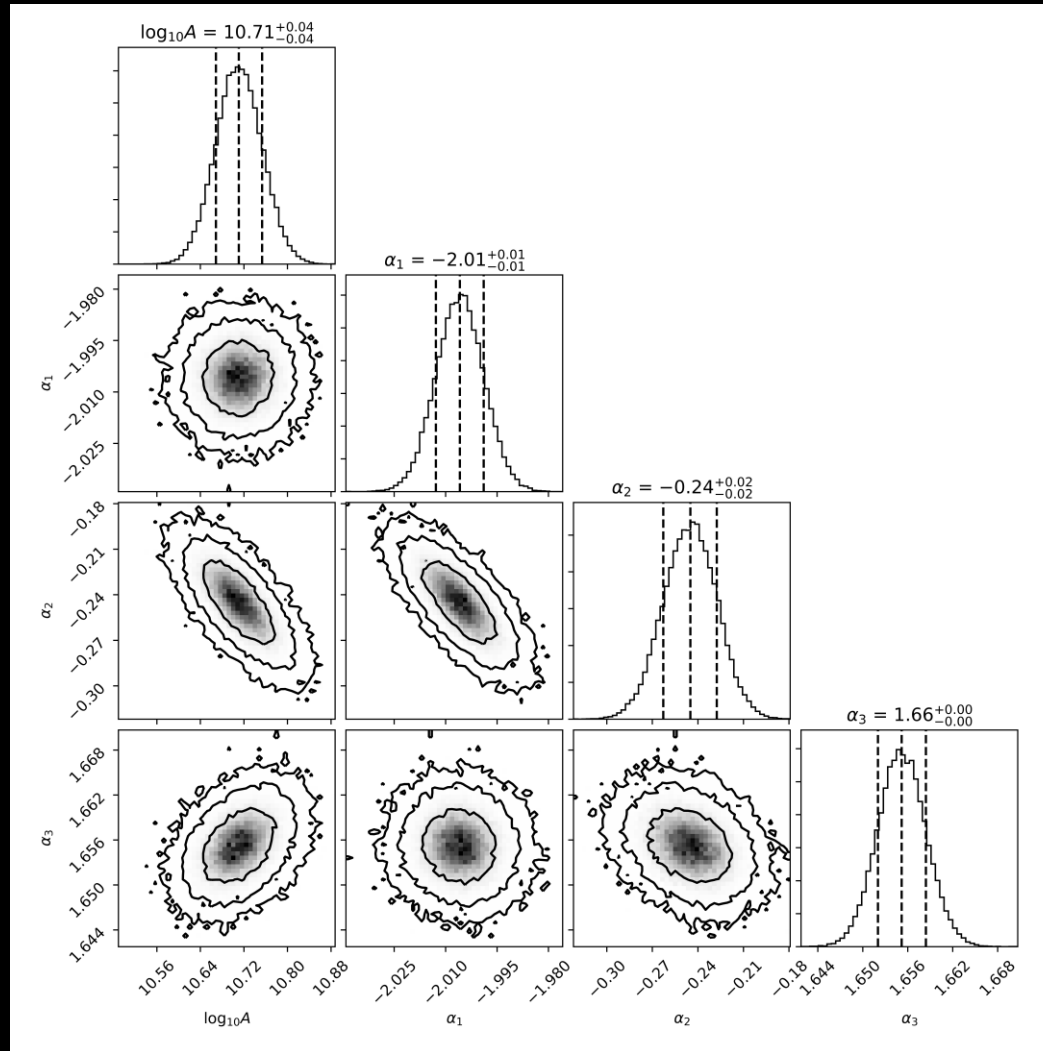
Planets, gravity scaling



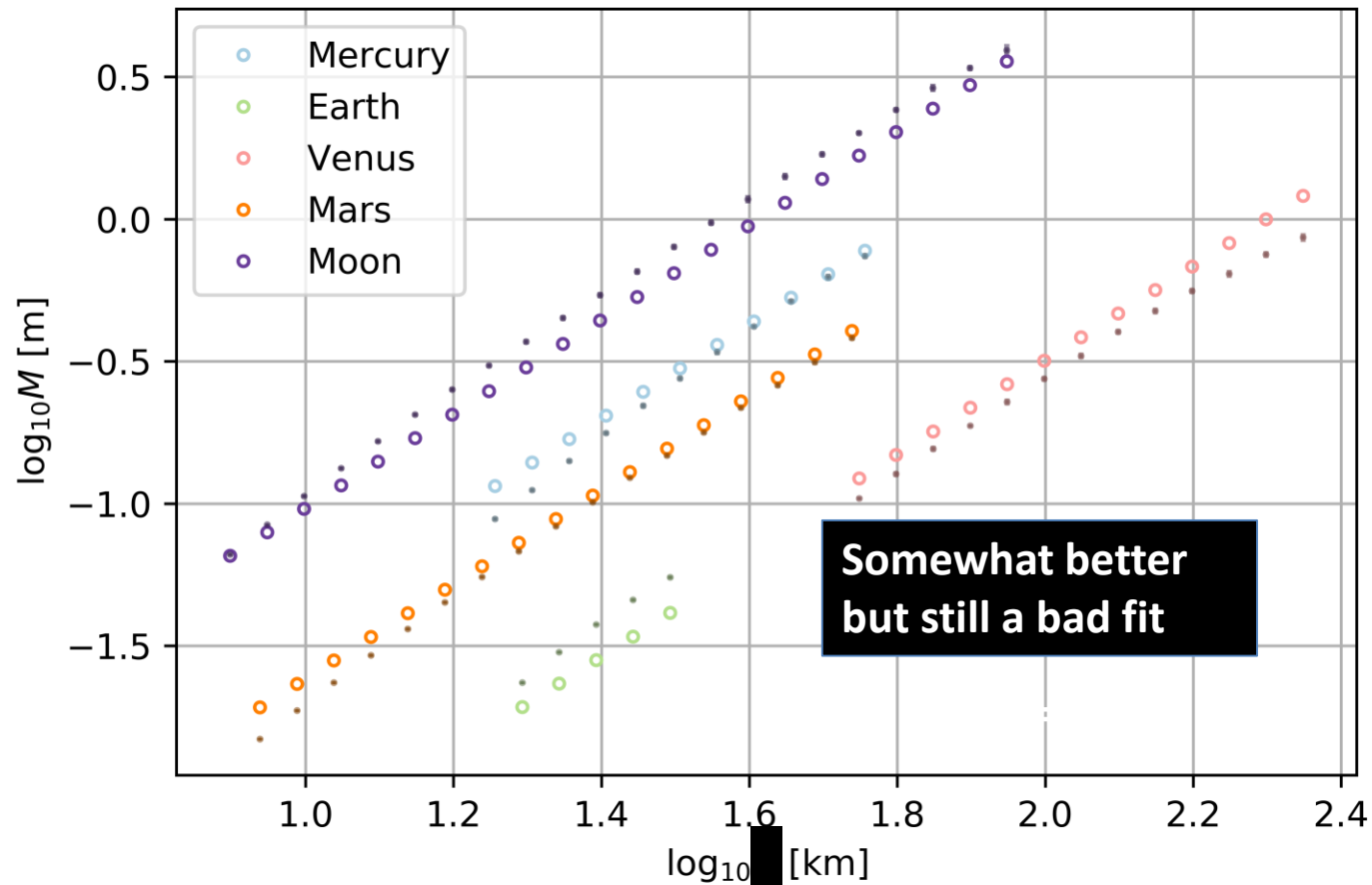
Planets, gravity scaling



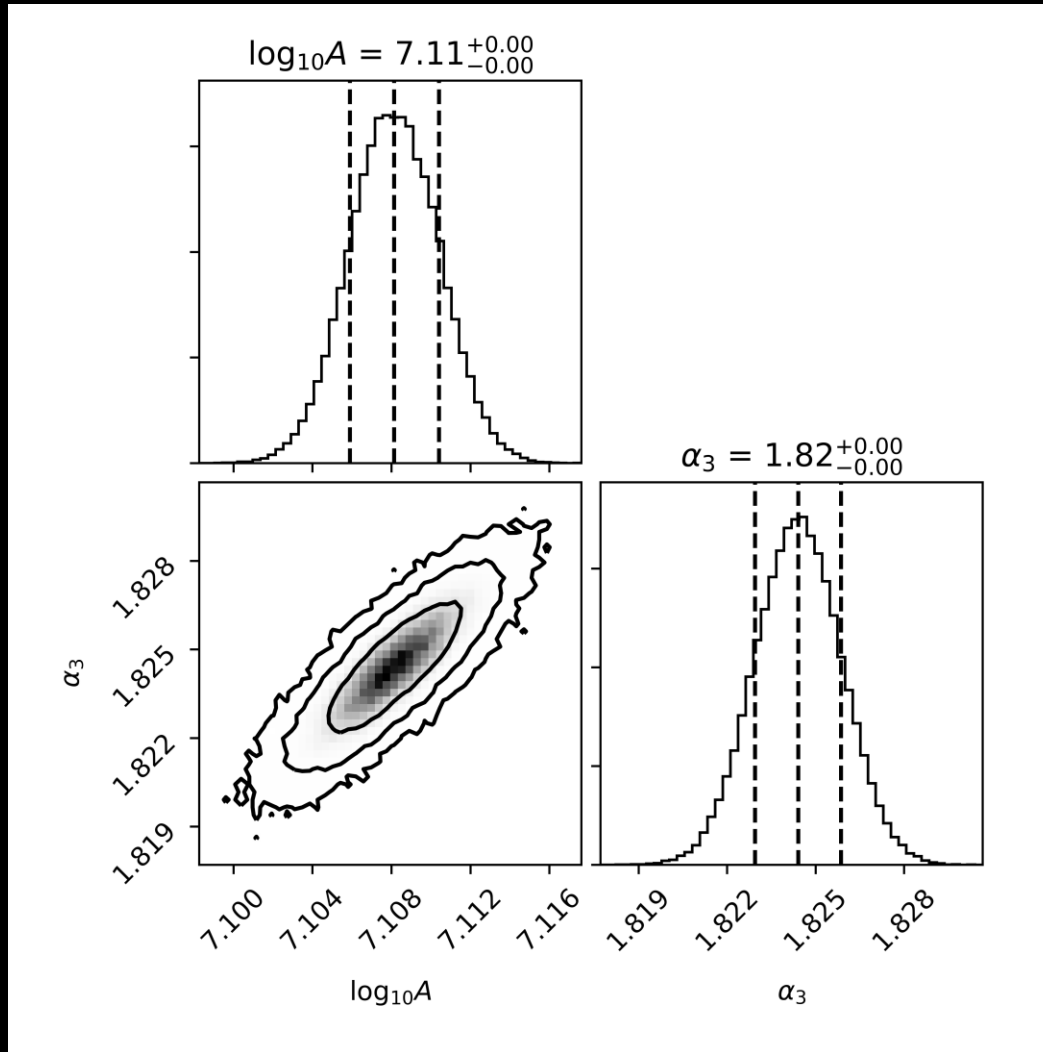
Planets, general scaling



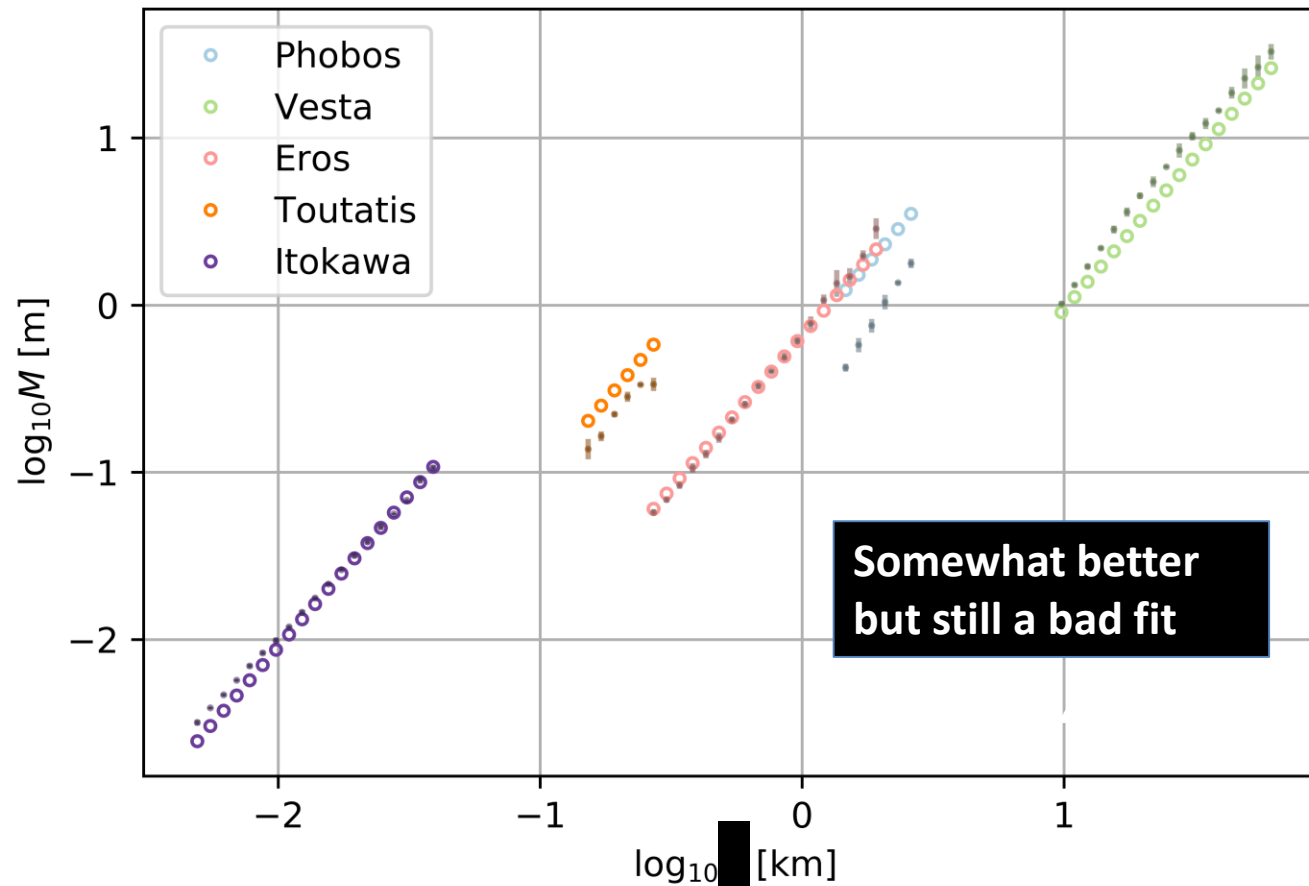
Planets, general scaling



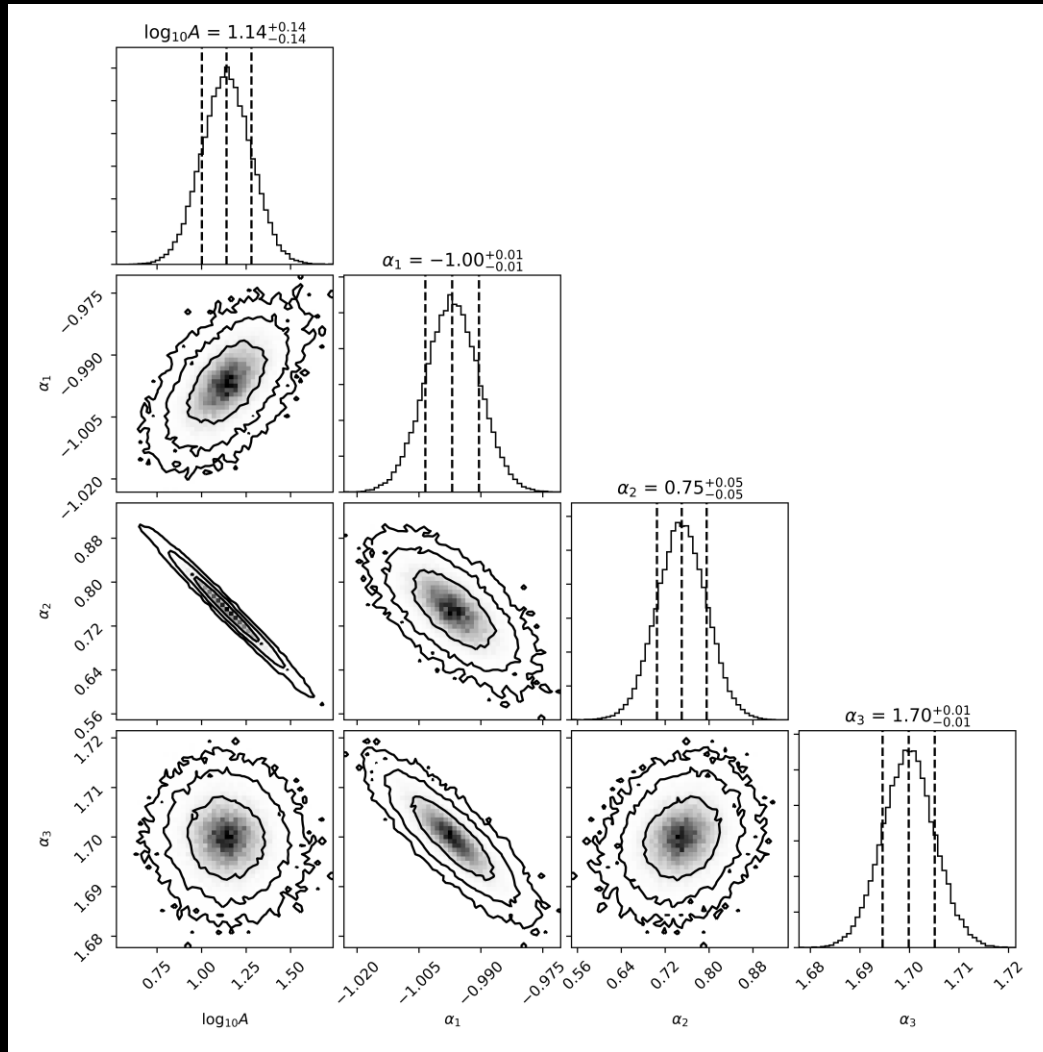
Asteroids, gravity scaling



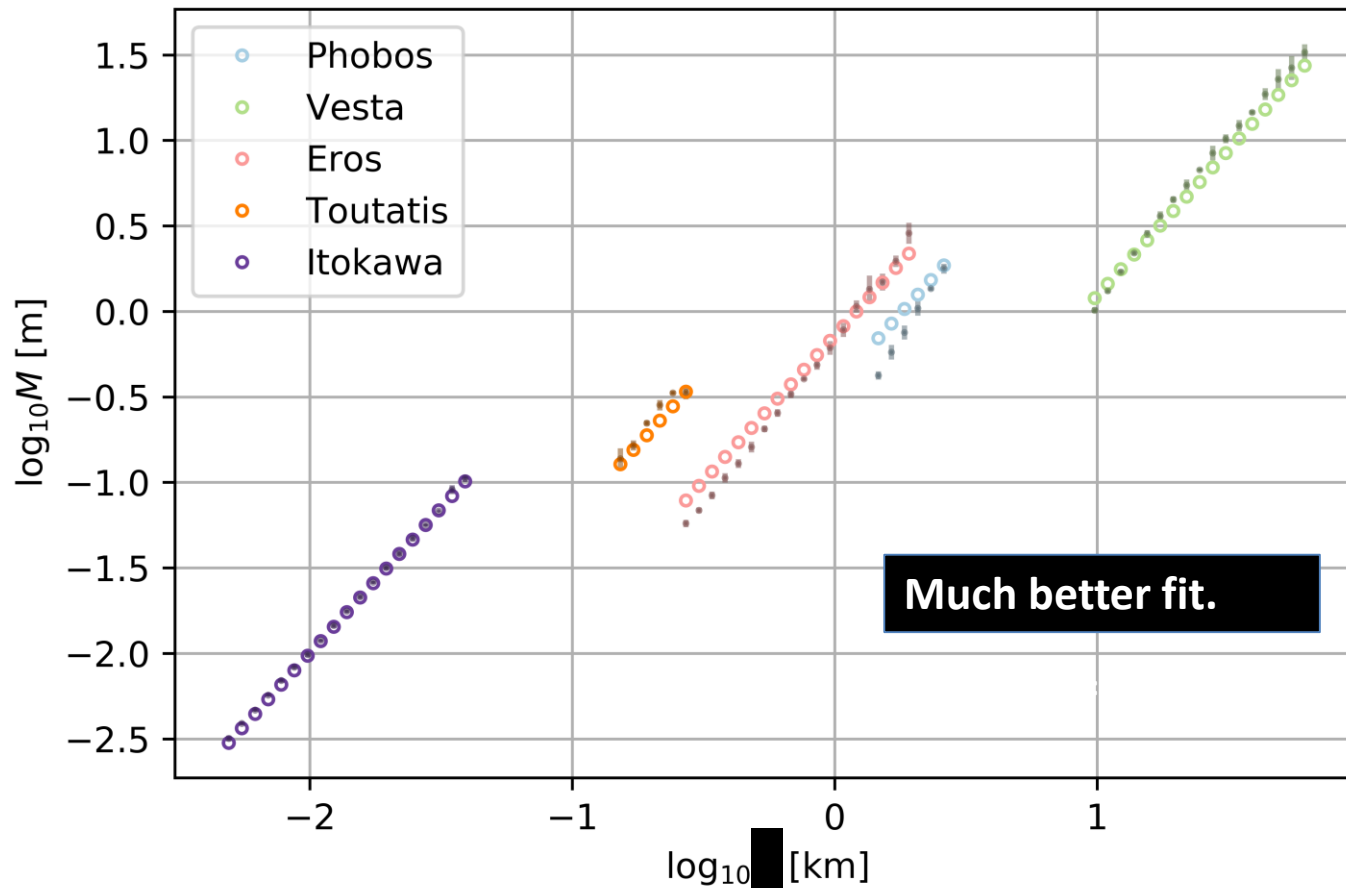
Asteroids, gravity scaling



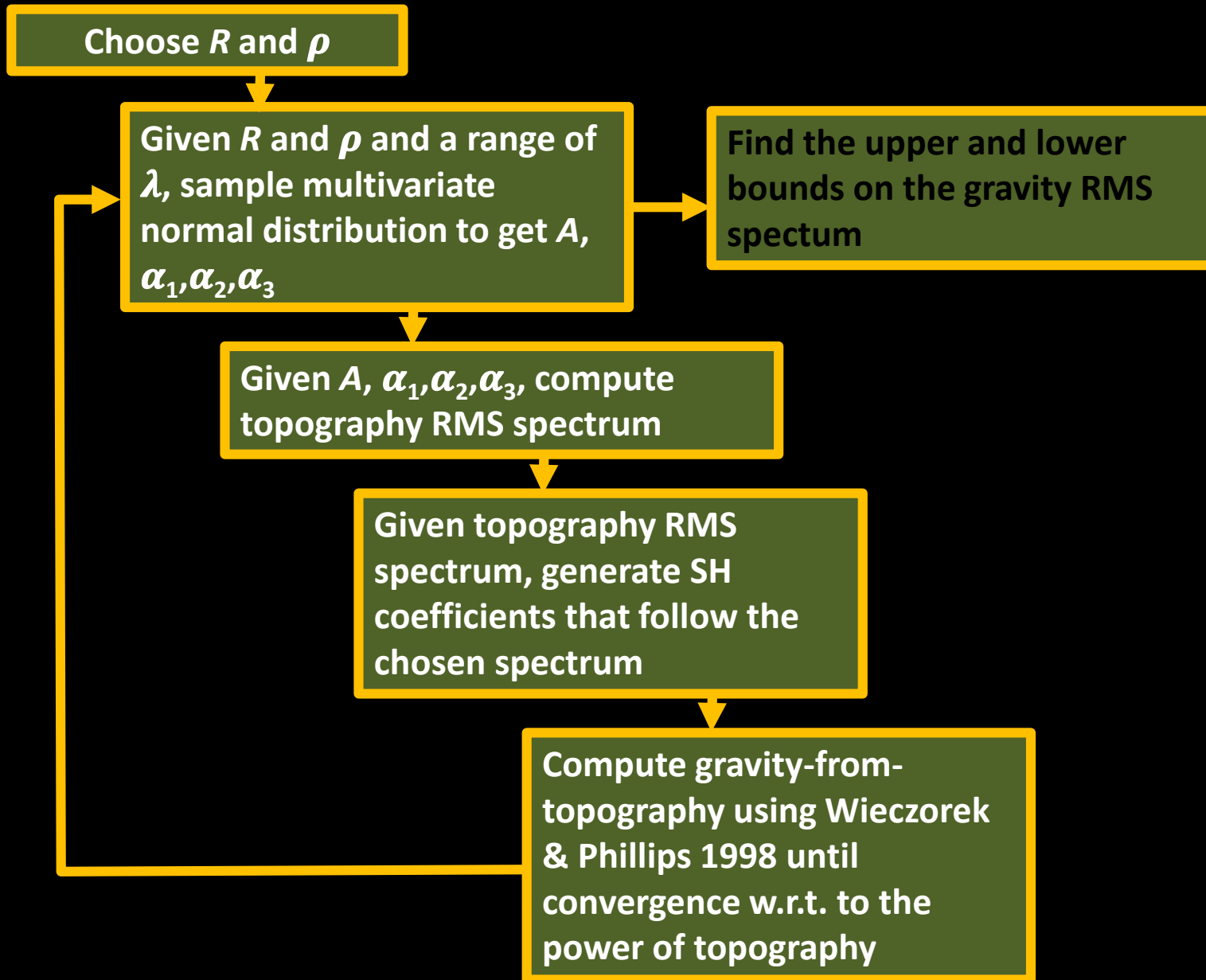
Asteroids, general scaling



Asteroids, general scaling



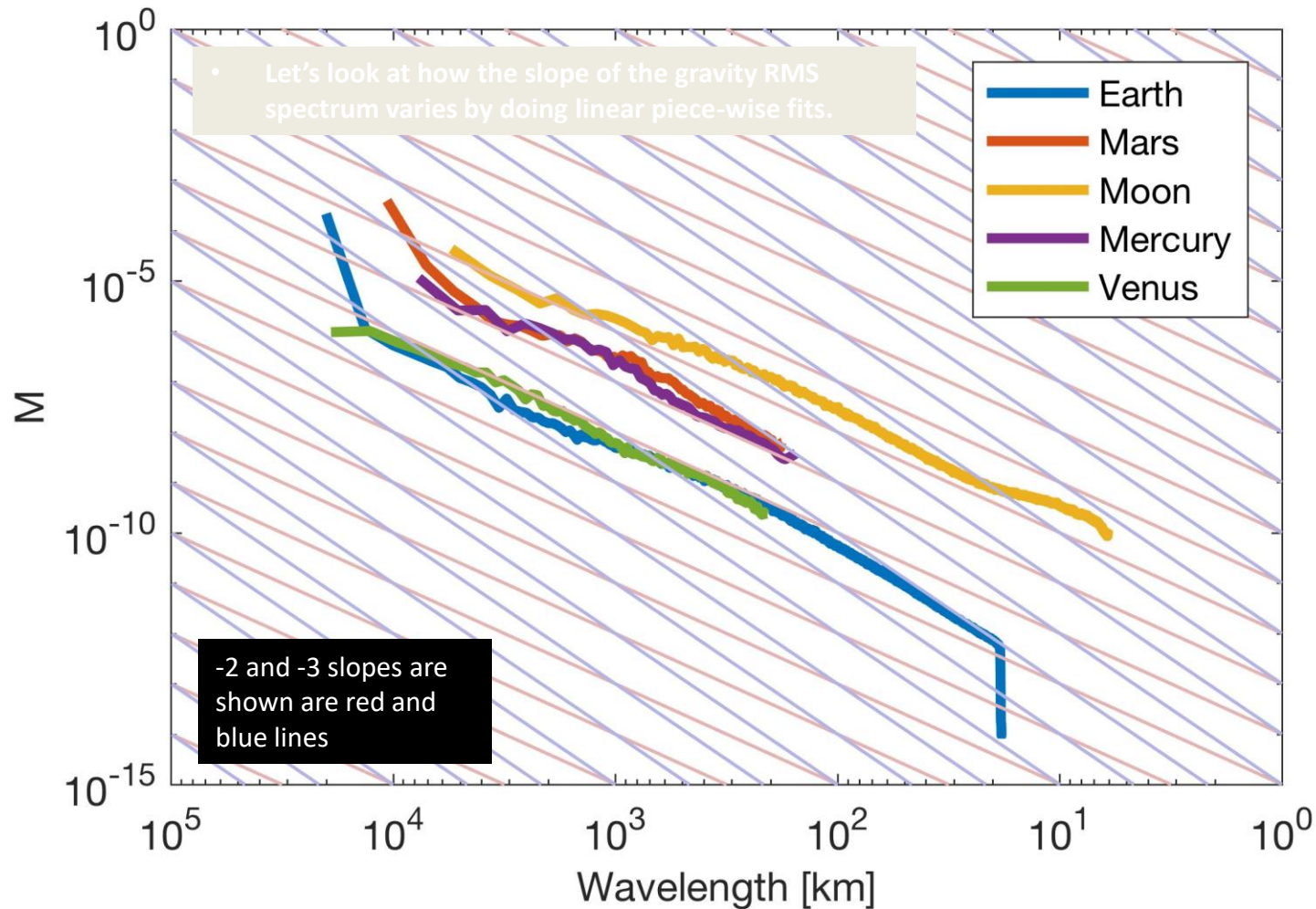
A priori constraint on gravity RMS



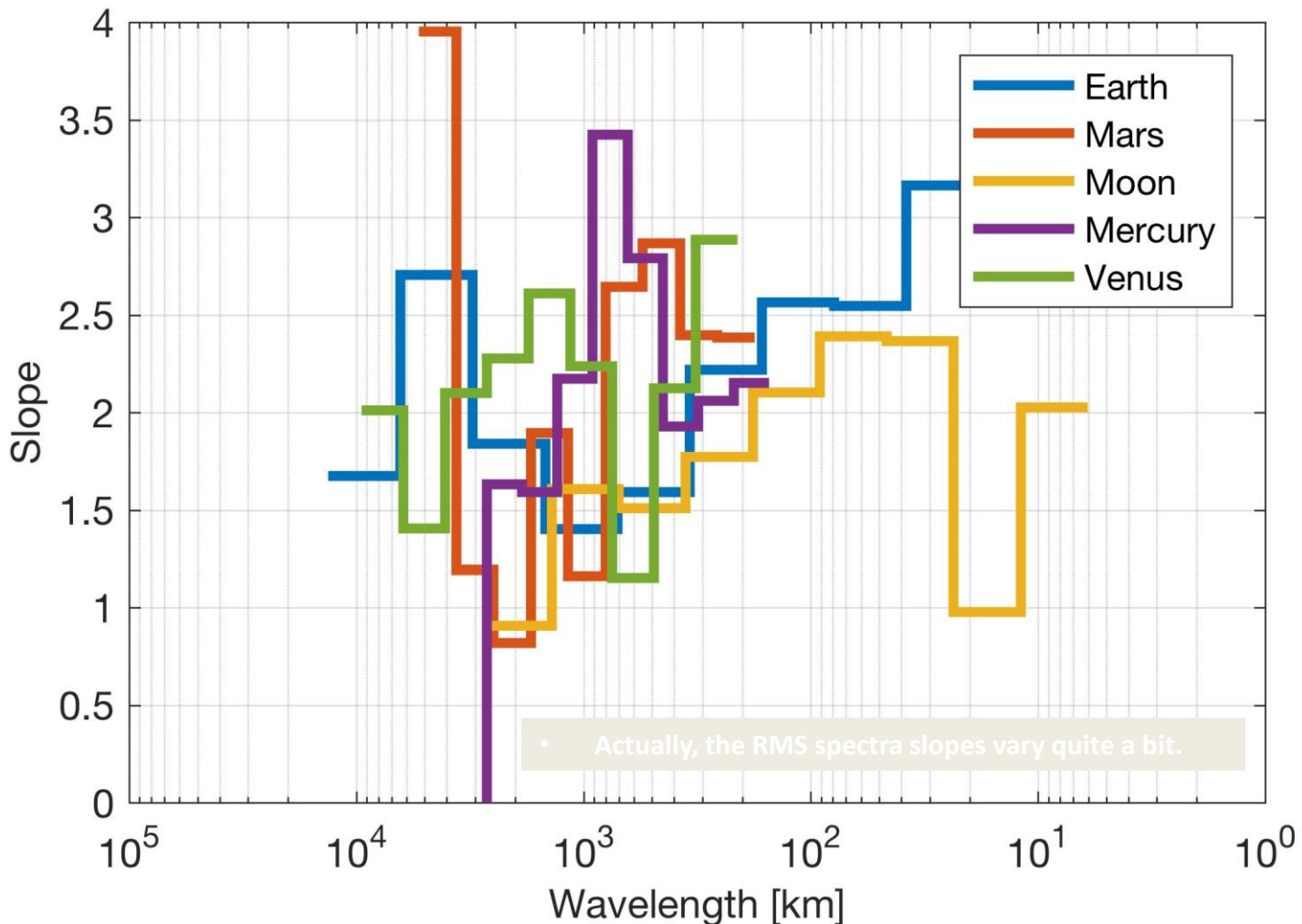
Summary

- Topography RMS spectra of 4 terrestrial planets and the Moon cannot be simultaneously fit with a single power law of the gravity-scaling or general form.
- Topography RMS spectra of asteroids **CANNOT** be *satisfactorily* fit with a power law the gravity-scaling form.
- Topography RMS spectra of asteroids **CAN** be *satisfactorily* fit with a power law of the general form.
- Despite having different internal structure, composition and mechanical properties of the surface layer, the asteroid topography spectra can be effectively modeled as a general power law

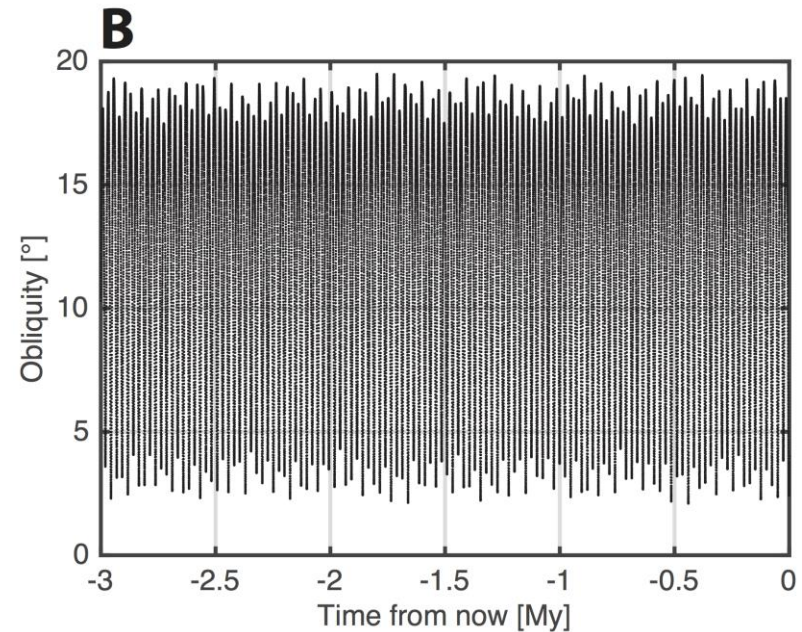
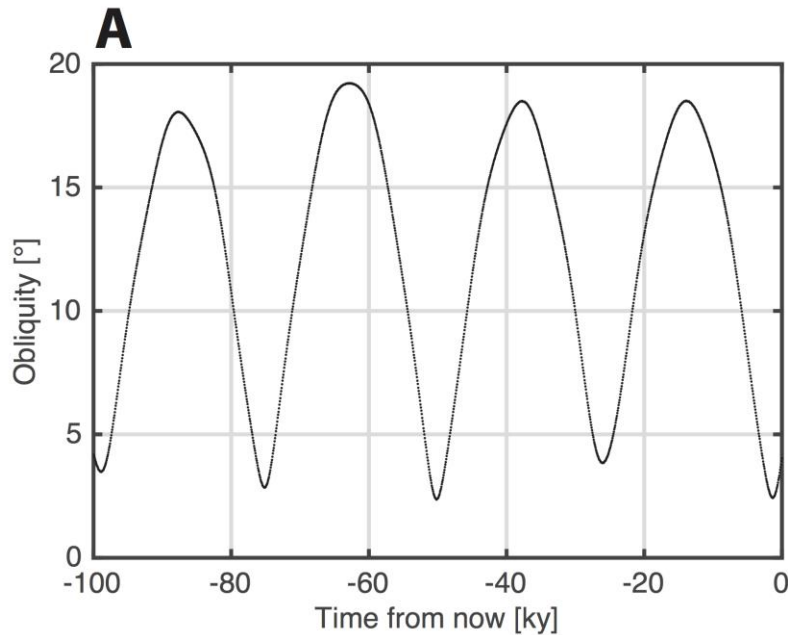
Gravity RMS spectra



Slopes of piecewise fitted gravity RMS spectra



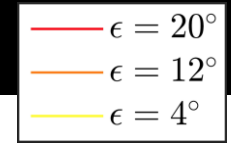
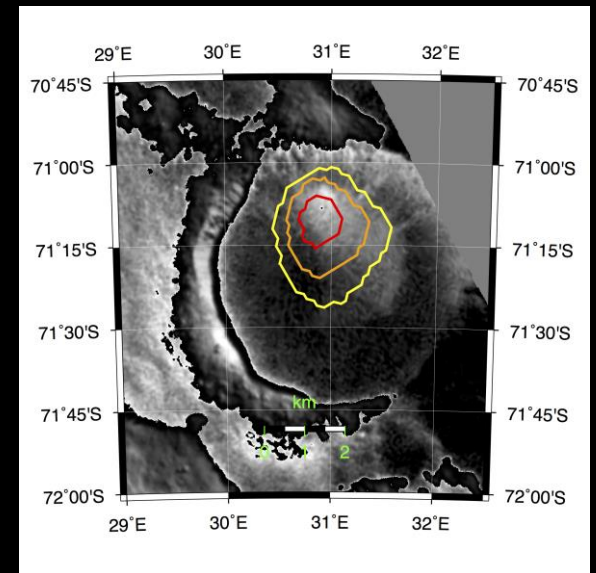
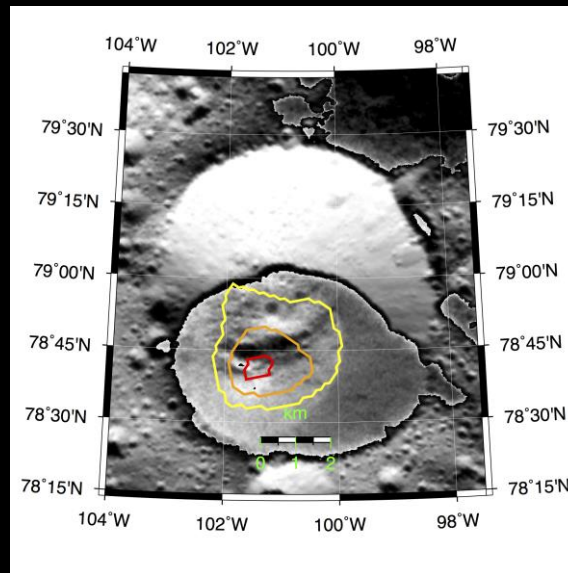
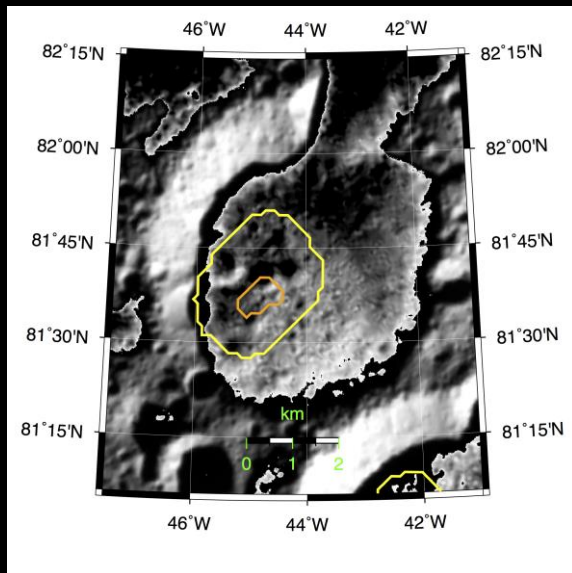
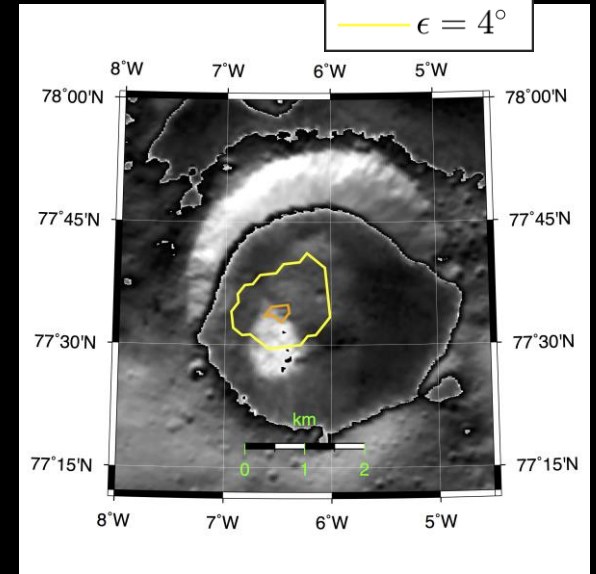
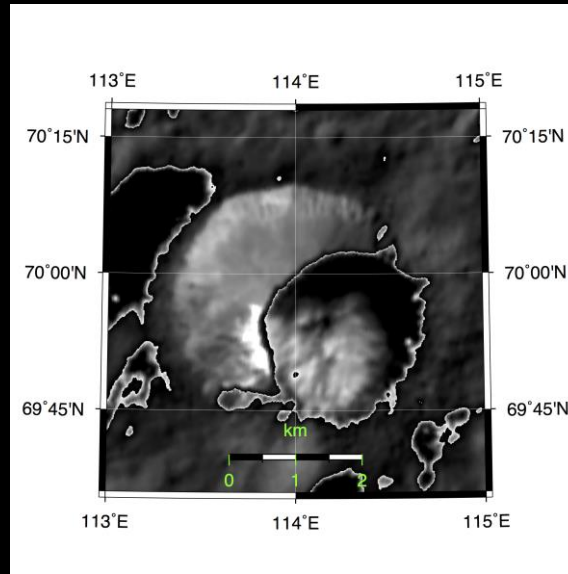
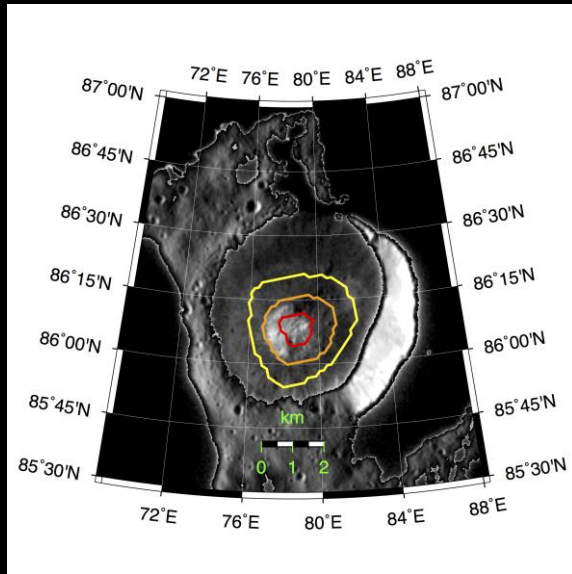
Ceres' obliquity history



- **Obliquity varies between 2.4° and 19.7°**
- **The main period is 24.5 ky**
- **We happen to visit Ceres when its obliquity is minimal**

Ermakov et al., in prep. for GRL

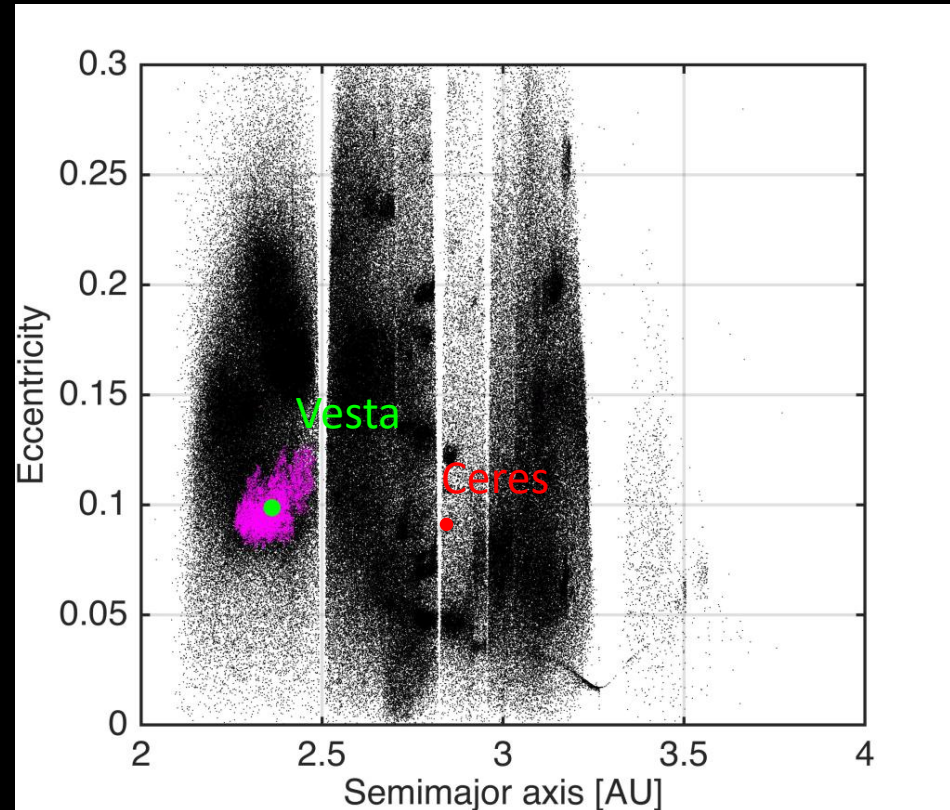
Bright Crater Floor Deposits (BCFDs)



Why Ceres?

- **Largest body in the asteroid belt**
- **Low density implies high volatile content**
- **Conditions for subsurface ocean**
- **Much easier to reach than other ocean worlds**

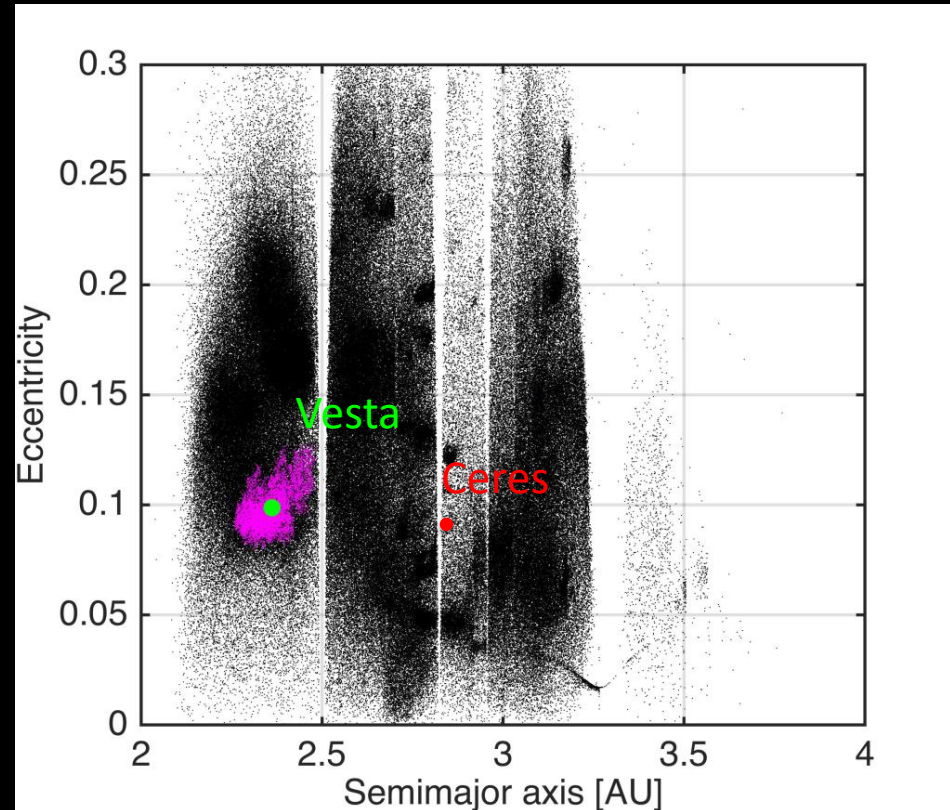
Ceres location in the asteroid belt



Why Ceres?

- **Largest body in the asteroid belt**
- **Low density implies high volatile content**
- **Conditions for subsurface ocean**
- **Much easier to reach than other ocean worlds**
- **Major unexplored object in the asteroid belt**

Ceres location in the asteroid belt



What did we know before Dawn

- **Castillo-Rogez and McCord 2010**

Ceres accreted as a mixture of ice and rock just a few My after the condensation of Calcium Aluminum-rich Inclusions (CAIs), and later differentiated into a water mantle and a mostly anhydrous silicate core.

What did we know before Dawn

- **Castillo-Rogez and McCord 2010**

Ceres accreted as a mixture of ice and rock just a few My after the condensation of Calcium Aluminum-rich Inclusions (CAIs), and later differentiated into a water mantle and a mostly anhydrous silicate core.

- **Zolotov 2009**

Ceres formed relatively late from planetesimals consisting of hydrated silicates.

What did we know before Dawn

- **Castillo-Rogez and McCord 2010**

Ceres accreted as a mixture of ice and rock just a few My after the condensation of Calcium Aluminum-rich Inclusions (CAIs), and later differentiated into a water mantle and a mostly anhydrous silicate core.

- **Zolotov 2009**

Ceres formed relatively late from planetesimals consisting of hydrated silicates.

- **Bland 2013**

If Ceres *does* contain a water ice layer, its warm diurnally-averaged surface temperature ensures extensive viscous relaxation of even small impact craters especially near equator